1-1-2014

Development of a Dynamic Performance Management Framework for Naval Ship Power System using Model-Based Predictive Control

Jian Shi

Development of a dynamic performance management framework for naval ship power system using model-based predictive control

By

Jian Shi

A Dissertation
Submitted to the Faculty of
Mississippi State University
in Partial Fulfillment of the Requirements
for the Degree of Doctor of Philosophy
in Electrical and Computer Engineering
in the Department of Electrical and Computer Engineer

Mississippi State, Mississippi

December 2014

Development of a dynamic performance management framework for naval ship power system using model-based predictive control

By

Jian Shi

Approved:

Sherif Abdelwahed
(Major Professor)

Randolph F. Follett
(Committee Member)

Yong Fu
(Committee Member)

Michael Mazzola
(Committee Member)

James E. Fowler
(Graduate Coordinator)

Jason M. Keith
Interim Dean
Bagley College of Engineering

Name: Jian Shi

Date of Degree: December 13, 2014

Institution: Mississippi State University

Major Field: Electrical and Computer Engineering

Major Professor: Dr. Sherif Abdelwahed

Title of Study: Development of a dynamic performance management framework for naval ship power system using model-based predictive control

Pages in Study: 170

Candidate for Degree of Doctor of Philosophy

Medium-Voltage Direct-Current (MVDC) power system has been considered as the trending technology for future All-Electric Ships (AES) to produce, convert and distribute electrical power. With the wide employment of high-frequency power electronics converters and motor drives in DC system, accurate and fast assessment of system dynamic behaviors , as well as the optimization of system transient performance have become serious concerns for system-level studies, high-level control designs and power management algorithm development.

The proposed technique presents a coordinated and automated approach to determine the system adjustment strategy for naval power systems to improve the transient performance and prevent potential instability following a system contingency. In contrast with the conventional design schemes that heavily rely on the human operators and pre-specified rules/set points, we focus on the development of the capability to automatically and efficiently detect and react to system state changes following disturbances and or damages by incooperating different system components to formulate an overall system-level solution. To achieve this objective, we propose a

generic model-based predictive management framework that can be applied to a variety of Shipboard Power System (SPS) applications to meet the stringent performance requirements under different operating conditions. The proposed technique is proven to effectively prevent the system from instability caused by known and unknown disturbances with little or none human intervention under a variety of operation conditions.

The management framework proposed in this dissertation is designed based on the concept of Model Predictive Control (MPC) techniques. A numerical approximation of the actual system is used to predict future system behaviors based on the current states and the candidate control input sequences. Based on the predictions the optimal control solution is chosen and applied as the current control input. The effectiveness and efficiency of the proposed framework can be evaluated conveniently based on a series of performance criteria such as fitness, robustness and computational overhead. An automatic system modeling, analysis and synthesis software environment is also introduced in this dissertation to facilitate the rapid implementation of the proposed performance management framework according to various testing scenarios.

DEDICATION

To my beloved family.

ACKNOWLEDGEMENTS

I want to take this opportunity to thank everyone who has ever been there for me during this long journey. It is hard, but we made it through TOGETHER.

Don't stop believin'

Hold on to that feelin'

TABLE OF CONTENTS

LIST OF TABLES

LIST OF FIGURES

CHAPTER I

INTRODUCTION

1.1 Background

Electrical power system is becoming the backbone of the next-generation naval ships as it supplies energy to various onboard system components including weapon system, service system, operation system and propulsion system [1]. Compared with the conventional ship designs which rely on auxiliary systems that are steam powered or hydraulically powered, electrical drive offers significant benefits in terms of reducing the life-cycle cost, increasing the payload and survivability. The next generation Navy warships are envisioned to be fully electricity driven and have a power demand of upto 100 Megawatts. In order to meet that such critical power requirements, the Integrated Power System (IPS) is proposed as a solution to provide the power to serve a variety of onboard loads [2]. Considering the critical role the power system is playing for ship operation, relying on the conventional self-recovery mechanism or manual control of the electric power system can no longer meet the performance standard. A dynamic performance-oriented power management framework for the analysis and design of SPS is necessary [3] and becomes an urgent requirement for the design of future onboard power control systems.

1.2 Challenges and Motivations

The rapid growth in computer science and communication technology has made smooth and flexible information sensing and transmission system possible. As information including system-wide voltage levels, directions of power flows and real-time component status has become available upon request, the new control schemes could take advantage of this information and perform dynamic performance management determined based on a cooperative global basis to enhance the system stability and optimize the performance.

Based on the prior discussion, there are three main challenges we need to overcome in this framework. One of the challenges is that the unique characteristics of SPS requires explicit high-resolution modeling of system components transient phases [4]. The models have to be developed specifically for the dynamic analysis of SPS, so they can provide precise insight for system dynamic behavior investigations. Another challenge is with the computational burden of time domain simulation to meet the stringent requirement of real-time operations. For the evaluation process, any small variations on system parameters would result in a complete re-computation of the whole system, thus making the performance assessment difficult for actual implementation. Lastly, the dynamic management framework should have certain degrees of flexibility so that it can be easily adapted to a variety of operation scenarios. It is also desirable that the dynamic management can be open-ended and extensible to be integrated with other management functions such as Quality of Service (QoS) management or fuel economy management to form a unified SPS energy management and regulation system [5].

For the last decade, model-based control has gained increasing attention in the different engineering fields as an attractive approach for system-wide automatic management [6]. Among various optimization and management techniques, the design concept of model predictive control (MPC) has been proven for its flexibility, accuracy, and effectiveness. A series of application designs utilizing MPC techniques can be found in [7-11]. MPC refers to the generic control techniques that predict the future system states over a certain length of "prediction horizon" based on a given objective function, a set of candidate control inputs, an accurate approximation of the system behavior, and the current system state measurements. The first element of the input sequence that results in the optimized future system state prediction is then chosen and applied to the current system. Previous works have demonstrated that MPC techniques can be used to generate a coordinated solution to optimize the operation of power systems and enhance the stability and reliability of systems affected by disturbances or faults. A combination of restoration procedures including system-level adjustments like load shedding and reconfiguration or component-level adjustment like system setting change can be utilized. The optimization objective is formulated based on system states represented in the form of nonlinear differential algebraic equations (DAEs) [8, 10] or linearized DAEs. While MPC has been found to have a great potential to solve the dynamic performance optimization problem and enhance the overall system reliability for terrestrial power systems, it has not been considered in analysis and design practice for SPS yet.

Another important factor for dynamic analysis practice, especially for power systems, is that the accuracy of the magnitude or frequency evaluation is closely related to the equivalent system model used to represent the actual physical behaviors over the

time frame of interest. In another word, there does not exist a set of "standard" component models that can be used for different types of performance analysis. The models have to be tailored to the scope of the specific study case by case [12, 13]. This factor needs to be carefully considered during the modeling phase for MPC design practice.

1.3 Research Statement

To start, an appropriate numerical modeling approach is developed specifically for the system-level analysis and control strategy design for MVDC SPS. The architecture of the latest MVDC base-line model and its notional functional block decomposition are illustrated with their exclusive modeling requirements respectively. Those functional blocks can be seen as the highly simplified abstractions of the physical shipboard power system components. A novel modeling strategy is then proposed as an extension to the existing literature to fully include the stator transient dynamics of the synchronous machines in order to accurately capture the dynamic characteristics of the system following local or system-wide disturbances that are necessary for system-level studies. The proposed modeling approach is verified against conventional steady-state modeling techniques and the corresponding equivalent Simulink models/RDTS models. Its simulation speed is also justified to meet the requirement for the system-level analysis and designs. Once the modeling strategy is fixed, the model-based performance management system can be developed.

In this dissertation, a flexible and automated system-level dynamic performance management framework with consideration of optimizing the dynamic transient responses following a system disturbance is proposed. In this framework, MPC technique

is used to achieve an overall system-side optimized solution that fulfills the requirement of operating conditions and fits the stringent performance specifications and various constraints. Time constraints (in another word computational efficiency) and the detailed performance criteria as suggested by the Electric Ship Research and Development Consortium (ESRDC) with regards to the dynamic transient responses regulation will be the main focus of this optimization work. In order to achieve the control objective, we assume that the system information transmission is instantaneous and always accurate, and all the system-level control resources are made available for the management framework [14] including: specification change for component-level controllers like motor drives and power converter ; shed non-vital loads; switch load feeder between port bus and starboard bus; shift power generations among main generators and auxiliary generators and reconfigure the distribution network. With the special characteristics of SPS taken into consideration, the proposed management framework mainly aims to achieve the bus voltage regulation and to prevent voltage oscillation simultaneously and efficiently. At the same time, it can be integrated with other types of power analysis tools like power balance analysis, fuel consumption analysis, and reliability/survivability assessment to provide an overall perspective of the system states and generate the optimal solution to facilitate the operation and design process.

Last but not least, a model-based software environment based on the principle of Model Integrated Computing (MIC) techniques is developed to support and facilitate the modeling and simulation process for the shipboard power system and the corresponding control and management framework design at a high level of abstraction called "meta-level." Meta-model generate models and specifications that can be directly used by

domain engineers to develop applications, test and simulate the performance with regards to a variety of different criteria, and synthesize control structures which can later be automatically translated to executable scripts for the management framework implementation.

1.4 Organization

The dissertation is organized as follows: the research scope of this dissertation is proposed in Chapter II followed by a detailed introduction of MVDC SPS including the system architecture and functional breakdowns, conventional dynamic performance techniques, average modeling techniques and model predictive control concept. Chapter III proposed the analytical modeling approach of SPS. The proposed modeling approach is verified against conventional steady-state modeling techniques, the corresponding equivalent Simulink models as well as hardware benchmark implemented on RDTS simulators. The design concept of the performance management framework, as well as the detailed script /algorithm formulation process is illustrated in Chapter IV; a series of case studies are presented to demonstrate the effectiveness and applicability of the proposed control techniques for system-level management strategy development. In Chapter V, the software tool is developed to facilitate the implementation of the proposed management framework as well as other types of power system analysis and simulation. Finally, in Section IV, the dissertation is concluded and future work is discussed.

CHAPTER II

BACKGROUND AND LITERATURE REVIEW

2.1 Research Scope

In order to set the stage for the following discussion, the specific type of analysis and design that we are focusing on in this dissertation needs to be defined first. A power system generally contains a variety classes of phenomenon that have different physical origin and occur within different time scales, as the result there does not exist an universal model for different types of studies [15]. The level of model fidelity heavily depends on the design purpose for the application. For SPS, the overall analysis and design process can be classified and represented using the form of system layers [16]. The hierarchical system architecture can be specified based on the required response time for the corresponding system operations. Specifically for the purpose of this dissertation, we consider three layers or levels of analysis and design which is a common practice for related research work [16, 17] as follows:

- System level (Level I): The response time is within the range of 1 *ms* upto 1 *Sec*. Under most circumstances, system level analysis is considered highly simplified and abstracted as it determines the overall topologies and functionalities of the system. The primary motivations behind the development of system-level model are: 1) for the early-stage design iterations where the parameters and the more detailed system

representations are not yet specified and 2) for the exploration and design process where system behaviors need to be repeatedly evaluated under a variety of conditions. Such practice includes high level control or optimization strategy design, system structure study, and harmonic resonance study.

- Application level (Level II): The response time is within the range of 100 μs upto 1 ms. Application level analysis and design mainly determine the operation status of system components and their local controllers.
- Physical level or hardware (Level III): The response time is in microseconds, depending on converter frequency. Analysis on this level primarily includes the switching operations of high-frequency power converters, fault protections, and gating signal generation.

While there is a variety of literature covering the modeling and simulation strategy for application level design and high-frequency component level analysis [18, 19], currently there is very little work focusing on the model formulation for system-level analysis. Therefore, when it comes to system-level design, usually the static model is used to approximate the system behavior during the time range of interest [20-23]. A more accurate model that specifically addresses the requirement of system-level dynamic studies needs to be developed. Based on the approximate time range of power system dynamic phenomenon shown in Figure 2.1 [12, 13, 15, 24] where the targeted time range is marked in red, the main dynamics studied in this dissertation are system resonances and synchronous machine stator transients. This is also the suggested objective of the ESRDC technical reports [17, 18]/IEEE standard for system-level dynamic analysis [25]

and to provide the essential criteria to observe the stability properties of the system, as from the system-wide perspective, the dynamics are mainly triggered by the mechanical and electrical power difference initiated by disturbance or system structure adjustment.

Based on the nature of performance evaluation criteria, for utility class AC power system the performance issues can be divided into two categories as rotor angular regulation and voltage regulation [12, 26]:

2.1.1 Rotor angular regulation

As the name suggests, the angular performance refers to the capability of power system to remain angular synchronous under disturbances. The performance is directly related to the generator speed governor and the damper circuit. Typically, angular desynchronization is represented in the form of aperiodic angular separation due to insufficient synchronizing torque and defined as "first swing instability." As the SPS is a tightly coupled system with shot cables and strong synchronizations, the electrical frequencies of the generators in MVDC system are considered well decoupled from the DC distribution bus compared with terrestrial AC power systems. The operation of the generators does not have to be phase locked or synchronized. With this in mind, rotor angle instability is very unlikely to occur [27]. Results in [28] also suggest that the inherited generator controls can strongly maintain the angular synchronization. With those factors taken into consideration, we can reach the conclusion that the angular performance is not the main objective for the performance management strategy design.

2.1.2 Voltage regulation

Voltage performance refers to the system's ability to maintain steady voltage within acceptable range at all buses. Voltage instability is usually caused by the excessive demand of reactive power and directly related to the performance of the generator excitation systems for the design and implementation of SPS applications. Especially considering the fact that multiple generators are connected to the same DC bus, the machines would interfere with others to regulate the bus voltage, and this easily leads to the large voltage swings. Therefore, for the MVDC SPS, the DC voltage of the distribution bus should be stringently regulated within desired margins both under "pre-fault" and "post-fault outage" conditions for improving security, reliability and survivability [29]. More specifically, the desired performance evaluation metrics have been mentioned in [30, 31] as the standard for voltage-regulation related system studies. This standard will be modified and adopted here as the performance criteria that the proposed management framework aims to achieve.

Table 2.1 Performance metrics for the voltage regulation [30]

Performance Metrics	General specification
Desired Bus Voltage	5 kV
Voltage Ripple	1.5%
Maximum Transient Recovery Time	0.1 Sec
Voltage Transient Range	+/- 10%

In other words, the voltage regulation needs to be achieved, and the voltage oscillation needs to be suppressed simultaneously and promptly to keep the system states within the desired region.

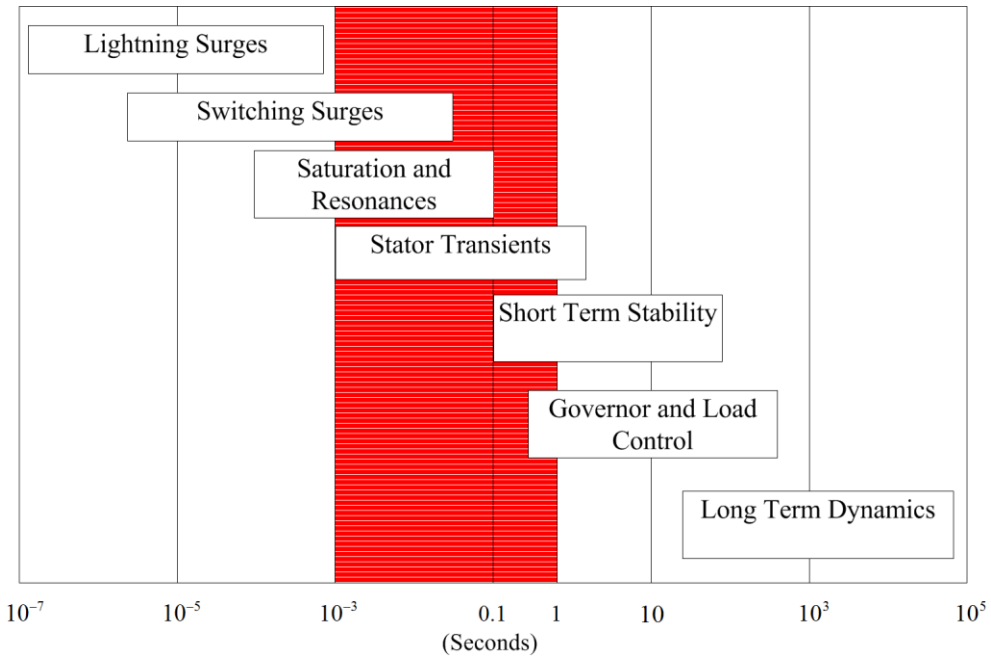

Figure 2.1 Time scale of dynamic phenomena [13, 24]

2.2 Overview of SPS: Definition and special characteristics

As a micro-grid power system, SPS is considered an independently controlled small electric network and is powered by the distributed generation system [32]. In order to determine an effective management approach for SPS, it is critical to capture the unique natures of SPS as a non-conventional power grid and pay special attention for the specific requirement for modeling, analysis and design based on the following characteristics [3, 33]:

- Length of power cables is limited by the size of the ship, which determines that the dynamics of transmission lines do not significantly affect the overall system behavior and can be ignored.

- System state information is transmitted very quickly within the system due to the close physical proximity, making the interconnections among different components important. The close electrical proximity also guarantees generators are strongly synchronized.
- With limited generation capacity and rotational inertia, generators are very sensitive to load changes, especially when the loads are rated at a significant fraction of the generating capacity of the system. Large dynamic load variations can lead to large voltage and frequency deviations on the interconnected distribution bus.

Overall, the tightly coupled nature of the distribution network, the limited generation capacity and the lack of generator inertia have determined that even tiny disturbance(s) within the system would cause large dynamic responses. Thus, compared with conventional power system grid, the SPS is more fragile and prone to faults and failures.

The uniqueness of SPS also leads to the conclusion that common assumptions and approximations that have been broadly used in the terrestrial power system; for example, the definition of infinite bus and slack generator does not apply to the SPS. With this in mind, common power system analysis tools/packages cannot be used to perform the dynamic analysis of SPS. Higher order models and real-time simulations are suggested especially for dynamic evaluations.

On the other hand, as the onboard power system is responsible for supplying energy to nearly all the vital modules, it is extremely critical to maintain the power system working properly under different operating conditions; thus, the reliability and

stability of an SPS is the top priority both under adverse conditions and normal operations regarding the ship designs. Damages to the power systems can directly lead to the failure of the ship's mission. Some real examples of such catastrophes are shown as follows:

- In January, 1988, USS Samuel B. Roberts struck an M-08 Naval mine in the central Persian Gulf. The engine room with two gas turbines were flooded and the ship used its auxiliary thrusters to get out of the mine field [34]. It did not lose full combat capability with radars and missile launchers.
- On February, 18, 1991, during Operation Desert Storm, USS Princeton was hit by two influence mines. It caused the ship to lose power and the weapon/combat system did not get back online until fifteen minutes later [35].

Figure 2.2 U.S. Navy's new 'all-electric' USS Zumwalt destroyer (DDG1000) [36]

2.3 MVDC SPS

A new system integration and power distribution architecture called medium-voltage DC (MVDC) has been developed for all-electrical naval vessels. As the name suggests, it refers to the power transmission system that relies on direct current (DC) as the transmission media. Compared with traditional AC-based architecture, the MVDC power system has several advantages [21, 31] including:

- Higher power transfer capability based on the DC level
- Easy connections and disconnections for both power sources and loads through the use of power converters as connection interfaces
- Potential number, size, weight and rating reduction and simpler cabling
- Improved management of faults and disturbances utilizing the controlled power electronics switchers

- Higher power density and potential better system efficiency

The general design concept of a typical MVDC system can be found in Figure 2.3.

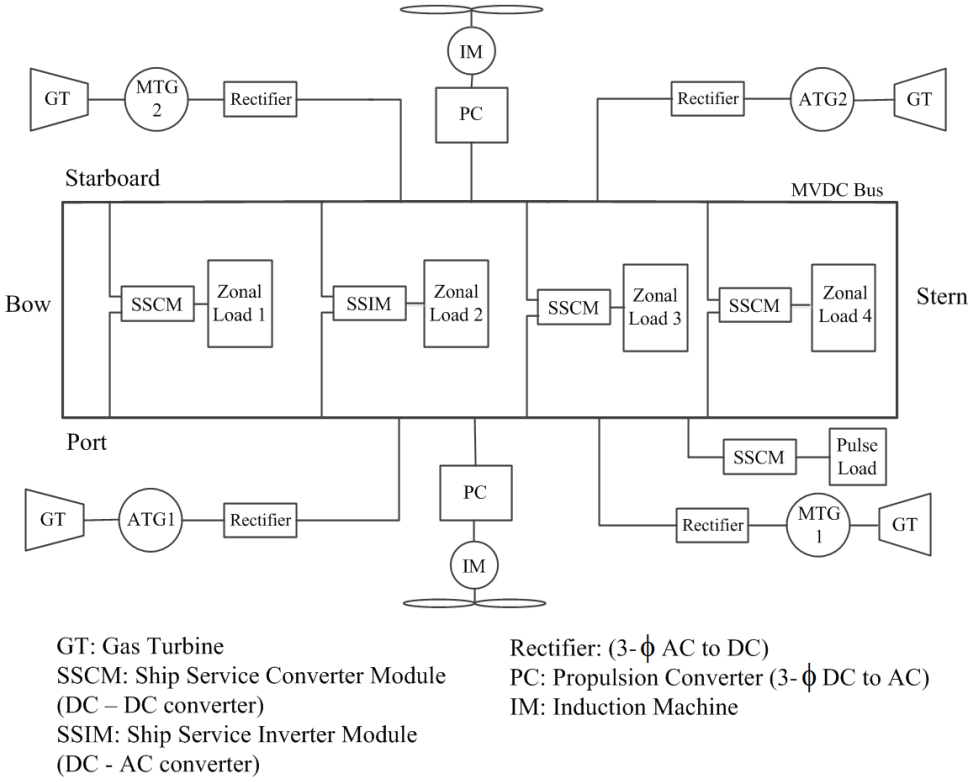

Figure 2.3 A design concept of MVDC SPS

To set the stage of this dissertation, a notional MVDC Next Generation Integrated Power System (NGIPS) model that was originally developed by the Office of Naval Research (ONR) and the ESRDC is used as the baseline topology for the corresponding model development [19, 25]. The standard modules and function diagrams in the preliminary model of a notional MVDC NGIPS include [18, 37]:

2.3.1 Propulsion modules

Electric power is converted into mechanical power through propulsion induction motors and propellers. The propulsion motors consist of two GE's Advanced Induction Motors (AIM) with 35MW rater power. A simplified one-line diagram of an induction motor along with its motor drive and propeller is shown in Figure 2.4.

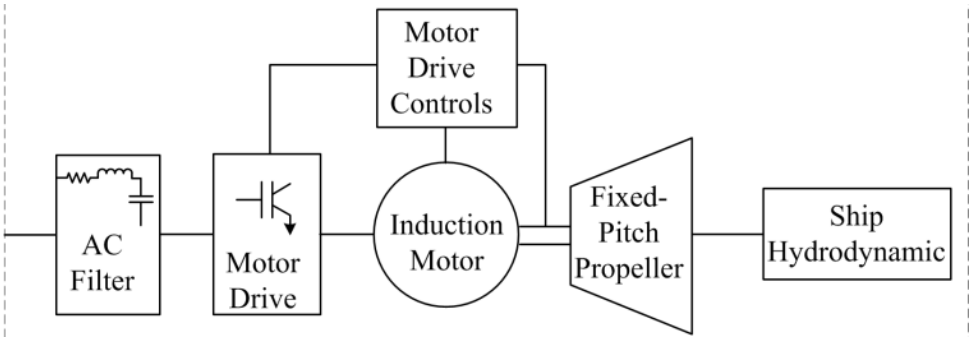

Figure 2.4 A simplified one-line representation of the propulsion system

2.3.2 Power generation modules

The electrical power is provided by two main generators (MTGs) rated at 36MW (45MVA) and two auxiliary generators (ATGs) rated at 4MW (5MVA). The generator modules consist of notional 3600 rpm twin shaft Rolls-Royce MT 30 gas turbines as the prime movers for MTGs and 14400 rpm single shaft General Electric LM500 gas turbines for ATGs, round rotor synchronous machines, the IEEE Type AC8B [38] exciters, and notional diode rectifiers [18]. A simplified one-line diagram representing a synchronous machine and its prime mover, exciter and rectifiers is shown in Figure 2.5 while the detailed structure of the generator with signal flows is illustrated in Figure 2.6.

For the current electric model, the gas turbine is represented in the form of a set of transfer functions.

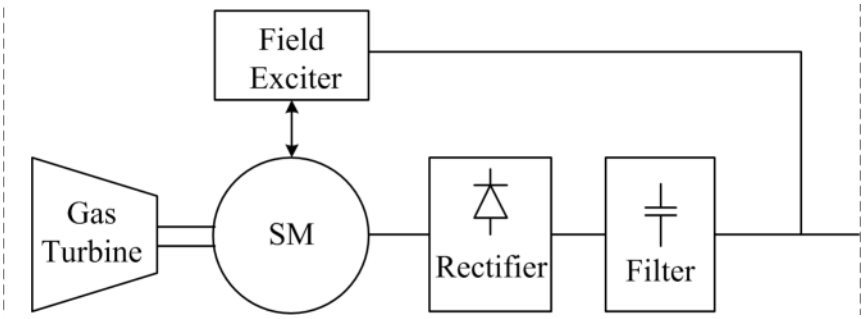

Figure 2.5 A simplified one line diagram of the generation module

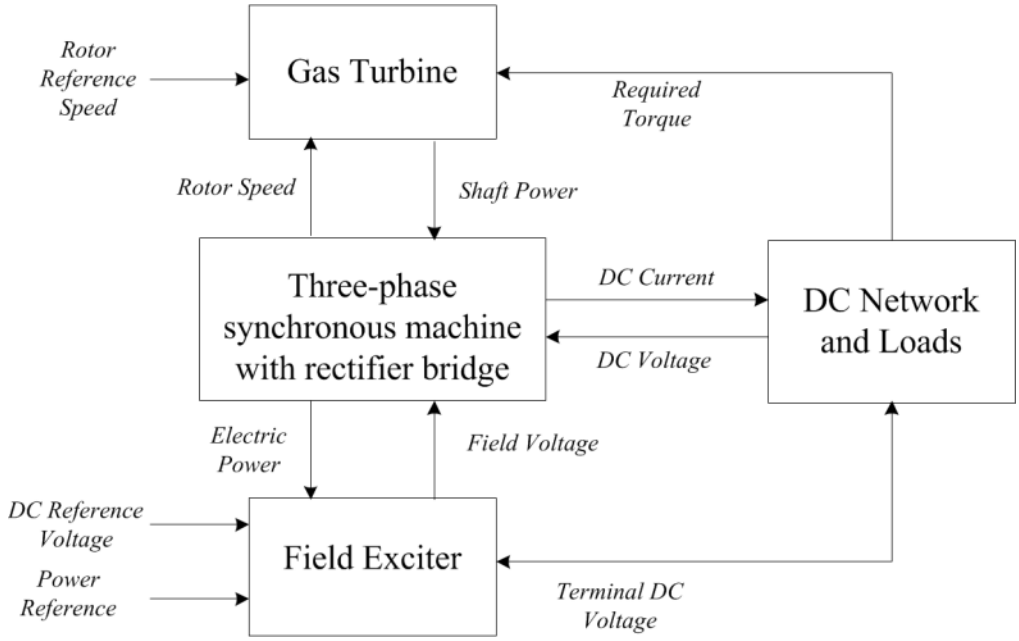

Figure 2.6 Detailed generator structure with signal flows

2.3.3 Power distribution modules

Zonal electrical distribution system is utilized in MVDC SPS. There are one main generator and one auxiliary generator on each side of the network (Port bus and Starboard bus) along with the induction motor drives. Ship loads are distributed in four zones from bow to stern and supplied from both port and starboard DC buses. The main bus of MVDC system is a 5kV DC bus.

2.3.4 Switching gears

All the electrical components are connected to the main MVDC bus with a disconnect device that determines the power flow directions, include simple disconnect means like switches, circuit breakers, or more complex ones like manual bus transfers (MBTs) and automatic bus transfer (ABTs). To handle unexpected possible damages, there are switches attached to the cross-hull connections as well. This creates a "split-plant" configuration to provide maximized reliability. For simplicity, it is assumed that switches are able to instantly connect and disconnect the corresponding component from the distribution network.

2.3.5 Power conversion modules:

Conversion modules convert electric energy from one form to another. Typical on-board conversion modules include power converters which convert energy between three phase AC components and DC distribution bus (AC/DC as rectifier, e.g. the generator rectifier or DC/AC as inverter, e.g. the propeller converter). For ship service loads distributed in different zones, there are also Ship Service Converter Modules (SSCMs) and Ship Service Inverter Modules (SSIMs) that are directly fed from the main

DC distribution bus and convert appropriate voltage to the zonal service loads either in the form of DC or AC. Power converters are considered as the main interface between the grid and corresponding components; thus, controls of converters are expected to facilitate the connection and removal operation in a fast and yet stable manner.

2.3.6 Power loads

Electric loads consume the power generated by the power generation module. Future electrical ships are expected to carry a variety of loads that range from conventional facility loads to high power radar loads and pulse loads. Based on their electronics characteristics, electrical equipment can be classified as resistive constant impedance/resistance loads, constant power loads and pulse loads, e.g. electromagnetic aircraft launch system, rail guns, and laser weapons. For the NGIPS model, there are a total of 22 lumped-parameter loads within 4 zones, including two AC zonal loads supplied from a 450V AC bus, two DC zonal loads supplied from an 800V DC bus and a pulse load as a stand-alone load center connected to the network. The load specification can be switched between different operation modes.

As various loads and induction motors within the system are directly fed from the main DC bus via high-bandwidth power conversion equipment, they would exhibit a behavior called "Constant Power Load (CPL) behavior", which suggests that loads tend to keep constant power consumption under fast current or voltage variations [39-41] and therefore act in the similar way as negative incremental resistances. The detailed systematic review of CPL theory can be found below.

2.3.6.1 CPL theory and application

With the increasing employment of power electronic converters and electric motor drives in the advanced electrical systems containing multi-voltage level AC and DC components. Assessment of the concept of CPL and the study of has been made in [42-44] for advanced automotive power system and aircraft power systems [45, 46]. An illustrative of CPL is a dc/ac inverter which is assumed to be tightly regulated with the rotating load that has one-to-one torque–speed characteristic i.e. linear relation between torque and speed, and drive an electric motor. For this inverter, it behaves as a CPL at the input terminal, as the input current decreases/increases when the input voltage increases/decreases. As a result, CPL has "negative impedance characteristic" and therefore introduces a destabilizing effect in the DC micro-grid that might cause the main distribution bus voltage to show severe oscillation. A demonstration of the typical CPL concept is shown as in Figure 2.7.

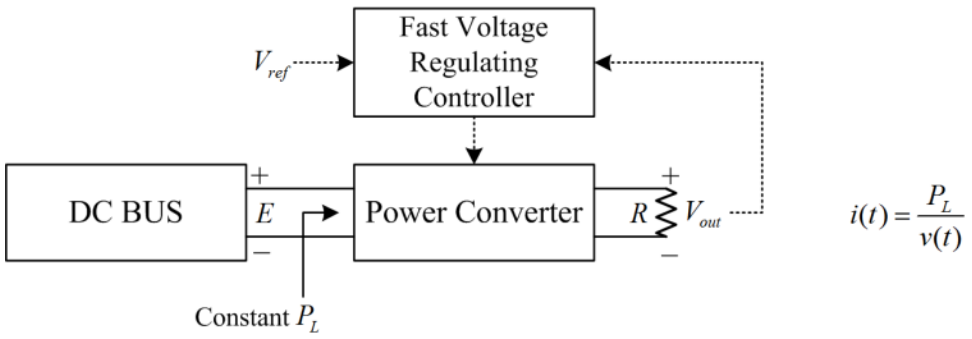

Figure 2.7 CPL characteristics [32]

Constant power load assumption is one of the most common hypotheses for simplifying model dynamics for system-level studies. Its validity is justified by the

employment of fast and robust converter controllers. As those high-frequency controllers effectively manage the current flow of the loads, the variation of load currents are not directly reflected as seen from the distribution network. CPL characteristic plays a very important role in simplifying the load characteristics [42] but also raises the issue of instability due to the negative impedance characteristics.

2.4 Modeling strategy for SPS

2.4.1 Overview

Based on the previous discussion, an appropriate modeling of shipboard power system is of critical importance to the design of shipboard applications. As a general modeling rule, it is impossible to develop models that include all the dynamics of the power system and can still of practical use. The level of fidelity of the model heavily depends on the design purpose for an application. In another word, for different design purposes, different modeling approaches are desired to facilitate corresponding evaluation. Based on the previous discussion, we have made the conclusion that for the design of the proposed dynamic performance management framework, a time-domain simulation based modeling approach would be desirable.

With the recent development of simulation software packages, a detailed model that considering all the details including the high-frequency converter switching actions has been developed and made available through various simulation platforms. The system is assembled in the form of Differential Algebraic Equations (DAEs) where the linear time-invariant part is represented in state-space equations and the time-domain transient responses are constructed by integrating the state-space equations using either fixed or

variable-step Ordinary Differential Equation (ODE) solvers that are provided with the embedded numerical engine i.e. Matlab.

Although the detailed model could be an option for the system-level study, due to the wide usage of power electronic converters within the system which requires relatively small simulation time steps and the complexity of detailed component structures, it inevitably suffers from the slow simulation speed [19, 37] which makes the high-fidelity model difficult and computationally expensive to be used for system-level analysis and design. Another important factor with power electronics switches is that the detailed switching actions make the system discontinuous which adds significant complexity and makes it impossible to be converted to linearized form for stability assessment and other form of analysis. In this case, a time-efficient and continuous representation of shipboard power system model is required.

A very common way to achieve that is by utilizing the reduced order modeling approach wherein the high-frequency dynamics of the system are "neglected" or "averaged" and the semiconductor switching is represented in the form of average-value formulation [47].With the implementation of average-value modeling techniques, it is expected that the numerical complexity can be reduced and the simulation efficiency can be improved with larger integration time steps to meet the requirement for management framework design.

Another way simplification can be implemented is to represent components in the abstracted forms based on the system-level analysis requirements and the proposed time range of interest rather than on the physical details. Combining the AVM techniques with the component simplifications, a much simplified representation of the originally

complicated system can be derived to specifically serve the need for high level studies and system-wide management design.

A general review of definitions and applications of dynamic average models for power system analysis can be found as in [48, 49] which was performed by IEEE Task Force on dynamic average modeling. The use of reduced-order average-value models is well established for distributed DC power system of spacecraft, aircraft, naval electrical systems and vehicular electric power systems. It has also been applied to variable speed wind energy systems [50-52]. For the purpose of this research work, we particularly consider the average-value modeling development for multi-phase rectifiers that have the typical configuration diagram as shown in Figure 2.8. Based on different cases, the power source could be a distribution AC power feeder (Case I) that is represented in its Thevenin equivalent voltages, series inductances and resistances, or a rotating machine (Case II) that is represented using the voltage-behind-reactance formulation which results in the similar form of Case I; the six pulse line commutated rectifiers could include an optional AC filter on the AC side and an optional DC filter on the DC side. The load(s) that is (are) connected to the DC network is (are) represented in the form of an equivalent resistor [53, 54]. Although this simplification representation ignores the inter-harmonics [55], it is commonly accepted in the low and medium power applications and considered valid for this work [49]. This configuration can be found as the input stage for a variety of medium power drives, motor loads and distribution networks.

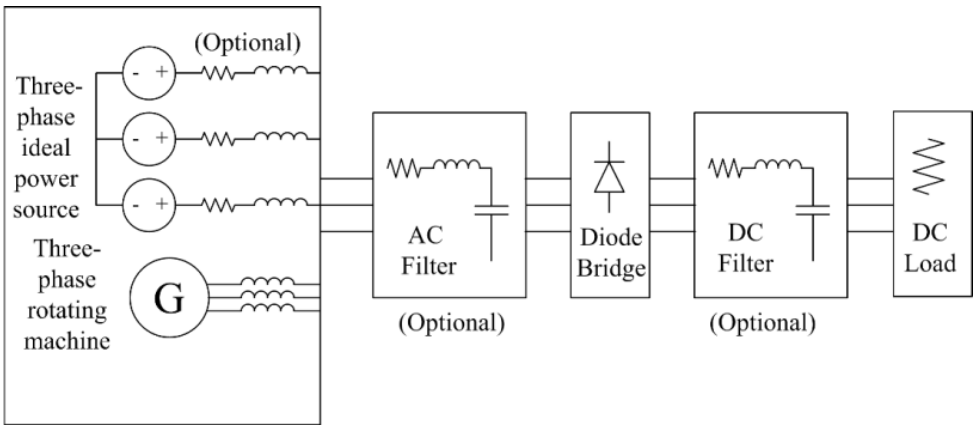

Figure 2.8 Typical configuration of a three phase line-commutated rectifier system

For the following discussion, it is assumed that the three-phase six-pulse rectifier is always working in the continuous conduction mode (CCM) and particularly under Mode1 where the commutation angle μ stays in the range of $0 < \mu < 60^\circ$ or under Mode 2 where $\mu = 60^\circ$. The reason behind this assumption is that CCM3 is an extreme condition and typically not considered in MVDC system while discontinuous conduction mode (DCM) is always intentionally avoided.

The generic fast averaging process over a prototypical switching interval can be defined as [56]:

$$\bar{f}(t) = \frac{1}{T_s}\int_{t-T_s}^{t} f(x)dx \tag{2.1}$$

where $f(x)$ indicates the system state equation and $\bar{f}(t)$ can be seen as the average value of $f(x)$ over a small period of time T_s.

2.4.2 Dynamic average modeling

For this three-phase diode rectifier model, various different modeling methodologies have been proposed in the literature. Those methodologies can be classified into two types of approaches: analytical and parametric. For the analytical approach, the system state variables like voltages or currents and their relationships are explicitly defined in the form of algebraic equations. With the pre-specified boundary conditions, the averaged representation of fast system state variations can then be derived analytically. Two analytical methods that are of particular interest of this dissertation can be found in [56-61] as the classic reduced order form (AVM-1) and [62-64] as the improved reduced order form (AVM-2) [48]. The details of those two modeling strategies and their essential difference will be briefed shortly in the following session:

2.4.2.1 Analytical approach

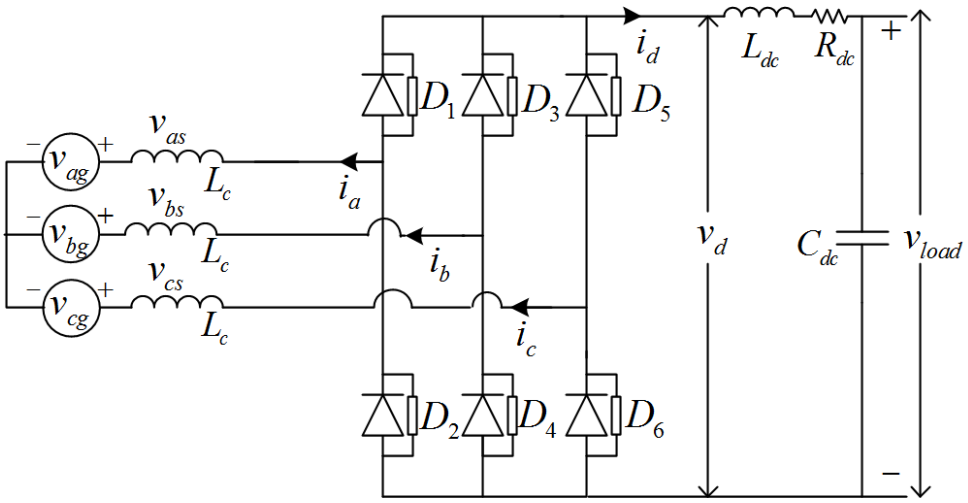

Figure 2.9 A three-phase voltage source fed load-commutated rectifier system [56]

A circuit diagram of the voltage source fed load-commutated rectifier system is shown in Figure 2.9. The AC source are represented in the form of an ideal three phase balanced voltage source v_{ag}, v_{bg} and v_{cg} with constant commutation inductance L_c. On the DC side, an RLC filter is deployed where the equivalent DC resistor and inductance is denoted as R_{dc} and L_{dc} respectively. The corresponding capacitor voltage is denoted as v_{load}. Given $\phi = \omega_g t$, and considering the phase delay effect caused by the commutation inductances, the over-all voltage that supplied from the AC side can be expressed as:

$$\begin{aligned} v_{as} &= E\cos(\phi) + L_c \cdot di_a/dt \\ v_{bs} &= E\cos(\phi - 2\pi/3) + L_c \cdot di_b/dt \\ v_{cs} &= E\cos(\phi + 2\pi/3) + L_c \cdot di_c/dt \end{aligned} \tag{2.2}$$

To further simplify the analysis procedure, it is assumed that the diode rectifier is lossless and its forward voltage drop and on-state resistance are neglected.

As the switching of the diode bridge is periodic in $\pi/3$ radian of the voltage angular displacement ϕ, any $\pi/3$ interval could be picked to develop the average representation of the voltage v_d. For this work, we will pick up the interval of $[0, \pi/3]$ as the averaging interval of interest. The dynamic average DC voltage on the DC side can be represented in the form of:

$$\bar{v}_d = \frac{3}{\pi}\int_0^{\frac{\pi}{3}} [(v_{ag} - v_{bg})]d\phi + \frac{3}{\pi} L_c \omega_g (i_a - i_b)\Big|_0^{\frac{\pi}{3}} \tag{2.3}$$

The over-bar is used to denote the fast average value during dynamical conditions which indicate that unlike steady-state operation, the corresponding system state variations (e.g. the variation of the amplitude of the voltage) are allowed; however, the

averaging operation is assumed to be relatively faster. Therefore the variation from one averaging interval to the next is relatively small. To find the boundary conditions to solve (2.3), the three phase conducted currents within the interval can be expressed as:

$$\begin{aligned} i_{abc}\big|_{\theta_g=0} &= [0, i_d(0), -i_d(0)] \\ i_{abc}\big|_{\theta_g=\mu} &= [-i_d(\mu), i_d(\mu), 0] \\ i_{abc}\big|_{\theta_g=\pi/3} &= [-i_d(\pi/3), i_d(\pi/3), 0] \end{aligned} \tag{2.4}$$

where μ refers to the commutation angle and $i_d(t)$ indicates the instantaneous value of DC current output on the DC side. To determine the representation of $i_d(t)$, AVM-1 and AVM-2 have provided different approximations.

In AVM-1, $i_d(0)$ is approximated by the representation of $\bar{i}_d$ and accordingly, $i_d(\pi/3)$ is represented as $\bar{i}_d + \Delta\bar{i}_d$ which yields the following boundary condition:

$$\begin{aligned} i_{abc}\big|_{\theta_g=0} &= [0, \bar{i}_d, -\bar{i}_d] \\ i_{abc}\big|_{\theta_g=\frac{\pi}{3}} &= [-\bar{i}_d - \Delta\bar{i}_d, \bar{i}_d + \Delta\bar{i}_d, 0] \end{aligned} \tag{2.5}$$

where $\Delta\bar{i}_d$ is used to denote the average DC current variation over the averaging interval due to long-time slow system dynamics and can be approximated as:

$$\Delta\bar{i}_d = \frac{\pi}{3}\frac{d\bar{i}_d}{d\phi} = \frac{\pi}{3\omega_g}\frac{d\bar{i}_d}{dt} \tag{2.6}$$

Substitute (2.6) into (2.3), the average DC voltage can be obtained as:

$$\bar{v}_d = \frac{3}{\pi}\sqrt{3}E + \frac{3}{\pi}L_c\omega_g\bar{i}_d - 2L_c\frac{d\bar{i}_d}{dt} \tag{2.7}$$

Considering the effect of the RLC filter, based on Kirchhoff's voltage law:

$$\bar{v}_d = R_{dc}\bar{i}_d + L_{dc}\cdot d\bar{i}/dt + v_{load} \tag{2.8}$$

Combine (2.7) and (2.8), the complete averaged formulation of DAE that describing the characteristics of the rectifier can be derived as:

$$\frac{d\bar{i}_d}{dt} = \frac{\frac{3}{\pi}\sqrt{3}E - (R_{dc} + \frac{3}{\pi}L_c\omega_g)\bar{i}_d - v_{load}}{L_{dc} + 2L_c} \tag{2.9}$$

with the commutation angle expressed as:

$$\mu = \arccos(1 - 2L_c\omega_g\bar{i}_d/\sqrt{3}E) \tag{2.10}$$

The approximation used in (2.6) only holds true when the variation of $\bar{i}_d$ during the averaging interval stays consistent; however, this may not always be accurate due to the possibility of large system state change. In another word, $\Delta\bar{i}_d$ need to be defined in a more specific way to capture the dynamic averaging variation during the switching interval. An attempt to improve the dynamic accuracy of AVM-1 approach is introduced in approach AVM-2, where i_d is approximated using its first-order Taylor expansion as:

$$i_d(\theta) = i_{d0} + k(\theta - 2/\mu) \tag{2.11}$$

where i_{d0} is defined as the average value of i_d during the commutation period and stays as a constant, μ is the commutation angle, and k is the coefficient that captures $di_d/d\theta$ during the averaging interval.

As AVM-2 has provided an explicit representation of i_d with respect of the time, a better accuracy is expected for the rectifier output voltage. With the new representation, the boundary conditions given in (2.4) can be updated correspondingly into:

$$
\begin{aligned}
i_{abc}\big|_{\theta_g=0} &= [0, i_{d0} - k\cdot\mu/2, -i_{d0} + k\cdot\mu/2] \\
i_{abc}\big|_{\theta_g=\mu} &= [-i_{d0} - k\cdot\mu/2, i_{d0} + k\cdot\mu/2, 0] \\
i_{abc}\big|_{\theta_g=\pi/3} &= [-i_{d0} - k(\pi/3-\mu/2), i_{d0} + k(\pi/3-\mu/2), 0]
\end{aligned}
\tag{2.12}
$$

Then the new formulation of $\bar{v}_d$ can be derived with the updated terminal current boundary conditions following the same procedure as AVM-1, which result in a new representation of DAE as:

$$
\frac{di_d}{dt} = \frac{\frac{3}{\pi}\sqrt{3}E - (R_{dc} + \frac{3}{\pi}L_c\omega_g)i_{d0} - v_{load}}{L_{dc} + L_c(2 - \frac{3\mu}{2\pi})}
\tag{2.13}
$$

where $\mu = \arccos(1 - 2L_c\omega_g i_{d0} / \sqrt{3}E)$

Compare (2.9) with (2.13), we could observe that the formulation of AVM-1 and AVM-2 are very similar with only different coefficient of the commutation inductance L_c. In another word, the improvement of AVM-2 approach is presented in the form of an additional inductance connected in series with L_c.

With the explicit form of averaged DC current, for AVM-1, the three-phase AC currents throughout the rectifier during the averaging interval can be established in d-q frame (the reference frame) as:

$$
\begin{aligned}
\bar{i}_q^r &= \bar{i}_{q,com}^r + \bar{i}_{q,cond}^r \\
\bar{i}_d^r &= \bar{i}_{d,com}^r + \bar{i}_{d,cond}^r
\end{aligned}
\tag{2.14}
$$

where the commutation and conduction component of the current can be found as:

$$
\begin{aligned}
\bar{i}^{r}_{q,com} &= \frac{2\sqrt{3}}{\pi}\bar{i}_d[\sin(\mu-\frac{5\pi}{6})+\sin(\frac{5\pi}{6})]\frac{3}{\pi}\frac{E}{L_c\omega_g}(\cos\mu-1) \\
\bar{i}^{r}_{d,com} &= \frac{2\sqrt{3}}{\pi}\bar{i}_d[-\cos(\mu-\frac{5\pi}{6})+\cos(\frac{5\pi}{6})]\frac{3}{\pi}\frac{E}{L_c\omega_g}\sin\mu-\frac{3E}{\pi L_c\omega_g}\frac{1}{2}\mu \\
\bar{i}^{r}_{q,cond} &= \frac{2\sqrt{3}}{\pi}\bar{i}_d[\sin(\frac{7\pi}{6})-\sin(\mu+\frac{5\pi}{6})] \\
\bar{i}^{r}_{d,cond} &= -\frac{2\sqrt{3}}{\pi}\bar{i}_d[\cos(\mu+\frac{5\pi}{6})-\cos(\frac{7\pi}{6})]
\end{aligned}
\tag{2.15}
$$

For AVM-2, similar formulations can be developed to capture the average line currents on the AC side. The detailed mathematical derivation process is not included here for simplicity and can be found in [56] and [62].

The accuracy of the reviewed average-value modeling methodologies have been verified with detailed computer simulations and hardware prototyping systems and proven to be able to capture the average-value system responses in both steady-state and under large-disturbances. It is generally reported in the literature that neglecting certain high-frequency elements may lead to certain degradation of model accuracy compared with hardware prototypes; however, it can significantly improve the simulation efficiency of power electronic systems. In the resulting AVM, the dynamics of the rectifier and DC-link are accurately described using a set of DAEs, which can then be easily utilized for mathematical implementation of time-domain simulations and other types of stability analysis.

2.4.2.2 Parametric approach

In parametric model [49], the inputs of the rectifier $\bar{v}_{abc}$ and $\bar{i}_{abc}$ are supposed to be connected to the outputs of the rectifier $\bar{v}_d$ and $\bar{i}_d$ with an algebraic block separately:

$$\begin{aligned} \bar{v}_{abc} &= \alpha(.)\bar{v}_d \\ \bar{i}_d &= \beta(.)\bar{i}_{abc} \end{aligned} \tag{2.16}$$

where $\alpha(.)$ and $\beta(.)$ are algebraic functions linking the input variables of the rectifier to the output variables.

In this representation the detailed formulation of $\alpha(.)$ and $\beta(.)$ are not required but as they may vary with operating conditions, the functions need to be extracted with repeated simulations and derived in the form of look-up tables. Parametric approach, compared with analytical approach, is considered to be more elegant, straightforward and easy to implement; however, it lacks the ability to support systematic studies and in order to get an accurate approximation of the algebraic function, a large number of repeated simulations under a variety of operating conditions are required beforehand. Weighing all the pros and cons, for this research work, we will focus on the analytical approach.

2.4.3 ESRDC suggested case studies

A series of case studies were suggested by ESRDC in [18] to assess the performance of the MVDC system under different scenarios. What of interest here is the set of case studies that require relatively short time scales (from μs to ms). They can be modified and adapted here to simulate the system dynamics, characterize the transient performance and evaluate the accuracy of the modeling strategy. Some of the representative case studies that are closely related to the dynamic study performed in this dissertation can be found as:

2.4.3.1 Scenario one: Load pick-up

Sudden connection of large load to ship grid such as a large uncontrolled motor or a pulse load directly connected to the grid, etc. The prime mover initially loaded around 50% and after connecting a large load, a certain percentage of power is added. Study of dynamics and transients during this process are suggested including deviations from nominal generator frequencies based on MIL standard 1399 and deviations from nominal main distribution bus voltage [65].

2.4.3.2 Scenario two: Load rejection

Study transient caused by sudden loss of large load that is triggered by load breakers trip.

2.4.3.3 Scenario three: Loss of generator

Study the transient caused by sudden loss of a generator under two cases:

- The remaining generation capacity is larger than connected loads
- The remaining generation capacity is less than the connected loads where load shedding is required

2.4.3.4 Scenario four: Power restoration to vital load(s)

One of two buses connected to a vital load supplying power is damaged. The second bus is already at full capacity supplying power to other interconnected loads. Non-vital loads are shed to preserve enough power for the vital load. Study of transients during the bus switching event and the estimated time required to restore the power are suggested.

Meanwhile, there also exist various case studies that are recommended for system-level studies include: power balance analysis, fuel consumption analysis, prime power optimization and reliability/survivability assessment. Of them the reliability assessment essentially solves the question that under given system topology and component settings, the proportion of the load that could be maintained following the event of system failures. As the system failure probability can be described with a probability distribution, the reliability of the system can also be accessed through quantitative indices to facilitate the early stage design.

2.5 MVDC Quality of Service (QoS)

In the previous chapters, we mainly focused on the evaluation of dynamic performance characteristics and the relative modeling strategy design. As a reference, in this chapter, we will briefly talk about the steady-state operation characteristics of MVDC SPS. Quality of Service (QoS) is introduced as one of the most important static criteria for SPS applications. QoS is defined in the form of reliability metric to quantize the ability of the system to supply power loads and fulfill their power requirements [1, 66]. The definition of the QoS metrics doesn't take into account survivability events as battle damage but does take into consideration of equipment failures and the transients caused by normal system operation.

From the QoS perspective, the ship may be operated under five different modes including: anchor, shore, cruising, functional, and emergency [67].

- Anchor: Also known as the minimum condition. This is the condition in which the ship supplies power while the ship is at anchor

- Shore: refers to the condition where the ship receives all the power from a shore facility
- Cruising: the ship cruises at a certain cruising speed, with reserved power for combat system
- Functional: the ship is performing certain functions under this condition. Common functions include: battle, air operation, store ships, repair, and etc.
- Emergency: ship is powered by the emergency generators/back-up power storage units with the service generators down

Accordingly, the power loads can be classified as: un-interruptible, short-term interruptible, long-term interruptible and exempt [1]. Load shedding is required to achieve QoS under adverse conditions including system failures or battle damages. Via the load shedding and other coordinated system reconfiguration, power supply to vital loads that of necessity of the specific operation can be maintained during and after the disturbances to avoid the QoS failure and by doing so, to enhance the system reliability.

Another criteria used to classify different categories of loads is the priority level. Priorities are determined based on the mode the ship is operating under. Commonly there are three types of priorities defined for SPS [68]:

1. Non-vital: load that can be immediately disconnected without adversely effecting ship operations.
2. Semi-vital: loads that are important but still can be shut down.
3. Vital: loads that affect the survivability of the ship which require continuous power supply and are not affected by the load shedding schemes.

These three categories of load priorities are being actively used in the current load shedding system of SPS. Other than the fixed priority levels commonly found in terrestrial power system, on board loads tend to change priorities depending the current operating conditions or the mission requirements.

A simple demonstration of priority level of loads under different ship operation mode is shown in the Table 2.2 [69].

Table 2.2 Example of Load priorities under different operation mode

Load Type	Ship operation mode	
	Cruise	Battle
Service loads	Semi-vital	Non-vital
Propulsion loads	Vital	Semi-vital
Weapon loads	Non-vital	Vital

2.6 Dynamic performance management for SPS

For MVDC system, stability problems are mainly associated with control functions and passive filter specifications [17]. Therefore in the existing literatures most of the researchers are focusing on the component level analysis and control designs. Relying on passive methods, it is expected to achieve the optimization of the dynamics of certain components or sub-areas without considering the over-all system-level responses. While management techniques for stability of conversional terrestrial power system have been well developed, for SPS very limited effort has been made towards the design of system-level dynamic management. Based on [25], the general requirement is that under normal conditions, the underlying power management framework could (re-)configure the system to provide sufficient power to all loads while preserve sufficient operation

margins to address possible load changes due to sudden events like pulse loads initialization and large motor starting.

2.6.1 Conventional DC Micro-grid control techniques

To damp the energy unbalance and to keep the oscillations of the main bus voltages within the safe limits or to eliminate it, in [70], a variety of solutions are proposed including the passive hardware structure modification approach including adding resistors, filters, energy storage elements and strategies that replying on control designs including linear/nonlinear controllers. The advantages and disadvantages are analyzed here respectively:

- Adding resistors: This is the most direct method to use extra resistors to dissipate energy in order to damp the oscillations; however, the contribution is proven to be insufficient by itself to achieve a stable operating point.
- Adding filters: stable operation can also be achieved by adding capacitance or reducing inductance. The latter is usually impractical in applications while the former results in the addition of large amount of capacitance. However, this method is greatly constrained when it comes to the shipboard power system where the physical size and weight of capacitance matters. Another concern with the employment of expensive large capacitors is that they have relatively low reliability for both short time operation and long term maintenance.
- Adding energy storage device: adding bulk energy storage unit like batteries, ultra-capacitors that acts as an extension to the previous

approaches and can help damp the oscillations. However, for a DC network, this solution is only considered effective when the storage devices to work effectively, they have to be connected directly to the main DC bus without intermediate power converter interfaces. Direct connections would raise issues like voltage equalizing and potentially compromise the reliability and safety of the system. The storage devices are also expensive to install and operate with.

- Linear controller: linear controller is considered as the simplest strategy to regulate DC voltage at the main bus. Those PID type controller is designed to control the duty cycle of the interface converter based on the state-space system representations in order to achieve the optimal voltage regulation. In contrast with previous passive methods, linear controllers have advantages like simplicity and effectiveness, but it has been indicated that linear controllers cannot guarantee global stability of the desired equilibrium point.

While most control designs reviewed here have been examined against simulation and hardware prototyping and proven to be effective, they are still insufficient for a system-level design due reason including: 1) the algorithms are pre-specified and can only handle specific situations. They lack the ability to communicate and coordinate for system-wide management; 2) most of the designs are based on the state space representation of the system which yields the solution in the form of "domain attraction", i.e. the safe region of operation. They do not provide direct information with regards to the detailed performance evaluation. Time-domain analysis is still required to be

repeatedly performed in order to examine the control design based on the metrics in Table 2.1.

2.6.2 Reconfiguration and restoration for SPS

Reconfiguration process for shipboard power system reroutes the electric power in order to achieve various objectives including maximizing service restoration, minimizing power loss and optimizing power dispatch. Reconfiguration has also been proven to be an effective solution on the reliable operation of power system at the post-disturbance stage [71]. It is no longer only an emergency solution to isolate the areas affected by contingency and to solve the post-disturbance system topology energy distribution scheme, but also an integrated global solution that can be utilized to optimize the system resources distribution and the electrical plant performance [72, 73]. However, reconfiguration unavoidably changes the original topology of the system with the switching on and off of circuit breakers, bus transfers and low voltage protective devices and these changes may cause the system in transition towards instability as the system dynamics are trigged [74].

Previous research conducted in the reconfiguration area mainly focuses on the static system performance with regards to certain optimization functions [72, 73, 75]. There is yet no salient research effort on the dynamic behavior of SPS under disturbance or operating status change. In most of the research work based on static analysis, it is just assumed that the system can reach a post-disturbance stable operating equilibrium and the reconfiguration process will not affect the safety/security operation margin [67, 73]. However, for SPS, this is not necessarily true. Some other techniques have been proposed to increase the voltage stability margin by taking into consideration of reconfigurable

reactive power control planning in the post-contingency stage [76-79]. However, those techniques are generally developed for terrestrial system and ordinary mathematical expediencies like "slack bus" or "infinite bus" are assumed to be valid in the formulation of power flow calculations [79]. In some of those approaches, the installation locations of costs of reactive power adjustment devices are considered as an important factor and the control objective is normally set as long-term voltage stability [76-78]. Those assumptions and design considerations are not always valid when it comes to naval SPS. Reconfiguration approach designed specifically for MVDC zonal loads can be found in [80, 81]; however, the objectives of those approaches fall in the category of static performance optimization including power loss minimization, optimal power dispatch and fuel economization. The authors in [82] provided some valuable insight into the SPS dynamic reconfiguration with an analytical basis for evaluation of stability margin using Lyapunov's energy functions, but it has not present a detailed control framework to work with this approach. Therefore a novel detailed dynamic analysis of the post-disturbance system behavior and the corresponding reconfiguration process that specially targets at SPS needs to be carefully invested for reliability enhancement.

2.6.3 Load shedding for SPS

When a power system is working in stable status at normal frequency, the total mechanical power input from the turbines to the synchronous machines should be equal to the total power consumption of all the running loads plus the transmission losses. Therefore, the balance between power supplied by the generator's prime mover, in our case the gas turbine, and the power consumed by loads plays an important role in maintaining the normal system frequency and overall stability. In case of mild overload

or gradual load increase, the speed governor of the gas turbine senses the power demand change, then increases the rotor speed to increase the power supply accordingly. However, if all the generators are already at full capacity and the spinning reserve is zero, it is necessary to automatically and rapidly disconnect a portion of the load equal to or greater than the generation deficiency to achieve power balance and maintain system stability.

In other cases which include sudden or large changes like loss of generator or pulse-load startup, the generator frequency would decline rapidly which puts the system at risk (a typical protective low-speed trip on gas turbine is set at 96% of the nominal system frequency). Under this circumstance, proper actions to disconnect load need to be taken immediately as well to mitigate the effect and drive system away from collapse and hazardous states. This is called Load Shedding. Load shedding is closely related to the QoS study that is previously mentioned in Section 2.5 as for the low-priority loads are always expected to be shed first while high-priority loads need to get continuous electrical power supply.

Based on the discussion above, an automatic and efficient load shedding system is necessary for shipboard power system as the disturbance usually happens too fast for the human operator to react. The load shedding system is responsible to generate a system level scheme which specifies the disconnection of selected loads from the main distribution network in a fast and reliable manner to optimize the overall system performance especially during the transient phase.

Based on the existing literature, current available onboard load shedding practices are normally achieved using the following approaches [83]:

2.6.3.1 Circuit breaker based/ Under-frequency/Under-voltage load shedding

Those approaches are well developed for large utility system and have been widely employed to handle load shedding. Circuit breaker based approach is the basic type of load shedding. For this scheme, the circuit breaker interdependencies are pre-arranged and the sequence of circuit-breaker tripping is hardwired. Once the load shedding sequence is triggered, loads will be shed instantaneously based on the present sequence. This scheme is considered to be the most straightforward and efficient approach. However, it also has a number of inherent drawbacks such as [83]: in most of the scenarios, more loads are shed than required as the scheme only has one-stage of operation based on the worst scenario, as the circuit-breaker interdependencies are hardwired it is also expensive to modify the design for different applications. For Under-frequency/voltage load shedding, the guideline is to reduce fixed amount of load based on a system frequency/voltage levels. Once the system frequency/voltage set-point is reached, the corresponding relay trips one or more load breakers at a time to reduce the load consumption. This process is performed within programming logic controllers (PLCs) and will be repeated until enough loads are tripped and the frequency deficiency caused by the power imbalance is recovered. A typical example of under-frequency load shedding scheme is that: for every 1% frequency reduction, shed 10% of the total load. Compared with basic circuit-breaker based scheme, under-frequency replay based load shedding is more flexible and adaptive for different operation scenarios with the consideration of the global system configuration and the utilization of the knowledge of load priority levels; however, as the scheme comes in the form of a set of programmed relay settings, its drawbacks are also quite obvious: highly trial and error based, slow

response time, inaccurate load shedding, lack of knowledge to the system-wide working conditions, dynamics and etc.

2.6.3.2 Intelligent automatic load shedding [68]

An intelligent real-time load shedding scheme for SPS is proposed in [68]. In contrast with the conventional load shedding schemes, it is more "intelligent" as it can formulate the load priority levels based on various operating conditions and the undergoing missions. The system critical natures of loads including inrush currents, harmonics injection, power factors, restoration time and cost are also taken into consideration of the decision making process of load shedding. A dynamic database that updated based on system state information include mission, load info, connectivity, switch status is utilized by the load prioritization module which prioritizes the load. This generated priority list is then sent to the "expert control actions module" which decides the loads to be shed based on the static objective like least number of control actions taken, maximizing system benefits and minimum load curtailment. This approach is essentially a multi-objective optimization problem.

Another SPS load shedding scheme can be found as in [84]. Similar to the previous scheme, the system information is gathered within a central database including the operating conditions like power consumptions, current drawn, harmonics and etc. Based on the collected information, a dynamic priority list is generated and sent for execution.

Intelligent dynamic load shedding is a great improvement over the fixed schemes. Although no effort has been made so far to perform the load shedding for the dynamic performance optimization, it is considered as a promising strategy.

2.6.4 Other management techniques

Other voltage regulation and voltage stability protection methods have been proposed for terrestrial power system and SPS [85-87]. They aim at detecting potential instability or safety degradation of the power system and perform corresponding management actions to mitigate the effects. The stability protection schemes are based on offline-calculation and essential rule-based. A rule-based management scheme monitors bus voltage measurements and their rates of change to trigger the control actions. It heavily relies on the off-line calculations therefore lacks flexibility. Besides that, the majority of traditional voltage management strategies only consider a single control approach, such as generator voltage settings, transformer tap settings, capacitor switching and load shedding separately. The discrete nature of control actions are only considered in very few literature [88, 89]. In [90-92], automatic voltage regulators (AVRs), power system stabilizers (PSSs) and speed governors have also been considered to be used for voltage stability enhancement. Those controllers fall in the category of uncoordinated single-input and single-output controllers and the control actions are determined solely based on the local measurement of system states. No extra data transmission is required. This approach has been approved to be effective for local control in most cases; however, it is also highly conservative as no interconnections are considered. At the same time, even those control components could be very well-tuned; there is no guarantee that they can handle any possible disturbances.

For a highly-nonlinear and complex system like SPS, design approaches that based on pre-specified plans are inflexible and not adapt well to constantly varying operating conditions [93].

2.7 Multi-objective optimization

Multi-objective optimization (MOO) involves the solving more than one objective function simultaneously in decision-making and design situations. A survey of common multi-objective optimization methods for engineering can be found in [94, 95] and mainly in book [96]. A general multi-objective optimization problem can be defined as:

$$\text{Minimize } F(x) = [F_1(x), F_2(x), \ldots F_k(x)] \tag{2.17}$$

subject to:

$$h_i(x) = 0 \;\; i = 1, 2, \ldots m \tag{2.18}$$

and

$$g_j(x) \le 0 \;\; j = 1, 2, \ldots n \tag{2.19}$$

where k indicates the total number of objective functions. $h_i(x)$ and $g_j(x)$ are used to represent the existing constraints for the optimization problem.

Objectives considered in the multi-objective optimization problem, i.e. $F_1(x), F_2(x), \ldots F_k(x)$ are often conflicting with each other, therefore the solution needs to take into consideration of the scaling of each objective based on design preferences while satisfying all of the constraints. A common example for multi-objective optimization for SPS is to maximizing the cruise speed while minimizing the fuel consumption and minimizing the power losses within the system. As the formulation of this type of optimization problem depends on varying operating conditions and involves system-wide consideration of relative constraints, it has caused difficulties for conventional single-objective control designs.

As MOO inherently contains multiple different mathematical objectives that may have different units or different orders of magnitude, in order to accurately compare the priorities of those objectives and make decisions based on a global basis, it is critical that objectives involved in a MOO problem to be transformed into unitless forms and possess similar orders of magnitudes [96].

2.8 Model predictive control

With the advance in control and mathematical programming techniques, Model Predictive Control (MPC) technique has made the design of an automated and efficient performance management framework for power system possible. Since the first introduction during the 60s of the last century, MPC has become more and more popular with both control theorists and control practitioners. The interest of applying MPC in industrial practice is constantly driven by the fact that today's system is more complex than ever, therefore it is more difficult to maintain the system in admissible operating region with tight performance specifications while satisfying a variety of regulations and constraints due to environmental, productivity and safety considerations. MPC, also referred to as moving horizon control or receding horizon control, has proven to be a well-suited approach to solve this category of problems.

In general case, when used in electrical power system, MPC refers to a class of algorithm that predict a sequence of future system states based a manipulated control input adjustment, dynamic model of the system, and the current system states, then choose the control input that result in the optimized future system states. The use of MPC to achieve automatic self-managing has attracted a lot of interests in both academia and the power industry. A detailed review and formulation of MPC theory can be found in

[26, 97, 98]. MPC, as an effective control technique, has been used in a wide range of industrial applications. MPC is suitable for circumstances where:

- Complex processes that are difficult to control with standard PID algorithm
- Multiple inputs with strong impacts on the system state evolution
- Flexible objective and time-varying constraints

It can be seen that MPC has provided an optimal solution for multi-objective optimization problem as mentioned in the previous section. The general idea behind MPC is shown in Figure 2.10.

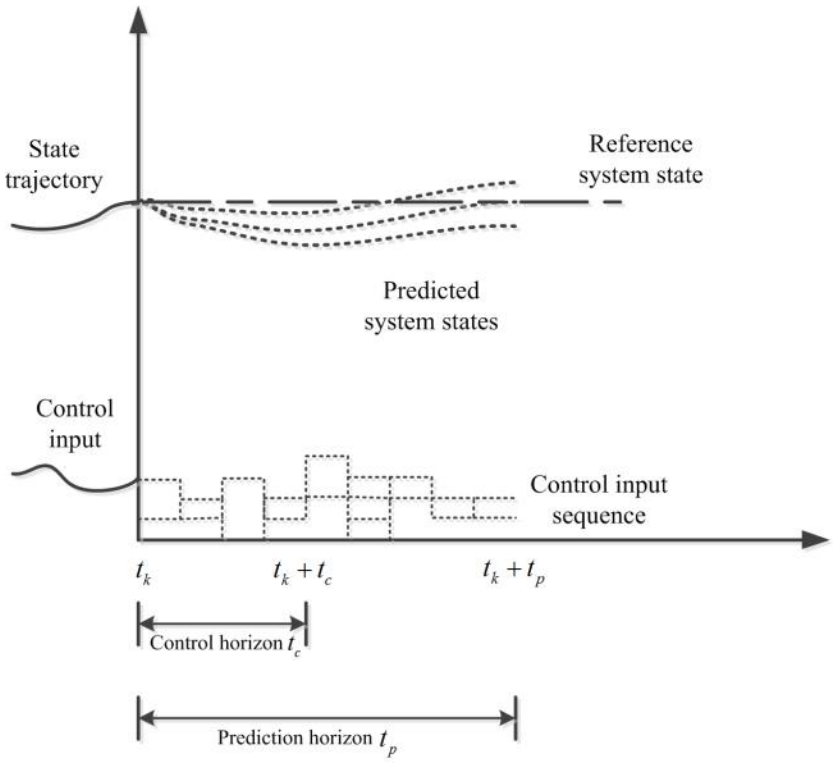

Figure 2.10 General principle of MPC [99]

A model predicative controller uses the system model to predict the future system trajectories (dotted lines) over a prediction horizon t_p based on the current system operating point x_0 which can be measured at time t_k and an accurate numerical system model [99].Based on the estimated future system states, an optimization solver determines the control over the control horizon t_c ($t_c \le t_p$) such that a predetermined performance objective function is optimized in over the prediction horizon. Assumed that there is not model mismatch and the optimization problem can be solved, then the derived control input can be applied at time t_k. The prediction cost function $J(x,u)$ can be referred to the deviation of each predicted trajectory from the reference system trajectory (dashed line).This process is repeated with the control and prediction horizon moving forward. The problem can be formulated in the form of:

$$\min \ J(x,u) \tag{2.20}$$

subject to $u \in U$, and $x \in X$ where U and X indicate the set of feasible input values and system states.

The key advantages of such a framework can be summarized as [93]:

- A variety of explicit performance control objectives as well as constraints of inputs and states can be combined and considered simultaneously within the same framework
- The management structure and the control solution is highly generic and abstracted, therefore it can be applied to a wide range of system structures, specifications, operating conditions and constraints

- Capability of handling the control design for non-linear and complex system models accurately and efficiently

There also exist a series of concerns about MPC techniques, mainly on the stability of the control scheme. As being pointed out the previous discussion, the optimization is made based on the assumption that the numerical system model used for prediction is always accurate and the predicted system states that derived from "open-loop" iterations. However, in general practice, the estimated open-loop system performance may not completely match with the corresponding close-loop response, therefore the stability of the MPC scheme as well as the model/plant mismatch need to be carefully evaluated especially when the prediction/control horizons are relatively long.

Another concern about MPC is the performance of the calculation. Ideally, one would want to extend the prediction horizon into infinite but this is impractical due to the fact that the open-loop optimal control problem cannot be solved sufficiently fast. From the computation effort point of view, short horizons are more desirable although long horizons are desired with from the performance point of view. The efficiency of the strategy much be taken in consideration when formulating the optimization problem.

More in-depth analysis of MPC design concept and relative problem formulation process can be found in Chapter IV.

2.9 Contributions

Compared with existing literature, the main contributions of this work include:

Overall, a novel dynamic performance management framework that developed specifically for MVDC shipboard power system is proposed. With the utilization of average-modeling techniques and model-based predictive control strategies, this

management framework is capable of performing effective and efficient dynamic management to optimize the system behavior during the transient phase caused by disturbances and other dynamic events; therefore enhancing the overall stability and reliability of the MVDC system. The detailed contributions included in this work can be listed as:

Contribution towards power system modeling and simulation:

- In order to develop an accurate baseline numerical model to facilitate the proposed dynamic management framework design, the latest MVDC shipboard power system architecture and its notional functional breakdowns are reviewed in details with their exclusive modeling requirements respectively.
- A highly simplified modeling strategy for MVDC SPS is developed in the form of Differential Algebraic Equations (DAEs) to evaluate the system-level dynamics. Compared with existing techniques and modeling approaches, it is more accurate and time efficient for the purpose of system level studies
- The presented modeling approach can be used as a convenient simulation tool for other research and application designs on shipboard DC power systems. The same modeling principle can be expanded for studies of short-term stability, governor and load control design, or even long term dynamics by including the appropriate level of details of the corresponding components.

Contribution towards model-based performance management and system optimization:

- A dynamic performance management system which targets at various classes of optimization problems is proposed in this dissertation. Compared with human operators and rule-based/strategy-based management system. It is able to automatically handle system dynamic responses triggered by faults, damages or other disturbances during the transient phase and by doing so, enhancing the over-all reliability of the MVDC system.
- The proposed framework has the capability of including a flexible multi-objective performance criteria, so compared with conventional dynamic control solutions that are fixed for certain specific objectives and missions, it can be flexibly used to manage the global system dynamics subjected to varying operating conditions, optimization criteria and real-time constraints
- This framework can also be integrated with other power management schemes, e.g. static system performance manager including fuel consumption optimization and QoS maintaining for the overall system reliability operation.

Contribution towards tool development/Software application design:

- A component based software environment has been designed for effective and automated implementation of the proposed management system

including system schematic design and control solution synthesis for SPS applications

- The proposed simulation and modeling environment is proven to be capable of cooperating with other power system simulators/hardware prototype benchmarks to make this tool flexible for different applications and different types of analysis.

CHAPTER III

SPS MODEL FORMULATION

3.1 Introduction

In this section, the modeling strategies for every function module as listed and reviewed in Chapter II are illustrated respectively. As a general modeling principle, power systems can be described by a set of parameter-dependent differential algebraic equations (DAEs) in the form of [100]:

$$\begin{aligned} \dot{x}(t) &= f(t, x(t), y(t), u) \\ 0 &= g(t, x(t), y(t), u) \end{aligned} \tag{3.1}$$

where x is the vector of continuous differential state variables for which the derivatives are present (in the form of $\dot{x}$), such as generator rotor angles and speed. y is the vector of algebraic variables like voltage magnitude and phase angles for which no derivatives are present, and u denotes the vector of discrete or continuous control input variables. x and the function f determine the differential attributes of the system while y and g determine the algebraic attributes. The term algebraic refers free of derivation and can be seen as a general representation of constraints applied to the found solution of f. While most power systems include SPS are non-linear, from the stability perspective, they are essentially time-invariant as the system's properties vary with the system states, not the time. In this case, the system representation can be simplified in the form of:

$$\dot{x}(t) = f(x(t), y(t), u)$$
$$0 = g(x(t), y(t), u) \tag{3.2}$$

In this chapter, the detailed MVDC system model will be derived and represented in the form of (3.1) to facilitate the analysis and control design in the following chapters.

3.2 System model formulation

Based on the review with regards to the modeling strategy in Chapter II, to study the influence of control techniques on the dynamics of shipboard power system, a scaled but representative model needs to be developed. This model should be abstracted and different than the conventional simulation-oriented power system model. At the same time, it needs to capture the dynamic behavior accurately to provide valuable insight into the transient phenomenon for the control framework design.

3.2.1 Power generation modules

Based on the previous discussion, an onboard generator module has essential elements including a prime mover (gas turbine), a field exciter, a synchronous machine and a three-phase diode rectifier.

While the prime mover and exciter play important roles on the synchronous machine operation, this process tend to have significantly larger time constants compared with the frequency range of interest. In another word, the turbine control units and the field excitation control loops are much slower compared with the time frame of interest. For example, the gas turbines, represented in the form of a set of transfer functions, have been reported to have an average of 8-10 seconds time constant due to the ignition delay and mechanical constant [21, 101]. The same situation applies to the excitation control loop due to the generator inertia. In this case, the full dynamics of those components do

not play an important role when it comes to the performance evaluation from the system-level perspective. Therefore, in order to simplify the simulations the corresponding excitation system and gas turbine transfer functions are modeled by means of constant values. Notice here the assumption is only suitable for the purpose of this particular design and frequency range. It may not be valid for other applications.

Based on the existing AVM techniques reviewed in Chapter II, the conventional dynamic average modeling technique can be modified and extended for the development of a synchronous machine fed load-commutated converter system. To start the discussion, it is good to first review the basic representation of the averaged DC voltage output:

$$\overline{v}_d = \frac{3}{\pi}\int_{\frac{\pi}{3}}^{\frac{2\pi}{3}} [(v_{bg} - v_{cg})]d\phi + \frac{3}{\pi} L_c \omega_g (i_b - i_c)\Big|_{\frac{\pi}{3}}^{\frac{2\pi}{3}} \tag{3.3}$$

With the synchronous machine as the voltage source, v_{ag}, v_{bg} and v_{cg} can no longer be approximated as an ideal three-phase balanced power source. Instead, they need to be expressed based on the dynamic relationship of the corresponding machine fluxes and currents. Notice that all the state variables that are related the synchronous machine will be represented in the classic d-q rotor reference frame which can be converted from three-phase domain using Park's Transformation (PT) as:

$$f_{qd0} = K_r(\phi) \cdot f_{abc} \tag{3.4}$$

where ϕ denotes the instantaneous rotor displacement angle and f denotes quantities like voltage, current or flux linkages. The transformation matrix K_r is defined as:

$$K_r = \frac{2}{3}\begin{bmatrix} \cos\phi & \cos(\phi - 2\pi/3) & \cos(\phi + 2\pi/3) \\ \sin\phi & \sin(\phi - 2\pi/3) & \sin(\phi + 2\pi/3) \\ 1/2 & 1/2 & 1/2 \end{bmatrix} \tag{3.5}$$

Similarly, to convert variables d-q frame back to three-phase domain, the Inverse Park Transformation (IPT) can be defined as:

$$f_{abc} = K_r^{-1}(\phi) \cdot f_{qd0} \tag{3.6}$$

$$K_r^{-1} = \begin{bmatrix} \cos\phi & -\sin\phi & 1 \\ \cos(\phi - 2\pi/3) & -\sin(\phi - 2\pi/3) & 1 \\ \cos(\phi + 2\pi/3) & -\sin(\phi + 2\pi/3) & 1 \end{bmatrix} \tag{3.7}$$

Particularly for this work, as the neutral connection is not presented, it can be assumed that f_0 is always zero and can thus be neglected.

To continue the analytical derivation, the detailed synchronous machine (SM) dynamic model in the form of DAE equations is necessary to determine the ever-changing stator outputs. A standard dynamic SM model [13, 102] is used here. In the subsequent development, the basic definitions and parameters in Table 3.1 are defined for the SM model.

Table 3.1 Parameters for the SM model (in p.u.)

Stator resistance: r_s	d-axis damper resistance: r_{1d}	Field resistance: r_{fd}	Load torque: T_M (N.m)
Stator leakage inductance: L_s	d-axis damper leakage inductance: L_{1d}	Field winding leakage inductance: L_{fd}	Electromagnetic torque: T_E (N.m)
Direct-axis magnetizing inductance: L_{md}	q-axis damper resistance: r_{1q}	Base speed: ω_g (rad/s)	Machine rotor angular speed: ω_r (rad/s)
Quadrature-axis magnetizing inductance: L_{mq}	q-axis damper leakage inductance: L_{1q}	Rotor (Load) angle: ϕ (rad)	Inertia constant: H

To start with, within the stator the basic representation of the relationship among flux linkage (λ), stator voltage (u) and the stator current flowing (i) in the reference frame can be written as:

For stator voltage:

$$\begin{aligned} v_d^r &= r_s i_d^r - \omega_g \lambda_q + d\lambda_d / dt \\ v_q^r &= r_s i_q^r + \omega_g \lambda_d + d\lambda_q / dt \end{aligned} \tag{3.8}$$

for rotor voltage:

$$\begin{aligned} v_{fd} &= r_{fd} i_{fd} + d\lambda_{fd} / dt \\ v_{1d} &= r_{1d} i_{1d} + d\lambda_{1d} / dt \\ v_{1q} &= r_{1q} i_{1q} + d\lambda_{1q} / dt \end{aligned} \tag{3.9}$$

where it is assumed that the damper windings are shot circuited so $v_{1d} = v_{1q} = 0$

The relationships between d-axis and q-axis stator/rotor flux linkages and currents:

$$\begin{aligned} \lambda_d &= L_s i_d^r + \lambda_{md} \\ \lambda_q &= L_s i_q^r + \lambda_{mq} \end{aligned} \tag{3.10}$$

$$\begin{aligned} \lambda_{1d} &= L_{1d} i_{1d} + \lambda_{md} \\ \lambda_{1q} &= L_{1q} i_{1q} + \lambda_{mq} \\ \lambda_{fd} &= L_{fd} i_{fd} + \lambda_{md} \end{aligned} \tag{3.11}$$

The mutual flux linkages can be described as:

$$\begin{aligned} \lambda_{md} &= L_{md}(i_d^r + i_{1d} + i_{fd}) \\ \lambda_{mq} &= L_{mq}(i_q^r + i_{1q}) \end{aligned} \tag{3.12}$$

The mechanical part of the generator can be represented as:

$$\begin{aligned} \dot{\phi} &= \omega_r - \omega_g \\ \dot{\omega}_r &= (T_M - T_E)\omega_g / 2H \\ T_E &= \lambda_d i_q^r - \lambda_q i_d^r \end{aligned} \tag{3.13}$$

With the assumptions made in (2.4) and (2.6), the second part of (3.3) can be rewritten in a similar manner. We can define that:

$$i_{abc}(\frac{\pi}{3}) = \begin{bmatrix} -\bar{i}_d \\ 0 \\ \bar{i}_d \end{bmatrix} \quad \text{and} \quad i_{abc}(\frac{2\pi}{3}) = \begin{bmatrix} 0 \\ -(\bar{i}_d + \Delta\bar{i}_d) \\ \bar{i}_d + \Delta\bar{i}_d \end{bmatrix} \tag{3.14}$$

Therefore, the remaining question is how to solve the first half of the equation with the given boundary condition. The detailed derivation is demonstrated as follow. Neglect the stator resistance, the stator voltages and stator flux linkages can be represented as:

$$\begin{bmatrix} v_{ag} \\ v_{bg} \\ v_{cg} \end{bmatrix} = \begin{bmatrix} \lambda_a / dt \\ \lambda_b / dt \\ \lambda_c / dt \end{bmatrix} \tag{3.15}$$

Substituting (3.15) into the first half of (3.3) yields

$$\overline{v}_d = \frac{3}{\pi} \omega_r (\lambda_b - \lambda_c) \Big|_{\frac{\pi}{3}}^{\frac{2\pi}{3}} + s.h \tag{3.16}$$

So now the problem becomes: finding the value of the expression $\lambda_b - \lambda_c$ at time instant $\frac{\pi}{3}$ and $\frac{2\pi}{3}$.

At time $\phi = \frac{\pi}{3}$, apply IPT and we could derive that:

$$\begin{aligned} \lambda_b(\frac{\pi}{3}) &= \frac{1}{2}\lambda_d(\frac{\pi}{3}) + \frac{\sqrt{3}}{2}\lambda_q(\frac{\pi}{3}) \\ \lambda_c(\frac{\pi}{3}) &= -\lambda_d(\frac{\pi}{3}) \end{aligned} \tag{3.17}$$

Thus, $\lambda_b(\frac{\pi}{3}) - \lambda_c(\frac{\pi}{3})$ can be represented as:

$$\lambda_b(\frac{\pi}{3}) - \lambda_c(\frac{\pi}{3}) = \frac{3}{2}\lambda_d(\frac{\pi}{3}) + \frac{\sqrt{3}}{2}\lambda_q(\frac{\pi}{3}) \tag{3.18}$$

Apply PT, the stator current in the rotor frame can also be evaluated based on the three phase current variable as shown in (3.14):

$$i_d^r(\frac{\pi}{3}) = -\overline{i}_d ; i_q^r(\frac{\pi}{3}) = \frac{\sqrt{3}}{3}\overline{i}_d \tag{3.19}$$

Similarly at time $\phi = \frac{2\pi}{3}$, apply IPT and the flux linkage can be represented as:

$$\lambda_b(\frac{2\pi}{3}) = \lambda_d(\frac{2\pi}{3})$$
$$\lambda_c(\frac{2\pi}{3}) = -\frac{1}{2}\lambda_d(\frac{2\pi}{3}) + \frac{\sqrt{3}}{2}\lambda_q(\frac{2\pi}{3}) \tag{3.20}$$

Thus,

$$\lambda_b(\frac{2\pi}{3}) - \lambda_c(\frac{2\pi}{3}) = \frac{3}{2}\lambda_d(\frac{2\pi}{3}) - \frac{\sqrt{3}}{2}\lambda_q(\frac{2\pi}{3}) \tag{3.21}$$

For the stator current, we can have:

$$i_d^r(\frac{2\pi}{3}) = -(\bar{i}_d + \Delta\bar{i}_d); i_q^r(\frac{2\pi}{3}) = \frac{\sqrt{3}}{3}(\bar{i}_d + \Delta\bar{i}_d) \tag{3.22}$$

with $\Delta\bar{i}_d = \frac{\pi}{3\omega_g}\frac{d\bar{i}_d}{dt}$

After considerable mathematical manipulation, the solution to (3.3) can be expressed as:

$$\bar{v}_d = -\frac{3\sqrt{3}}{\pi}\omega_r(L_{mq}\cdot i_{1q}) - \frac{3}{\pi}\left[\omega_r(L_s + L_{mq}) + L_c\omega_g\right]\bar{i}_d - \left[\frac{\omega_r}{\omega_g}(2L_s + \frac{1}{2}L_{mq} + \frac{3}{2}L_{md}) + 2L_c\right]\frac{d\bar{i}_d}{dt} \tag{3.23}$$

From the discussion, it can be observed that if i_q^r and i_d^r are considered known, and the detailed form of i_{1q} and ω_r can be derived, then the differential equation (3.23) could be solved. In order to solve the value of i_{1q} and ω_r which is the directly generated from the generator DAE set. Combine the aforementioned equations, the differential and algebraic variables can be determined respectively as:

$$x = [\lambda_{fd}, \lambda_{1d}, \lambda_{1q}, \omega_r, \phi]$$
$$y = [\lambda_d, \lambda_q, i_{fd}, i_{1d}, i_{1q}] \tag{3.24}$$

With f as:

$$\begin{cases} \dot{x}_1 = \omega_g \cdot (-r_{fd} \cdot y_3 + v_{fd}) \\ \dot{x}_2 = \omega_g \cdot (-r_{1d} \cdot y_4) \\ \dot{x}_3 = \omega_g \cdot (-r_{1q} \cdot y_5) \\ \dot{x}_4 = [T_M - (y_1 i_q^r - y_2 i_d^r)]\omega_g / 2H \\ \dot{x}_5 = x_4 - \omega_g \end{cases} \tag{3.25}$$

and g as

$$\begin{cases} x_1 = L_{fd} y_3 + L_{md}(i_d^r + y_4 + y_3) \\ x_2 = L_{1d} y_4 + L_{md}(i_d^r + y_4 + y_3) \\ x_3 = L_{1q} y_5 + L_{mq}(i_q^r + y_5) \\ y_1 = L_s i_d^r + L_{md}(i_d^r + y_4 + y_3) \\ y_2 = L_s i_q^r + L_{mq}(i_q^r + y_5) \end{cases} \tag{3.26}$$

This ODE set can be solved over a small time span $[t_{current}, t_{current} + t_s]$ with the latest system state variables and the current input variables including i_d^r, i_q^r, v_{fd}, and T_M. The output from the ODE include the rotor angular speed ω_r and the rotor q-axis current i_{1q}. This process can be implemented in Matlab using:

$$[t, x_{t+1}] = ode23(@DAE, tspan, x_t, DAE\_options) \tag{3.27}$$

The terminal voltage can then be derived based on the output of this DAE.

Considering the voltage drop caused by the stator resistor, the final differential equation can be derived as:

$$\bar{v}_d = -\frac{3\sqrt{3}}{\pi}\omega_r(L_{mq}\cdot i_{1q}) - \frac{3}{\pi}\left[\omega_r(L_s + L_{mq}) + L_c\omega_g\right]\bar{i}_d - 2r_s\bar{i}_d - \left[\frac{\omega_r}{\omega_g}(2L_s + \frac{1}{2}L_{mq} + \frac{3}{2}L_{md}) + 2L_c\right]\frac{d\bar{i}_d}{dt} \quad (3.28)$$

Notice that in (3.28), if we assume that $E_{equv} = -\omega_r L_{mq} i_{1q}$, $L_{cr} = \omega_r(L_s + L_{mq}) + L_c\omega_g$, and $L_{cl} = \frac{\omega_r}{\omega_g}(2L_s + \frac{1}{2}L_{mq} + \frac{3}{2}L_{md}) + 2L_c$, then (3.28) can be rewritten in a more simplified form as:

$$\bar{v}_d = \frac{3\sqrt{3}}{\pi}E_{equv} - (\frac{3}{\pi}L_{cr} + 2r_s)\bar{i}_d - L_{cl}\frac{d\bar{i}_d}{dt} \quad (3.29)$$

Similar forms of numerical models describing the characteristics of a machine fed rectifier system can be found in [57-59]. The model proposed in the existing literature is formulated using the form of sub-transient reactance X_d'' to represent the machine dynamics. This approximation could work as the commonly assumed "sub-transient dynamics" include the dynamic phenomenon of interest with regards to the system level study. However, the sub-transient reactance representation is limited to a specific stage of the system transient responses. Therefore the proposed modeling strategy of the LCC system provides a more generic representation that is desirable to capture the system states during every stage of the transient period. It can be seen as an extension to the existing modeling formulation, but with the improvement on capturing the complete transient machine dynamics during the time range of interest. Meanwhile, the calculation of the proposed approach is very straightforward and no additional mathematical manipulation or variable conversion is necessary. Considering the DC link dynamics which can be described as:

$$\bar{v}_d = R_{dc}\bar{i}_d + L_{dc} \cdot d\bar{i}/dt + v_{load} \tag{3.30}$$

Combine (3.28) with (3.30), we can now have the complete representation of the power generation module as:

$$\frac{d\bar{i}_d}{dt} = \frac{\frac{3\sqrt{3}}{\pi}E_{equv} - v_{load} - (\frac{3}{\pi}L_{cr} + 2r_s + R_{dc})\bar{i}_d}{L_{cl} + L_{dc}} \tag{3.31}$$

One interesting factor of this representation is that it is in a very similar form compared with (2.9), where the ideal three-phase voltage magnitude E is replaced by the equivalent stator flux linkages E_{equv} and the constant phase frequency ω_g is replaced by the rotor angular speed of the SM ω_r. This representation is denoted as the "*dynamic model*."

Now, the dynamic DC-link model can be used to approximate the behavior of the load-commutated synchronous machine systems. The concept of the proposed *dynamic model* can be represented in Figure 3.1. An equivalent circuit representation of Equation (3.29) is shown in Figure 3.2.

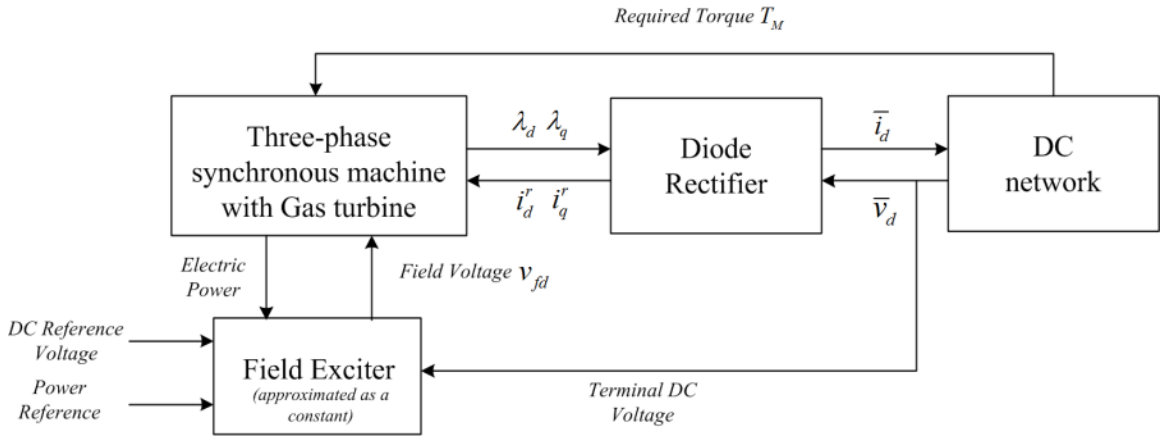

Figure 3.1 Concept diagram of the proposed average value model

Similar to (2.14), the commutation angle and the stator currents on the AC side can be derived from (3.29) as:

$$\mu = \arccos(1 - 2L_{cr}\omega_r \bar{i}_d / \sqrt{3}E_{equv}) \tag{3.32}$$

and the AC side current components can be derived as

$$\begin{aligned}
\bar{i}_{q,com}^r &= \frac{2\sqrt{3}}{\pi}\bar{i}_d[\omega_r(L_s + \frac{1}{2}L_{mq} + \frac{3}{2}L_{md})\sin(\mu - \frac{4\pi}{3}) + \\
&L_c\omega_g \sin(\frac{4\pi}{3})]\frac{3}{\pi}\frac{E_{equv}}{L_{cr}\frac{\omega_r}{\omega_g} + \frac{1}{2}L_{cl}}(\cos\mu - 1) \\
\bar{i}_{d,com}^r &= \frac{2\sqrt{3}}{\pi}\bar{i}_d[-\omega_r(2L_s + \frac{1}{2}L_{mq} - \frac{3}{2}L_{md})\cos(\mu - \frac{4\pi}{3}) + \\
&L_c\omega_g \cos(\frac{4\pi}{4})]\frac{3}{\pi}\frac{E_{equv}}{L_{cr}\frac{\omega_r}{\omega_g} - \frac{1}{2}L_{cl}}\sin\mu - \frac{3E_{equv}}{\pi L_{cr}\omega_g}\frac{1}{2}\mu \\
\bar{i}_{q,cond}^r &= \frac{2\sqrt{3}}{\pi}\bar{i}_d[\omega_r(L_s + L_{mq})\sin(\frac{2\pi}{3}) - L_c\omega_g \sin(\mu + \frac{2\pi}{3})] \\
\bar{i}_{d,cond}^r &= -\frac{2\sqrt{3}}{\pi}\bar{i}_d[\omega_r(L_s + L_{mq})\cos(\mu + \frac{2\pi}{3}) - L_c\omega_g \cos(\frac{2\pi}{3})]
\end{aligned} \tag{3.33}$$

The calculation of the proposed model involves the simulation of a standard SM which adds the complexity and requires more computational resources to solve. At this point, in some of the previous works, further simplification was made so that the transient saliency is neglected; instead (2.9) is used to model the SM dynamics with the assumption that the SM stays in its steady-state operation status during the transient phase. This approach is referred to the "*steady state model*." With this approximation, a more reduced model can be derived as shown in Figure 3.3 which contains only the steady-state characteristics of the average model and does not require a SM model.

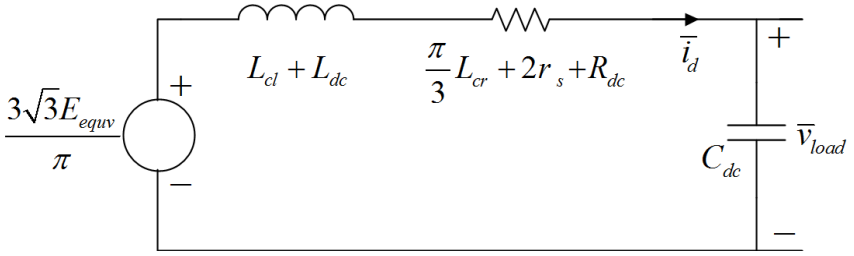

Figure 3.2 The equivalent representation of the *dynamic model*

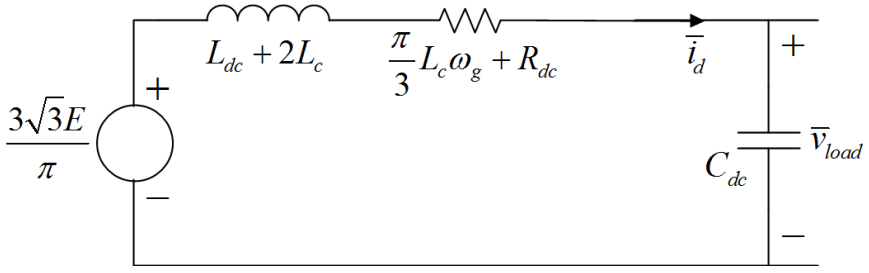

Figure 3.3 The equivalent representation of the *steady-state* model with transient neglected

However, in our case, this approximation may not stand true as the machine dynamics could potentially impact the overall system dynamic performance during the short period of transient phase. Therefore, in the following discussion our main focus will be on the evaluation of the *dynamic model* where SM dynamic variables are kept, while using the *steady state model* as a reference to compare the system responses generated from different modeling approaches.

3.2.2 Power distribution modules

As the SPS is closely coupled, the line reactances are considered to be small and therefore are combined with the filters. The distribution network is formulated so that the currents of interconnected branches on each bus should satisfy $\sum_{k=1}^{n} i_k = 0$ and $V_1 = V_2 \cdots = V_k$.

3.2.3 Switching gears and power conversion modules

For the switching gears, the status of components connecting or disconnecting to the distribution network is simply represented by a binary variable: 0 indicates disconnection while 1 indicates connection. For power conversion modules, as the interface converters are properly integrated with their interconnected components, the detailed high-frequency dynamics contained within power electronics converters (inverters) are not considered here separately.

3.2.4 Load modules

3.2.4.1 Resistive loads

Resistive loads are assumed to be connected the DC bus directly and then can simply be represented as a constant resistor. A typical resistive power load can be found in Figure 3.4.

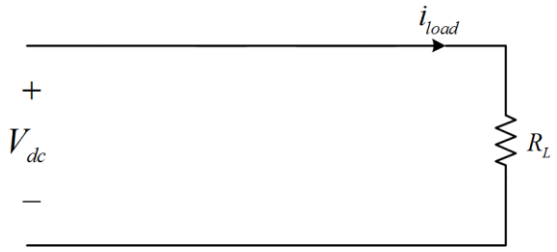

Figure 3.4 A typical representation of resistive load based on CPL assumption

3.2.4.2 Induction motor loads/CPLs

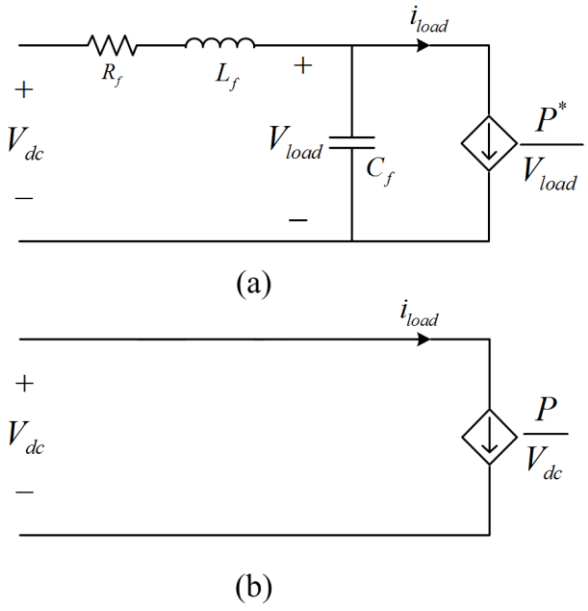

Figure 3.5 The equivalent average-value model of induction motor drives with filter

A typical representation of induction motor load with capacitive filter is shown in Figure 3.5(a) while a typical CPL load is shown in Figure 3.5(b). Without the consideration of losses in the interface inverter and the rotating machine itself, the induction motor can be seen as an ideal controller current source where the current is assumed to be equal to the instant power consumption P divided by the terminal voltage V_{load}. Typically for induction motors, the value of P is set as P^* where $P^* = \omega_r T^*_e$ and T^*_e represents the desired toque required by the mechanical loads.

3.2.4.3 Pulse loads

Pulse load refers to the kind of loads that draw a very high, short time current in an intermittent pattern [18]. A generic pulse load model as shown in Figure 3.6 is used here. From the system perspective, the behavior of pulse load can be seen as a parallel combination of two resistive elements, one with a very large value and the other with negligible value, and a switch is used to choose between the two resistors [103].

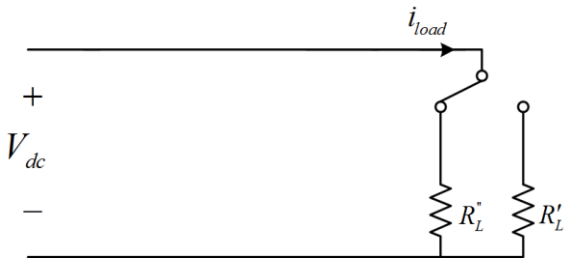

Figure 3.6 A generic representation of pulse load [103]

3.2.5 System DAE formulation

Based on the previous discussion, the individual component models can be combined and form a basic single-machine system model which contains a power generator as the power source, a notional uncontrolled diode rectifier, and a single induction motor load with filters which can be shown as in Figure 3.7.

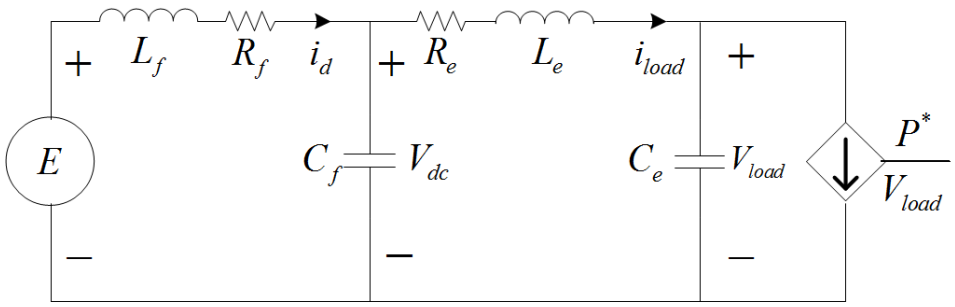

Figure 3.7 Average-value equivalent representation of a single-generator system

The following DAE can be formulated to describe the system states:

$$\begin{aligned} \frac{dv_{bus}}{dt} &= \frac{1}{C_f}(i_g - i_{load}) & \frac{di_d}{dt} &= \frac{1}{L_f}(E - R_f i_d - v_{bus}) \\ \frac{dv_{load}}{dt} &= \frac{1}{C_e}(i_{load} - \frac{P^*}{v_{load}}) & \frac{di_{load}}{dt} &= \frac{1}{L_e}(v_{bus} - R_e i_{load} - v_{load}) \end{aligned} \tag{3.34}$$

With the consideration of the general system structure demonstrated in Figure 2.3 and the individual component models developed in this Chapter, an extended system that includes multiple power sources and multiple loads can be developed as shown in Figure 3.8 by using the same modeling principle that has been used for the single-machine system. For power generation, two generators are used to supply power to the power grid and they are denoted as "G1" and "G2". To closely relate the system representation to the

baseline MVDC model, it is assumed that generator "G1" is acting as the main generator and "G2" is acting as the auxiliary generator. For the power loads, Load 1 and 2 are typical resistive loads and indicated as "L1" and "L2". Load 3 is a pulse load which is denoted as "L3". Load 4 and Load 5 are two propulsion loads denoted as "L4" and "L5". Combine all of the filter capacitors on the generator side as a total capacitor denoted as C_{gf} .The system state model can then be summarized and represented as:

On the generator side:

$$\begin{aligned} \frac{dV}{dt} &= \frac{1}{C_{gf}}\left(\sum_{k=1}^{2} I_{gk} - \sum_{j=1}^{5} I_{Lj}\right) \\ \frac{dI_{gk}}{dt} &= \frac{1}{L_{gk}}\left(E_{equv}^{k} - I_{gk}R_{gk} - V\right) \qquad \forall k = 1,2 \end{aligned} \tag{3.35}$$

On the load side:

For induction loads:

$$\begin{aligned} \frac{dV_{Lj}}{dt} &= \frac{1}{C_{Lj}}\left(I_{Lj} - \frac{P_j}{V_{Lj}}\right) \qquad \forall j = 4,5 \\ \frac{dI_{Li}}{dt} &= \frac{1}{L_{Li}}\left(V - R_{Li}I_{Li} - V_{Li}\right) \qquad \forall i = 4,5 \end{aligned} \tag{3.36}$$

For resistive and pulse loads:

$$\begin{aligned} V_{Lj} &= V \qquad \forall j = 1,2,3 \\ I_{Li} &= \frac{V_{Li}}{R_{Li}} \qquad \forall i = 1,2,3 \end{aligned} \tag{3.37}$$

The proposed DAEs can be combined with the formulations of (3.29) to produce the *dynamic* MVDC system model and with (2.7) to formulate the *steady-state* MVDC system model. As the proposed model only provides an abstracted concept for over-all

system formulation, it needs to be combined with detailed system specifications and simulation settings to form a "complete" mathematical representation of the actual system.

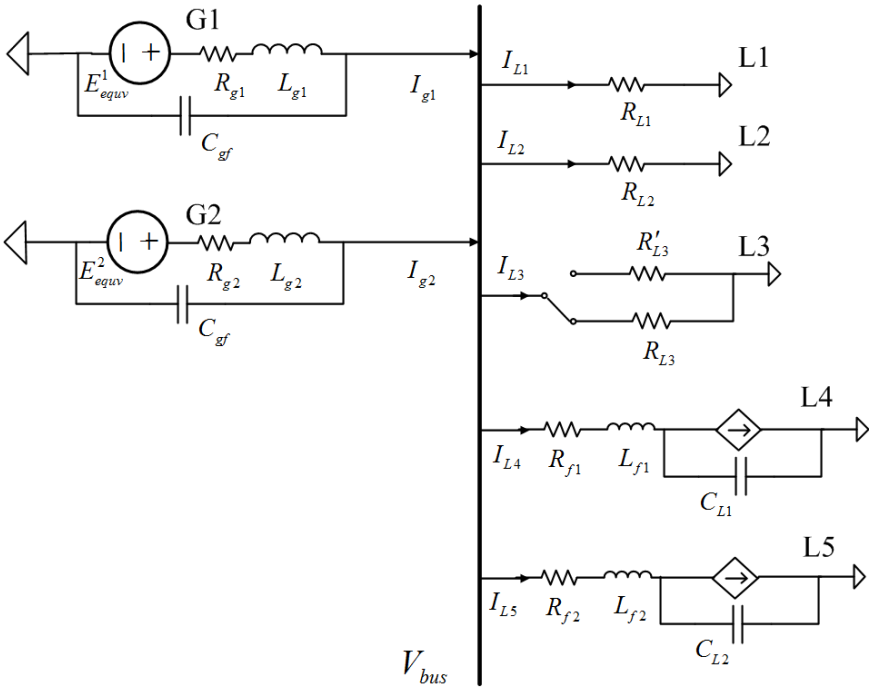

Figure 3.8 Average-value model of the multi-machine DC system

3.3 Model implementation and validation

3.3.1 System specifications

To start with, all the relative system parameters are converted to per-unit (p.u.) quantities. For the experimenting purpose, the following p.u. parameters are used based on the specification of MVDC IEEE standard [25]: V_{base} = 5000V, S_{base} = 47 MVA, and $Z_{base} = V_{base}^2 / S_{base} = 0.53\,\Omega$.

The specifications of the generator specifications and filter parameters can be found in Table 3.2, 0 and 0. The proposed modeling strategy is implemented in Matlab environment by using the default Matlab ODE solver.

Table 3.2 Parameters for generator one in the testing system in p.u.

$R_s = 0.002$	$L_d = 1.15$	$L_q = 0.7$	$L_{ls} = 0.15$
$R_f = 0.001$	$L_{lfd} = 0.09$	$R_{1d} = 0.045$	$L_{l1d} = 0.025$
$R_{1q} = 0.01$	$L_{l1q} = 0.045$	$H = 6$	$freq = 60$ Hz

Table 3.3 Parameters for generator two in the testing system in p.u.

$R_s = 0.001$	$L_d = 1.5$	$L_q = 1.5$	$L_{ls} = 0.15$
$R_f = 0.005$	$L_{lfd} = 0.05$	$R_{1d} = 0.03$	$L_{l1d} = 0.025$
$R_{1q} = 0.045$	$L_{l1q} = 0.045$	$H = 6$	$freq = 60$ Hz

Table 3.4 Passive filter specifications

$R_{g1} = 0.024\,\Omega$	$L_{g1} = 13.9$ mH	$R_{g2} = 0.05\,\Omega$	$L_{g2} = 15$ mH
$R_{f1} = 0.1\,\Omega$	$L_{f1} = 5$ mH	$C_{L1} = 1$ mF	$C_{gf} = 5$ mF
$R_{f2} = 0.15\,\Omega$	$L_{f2} = 15$ mH	$C_{L3} = 0.5$ mF	n/a

3.3.2 Validation with Simulink model/RTDS model

3.3.2.1 Equivalent Simulink model development

To validate the proposed multi-machine system, an equivalent Simulink system that has the same structure as in Figure 3.8 is developed. The specifications of the corresponding components are based on Table 3.2, 0 and 0 as well. The model is shown in Figure 3.9.

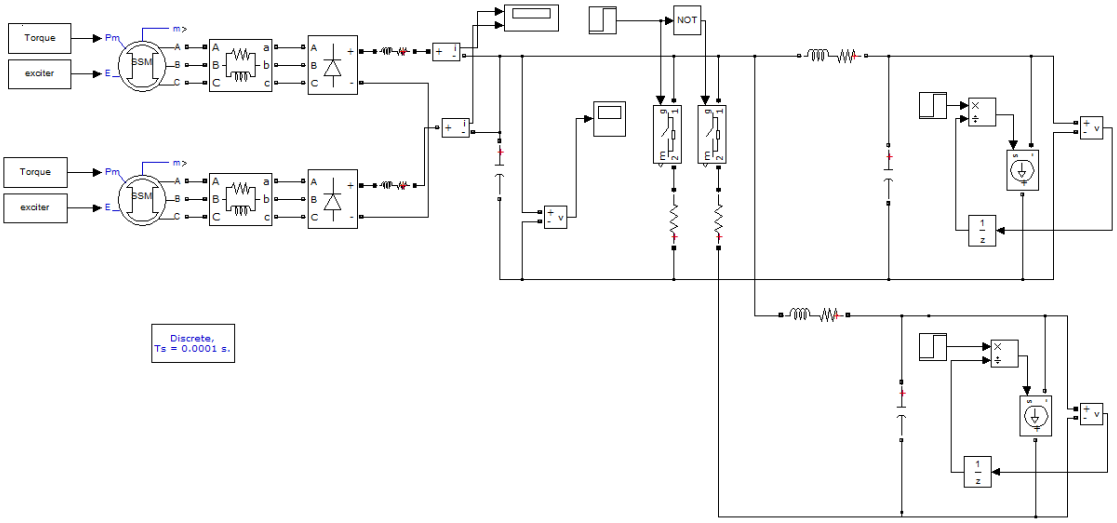

Figure 3.9 Simulink model of multiple-machine system

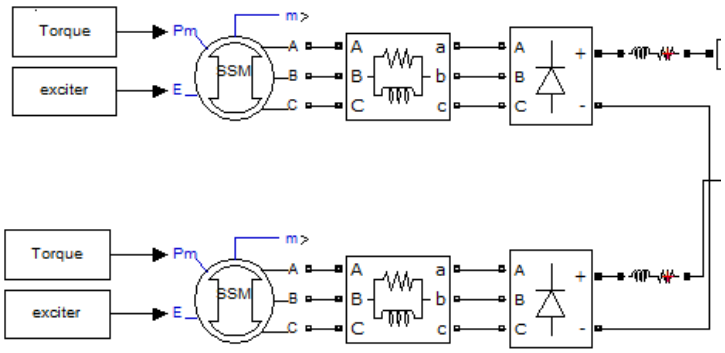

Figure 3.10 Generator side of the equivalent Simulink system

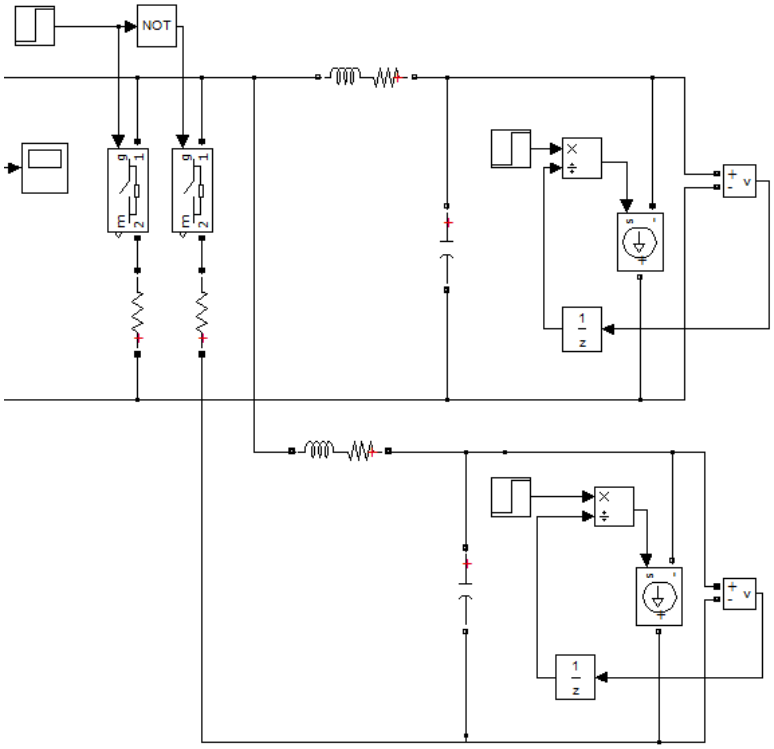

Figure 3.11 Load side of the Simulink system

Figure 3.10 shows the power generation units of the Simulink model. A standard "Simplified Synchronous Machine" from the Simpower library is used to represent the SM while the "Torque" and "Exciter" blocks are simply represented as constant values based on the previous assumption. The power converter used here is a three-phase universal bridge with diodes whose forward voltage is set as "0". Note that the simplified synchronous machine model needs to be carefully initialized to assure that the machine is working under steady-state mode from the starting point as the regular generator start-up operation needs the regulation signal from exciters/torque inputs.

Figure 3.11 shows the load model of the Simulink model. Different than the system concept diagram, resistive loads L1, L2 and pulse load L3 are combined as they

can all be are represented in the form of simple resistors while the pulse load is represented in the form of a resistive load that switch between two values. Motor loads are represented as controlled current sources with capacitive filters. Notice that the detailed values of the loads are not consistent and will be defined based on different operating conditions later.

3.3.2.1.1 Equivalent RTDS model development

To further validate the proposed formulation, we created the same system model in RSCAD and implemented it on RTDS rack as real-time hardware testament. The RTDS is a special purpose multi-processor simulation system that is optimized for high speed power system simulations and closed-loop control and hardware testing [104]. Unlink Matlab and other simulation tools that perform simulations in non-realtime, its capability to solve the electromagnetic transient in real time has made RTDS simulator a powerful tool when it comes to power system and power electronics studies. A series of technical publication about RTDS and the corresponding software suite RSCAD can be found in [105].

RTDS simulator takes advantage of advanced parallel processing techniques and hardware architecture to achieve the real-time calculation speed time. The simulator is assembled in forms of modular units called "racks" which contains slots and rail-mounted processor cards. For the software interface, RSCAD console is employed for the users to create system models, perform simulation, and collect data for analysis.

To perform the RTDS validation of the proposed modeling approach on the RTDS racks of Mississippi State University, the default processor card "3PC" and "GPC"

is used. The components consisted in the model are from the standard component library provided with RSCAD console.

The testing system schematic representing the equivalent MVDC SPS model is shown in Figure 3.12 where the detailed specifications of the each component are based on Table 3.2, 0 and 0. Similarly to the testing Simulink model, it has two generators connected to the main DC bus as power supply through diode rectifiers. The generator settings used for this dissertation is shown in Figure 3.13. Resistive loads, as well as constant power loads with filters, are fed from the distribution bus directly.

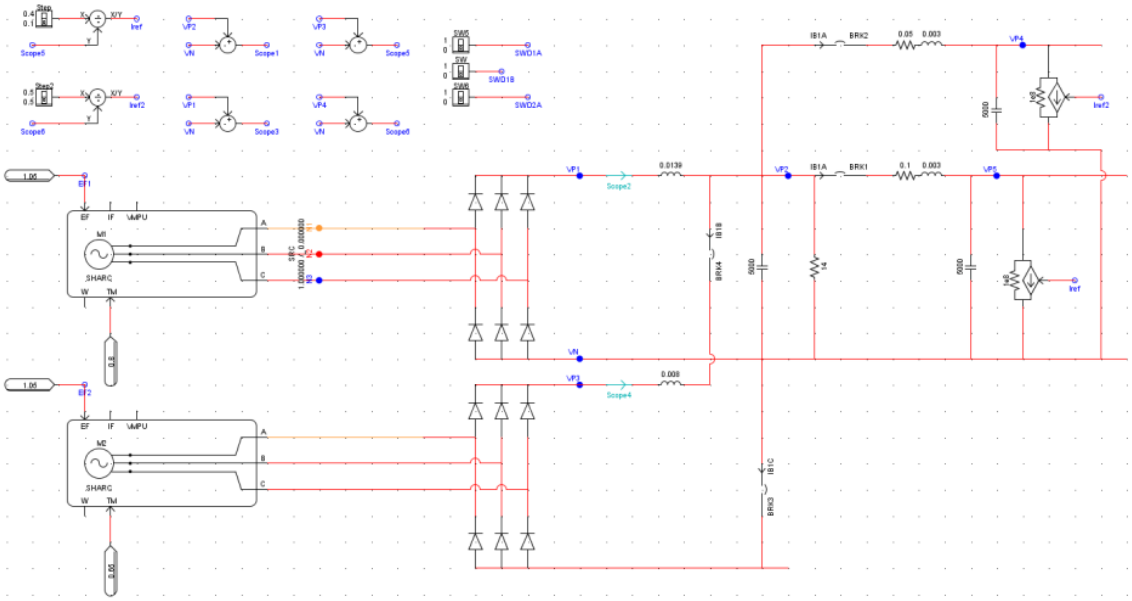

Figure 3.12 The RSCAD testing system

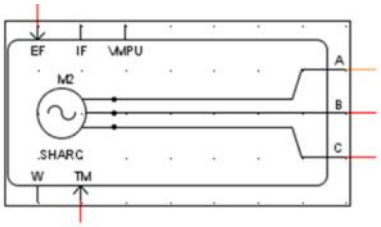

Name	Description	Value	Unit	Min	Max
Name	Machine name:	M2			
cnfg	Format of Machine electrical data input:	Generator			
cfgr	Number of Q-axis rotor windings:	Two			
trfa	Is D-axis transfer admittance known ?	No			
mmva	Rated MVA of the Machine:	28	MVA	0.0001	
VbsII	Rated RMS Line-to-Line Voltage:	4.16	kV		
HTZ	Base Angular Frequency:	60.0	Hertz		
satur	Specification of Mach Saturation Curve	Linear			
MM	Get Delta Speed Order (r/s) from CC ?	No			
spdin	Initial Speed in the first time steps is:	Rated			
tecc	Send Elect Torque in PU, TE to CC ?	No			
vtcc	Send Mach Bus V in PU, VMPU to CC ?	Yes			
trfmr	Include Optional Y-D Transformer ?	No			
ldmh1	Include Optional Machine Load No. 1 ?	No			
ldmh2	Include Optional Machine Load No. 2 ?	No			
prtyp	Solve Model on card type:	3PC		0	2

Figure 3.13 Demonstration of the generator settings in RSCAD

3.3.3 Testing Scenarios

3.3.3.1 Scenario I: Motor load pick up

In order to test the accuracy of the modeling method under various dynamic conditions, a series of case studies developed based on the recommended ESRDC practice are implemented using different simulation approaches and their results are documented and compared. For the first testing scenario, it is assumed that system is working under the cruising condition where only MTG G1 is running under half of the generation capacity and ATG G2 is offline. For the onboard lords, it is considered that total resistive load is R_L =2 p.u. and propulsion load is P^* =0.25 p.u.. At Simulation time T=10 sec. another motor load is picked up by the system so that P^* becomes 0.5 p.u..

The machine states including the rotor speed ω_r and the equivalent voltage E_{equv} following the load step change are shown in Figure 3.14. The DC bus voltage V_{bus} and current i_{gen} can be found in Figure 3.15, Figure 3.16, Figure 3.17 and Figure 3.18 with zoomed-in comparison. It is noticeable that the proposed *dynamic* model shows significant difference compared with *steady state* model which doesn't take machine dynamics into consideration. Therefore, the simulation results provide solid support for the previous statement that the machine transients could potentially affect the overall system behavior during the period of transients if not taken into consideration properly.

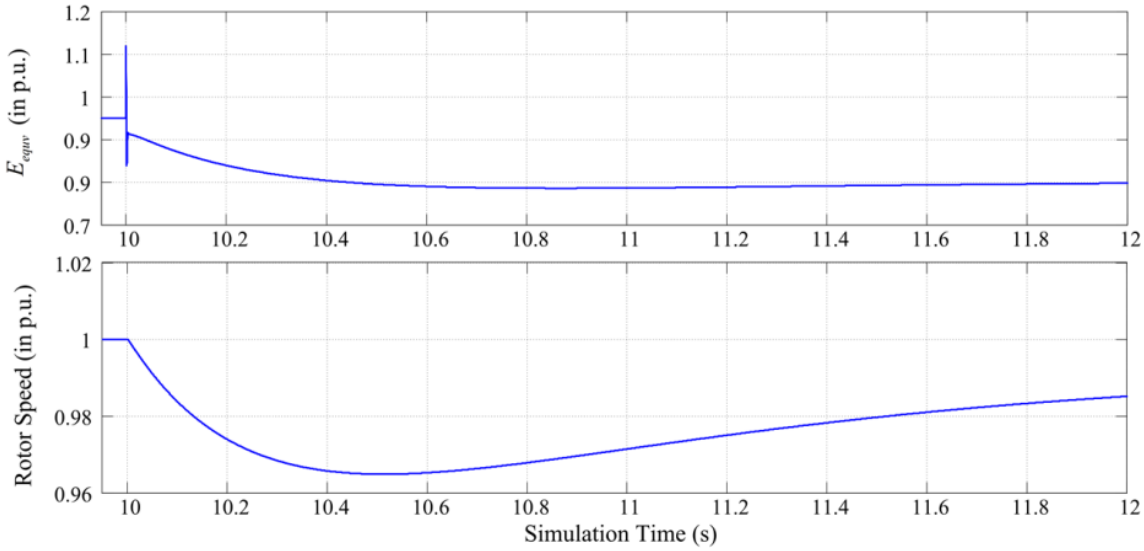

Figure 3.14 Machine states variation

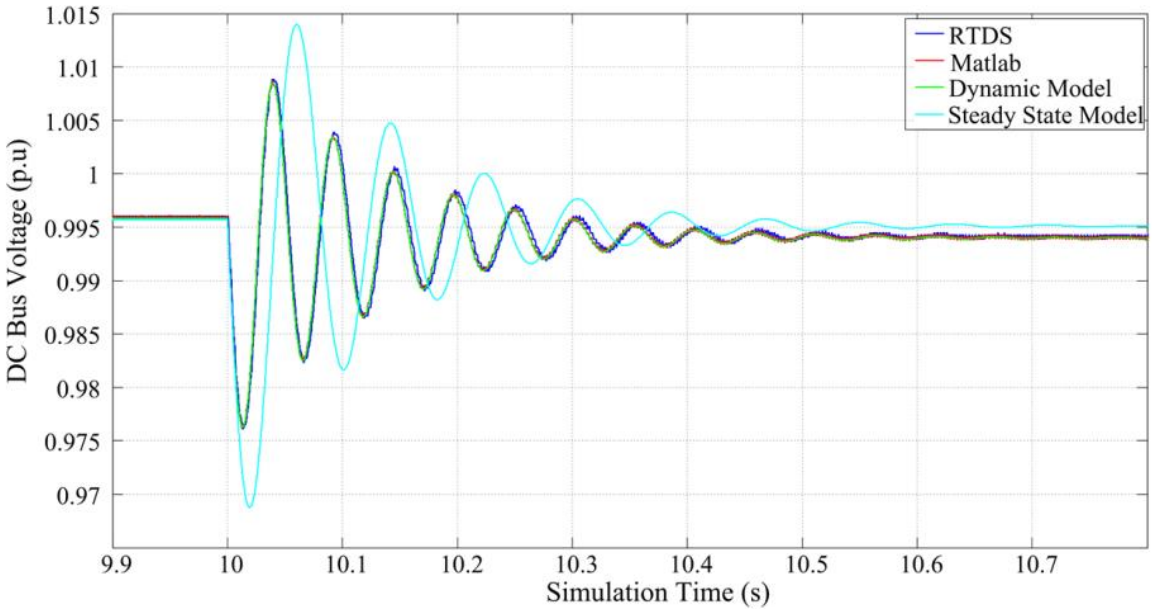

Figure 3.15 Main bus voltage

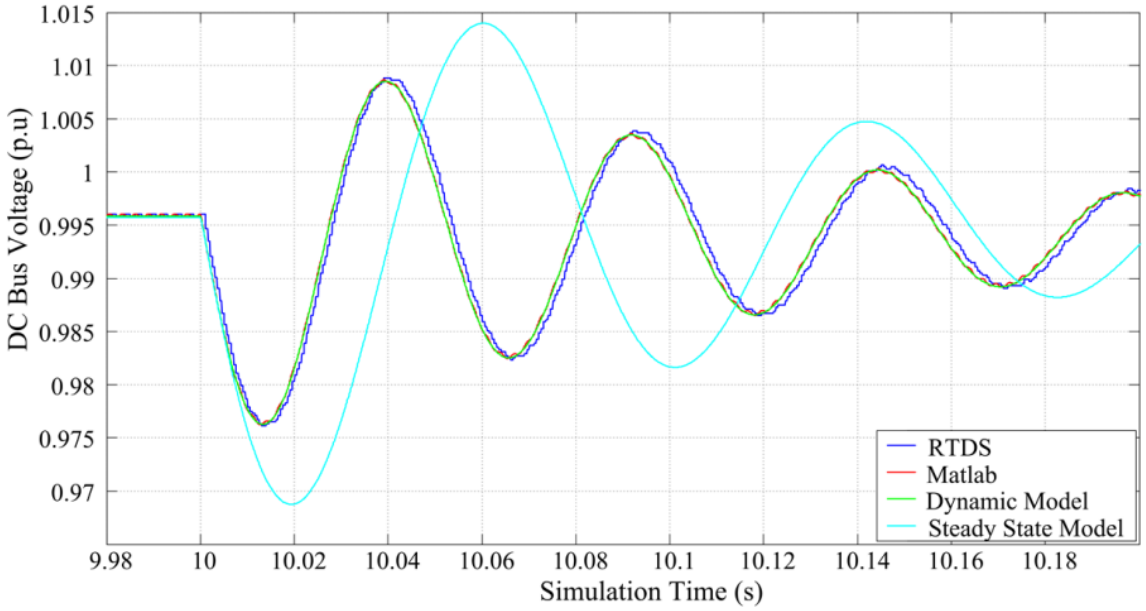

Figure 3.16 Main bus voltage: zoomed-in comparison between different approaches

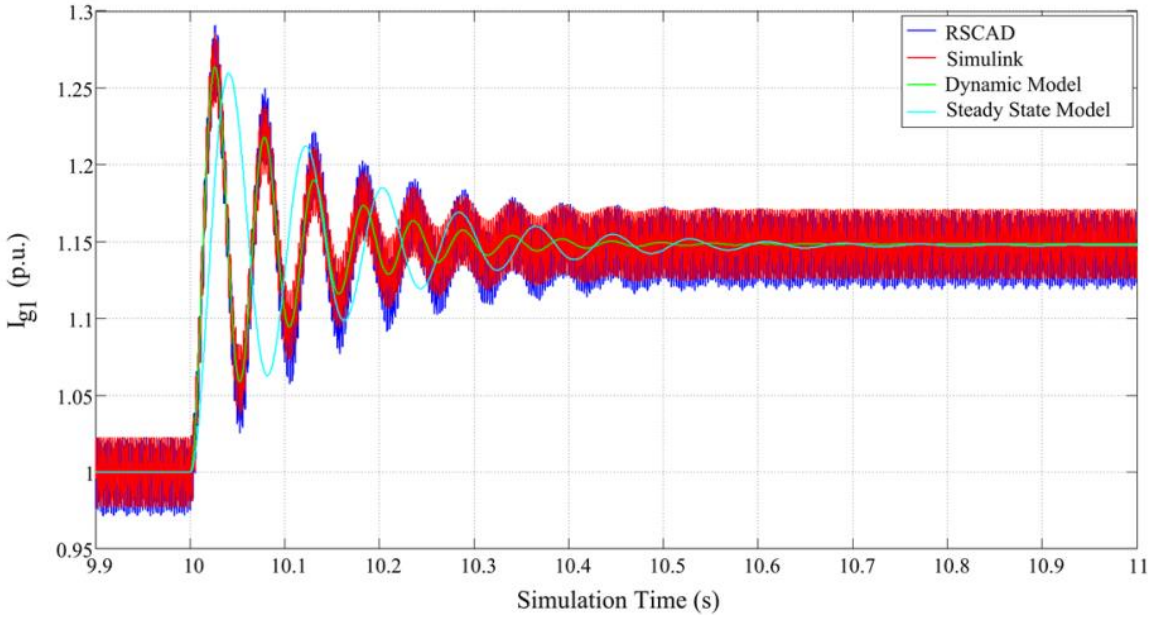

Figure 3.17 Generator one output current I_{g1}

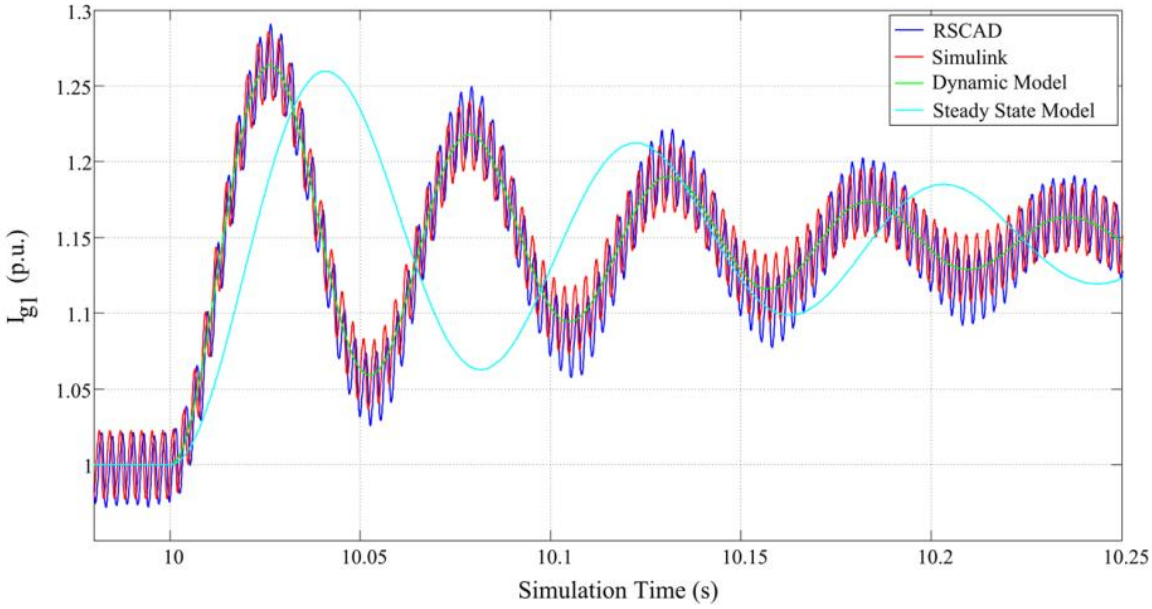

Figure 3.18 Zoom-in comparison between different approaches

Besides the comparison of time-domain waveforms, a more quantified result analysis is needed to characterize the performance of different simulation strategies. Here we use the standard "Percentage Error (PE)", as known as "approximation error" to quantify the accuracy of the modeling approach. The formulation for the PE can be defined as:

$$PE = 100 \times \left\| \frac{v - v_{predicted}}{v_{predicted}} \right\| \tag{3.38}$$

where v represents the simulation results generated from the *steady state* model, the equivalent Simulink model and RTDS model while $v_{predicted}$ represents the results generated by the proposed *dynamic* modeling approach. The current and voltage magnitude approximation error between the *steady-state* model and the *dynamic* model can be found in Figure 3.19. The comparison between the *dynamic* model and the equivalent Simulink model, as well as the comparison between the *dynamic* model and the RSCAD model is shown in Figure 3.20 and Figure 3.21 respectively.

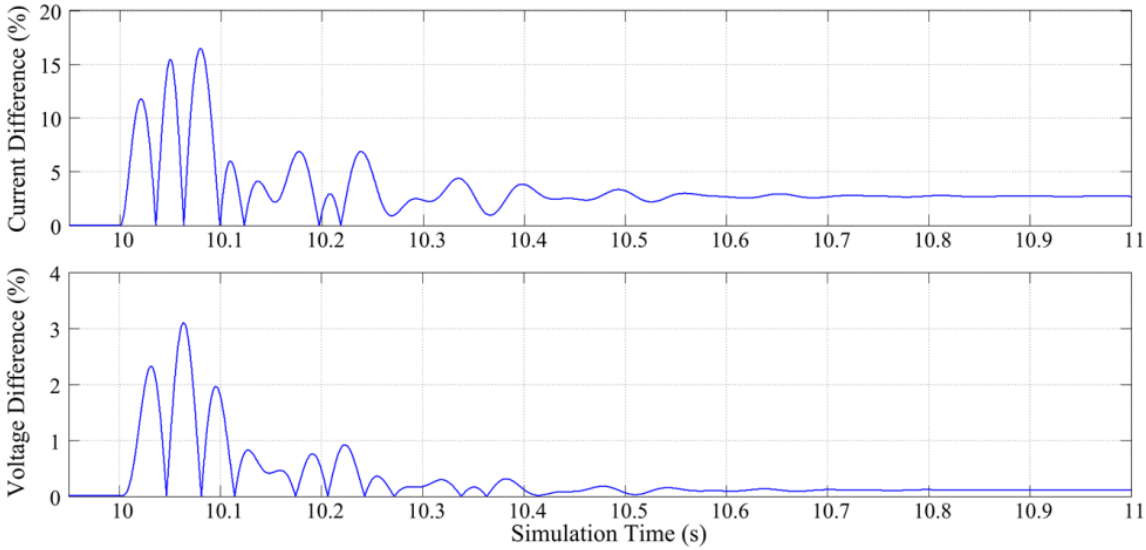

Figure 3.19 Voltage and current difference between dynamic model and steady state model

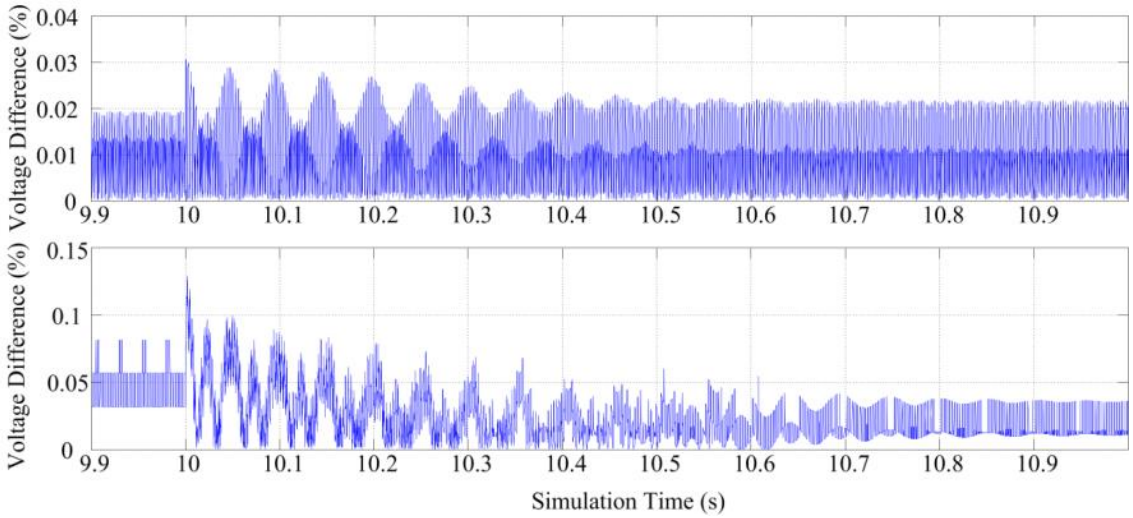

Figure 3.20 Voltage comparison between Simulink/the dynamic model (on top) and RTDS/the dynamic model (on bottom)

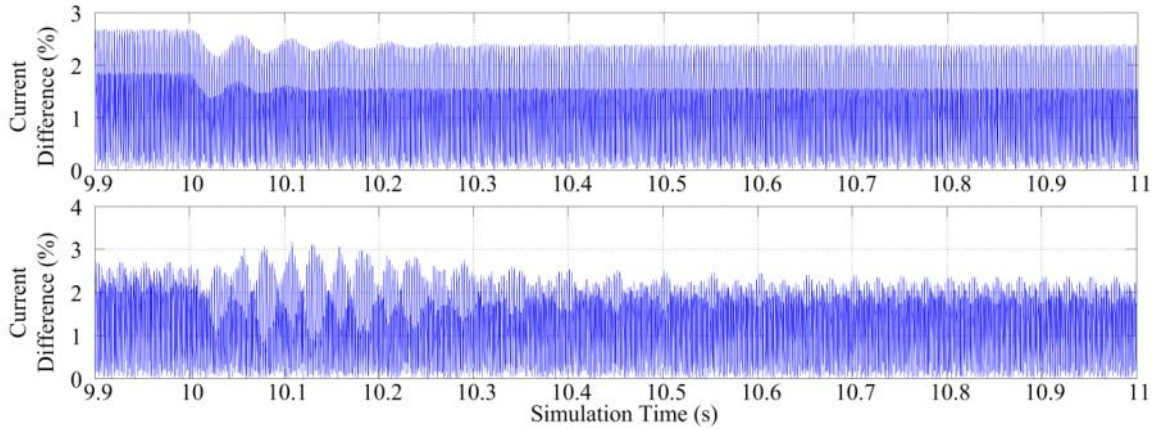

Figure 3.21 Current comparison between Simulink/the dynamic model (on top) and RTDS/the dynamic model (on bottom)

From the comparison, it can be observed the current approximation error between the *steady-state* model and the *dynamic* model is varying from 16% (during the transient) to 3% (under steady-state). Similarly, the voltage approximation error is varying from 4% (during the transient) to less than 1% under steady-state. Meanwhile, the comparison among the proposed *dynamic* model, the RTDS model and RSCAD model has shown that the proposed model has the capability to accurately capture the system dynamics during both transient period and steady-state operation with a maximum approximation error under 3% for i_{gen} and under 0.15% for V_{bus}.

3.3.3.2 Scenario II: Load rejection

Opposite to the previous test, for this scenario, it is assumed that the system is working under normal cruise condition where both MTG and ATG are online. Then the operation profile of the system changes due to an emergency battle condition and a fraction of motor load is removed at simulation time T=10 sec. In another word, the total

propulsion load drops from P^*=1 p.u. to 0.6 p.u. This case study can also be used to simulate the speed step-down scenario of ship in the form of reducing the rated power of propulsion loads. The DC bus voltage V_{bus}, generator current output for MTG I_{g1} and ATG I_{g2} can be found as in Figure 3.22, Figure 3.23 and Figure 3.24.

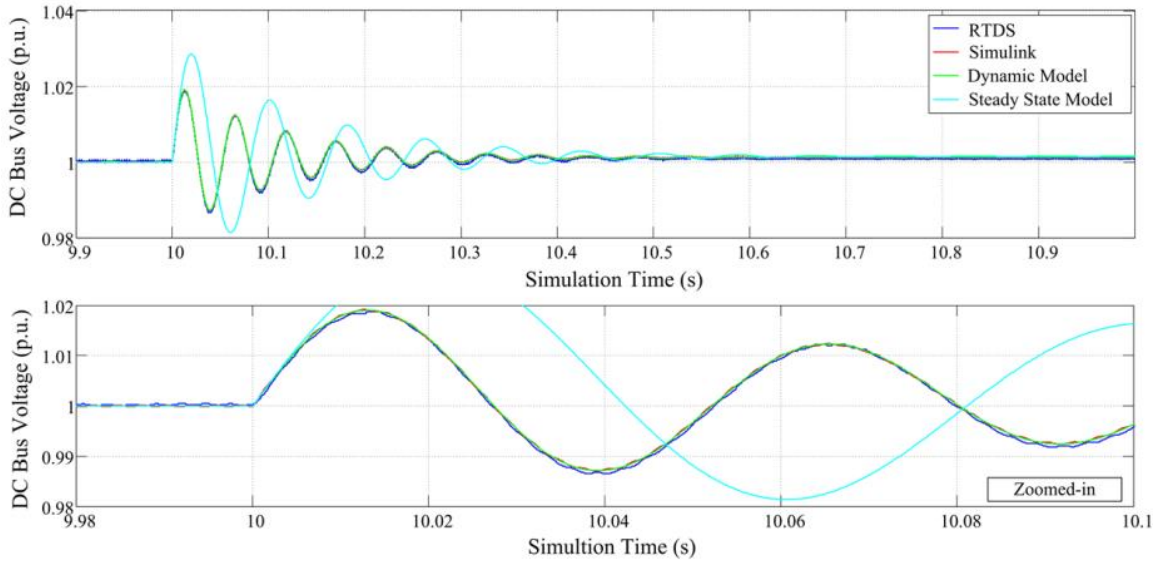

Figure 3.22 Main bus voltage with zoomed-in view

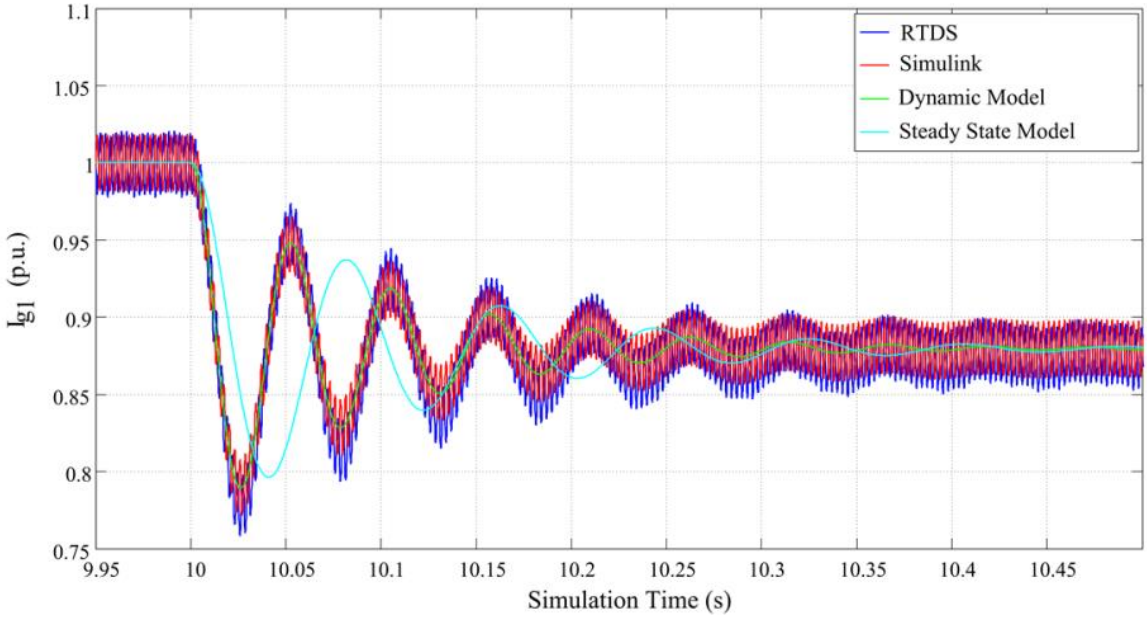

Figure 3.23 Main generator current I_{g1}

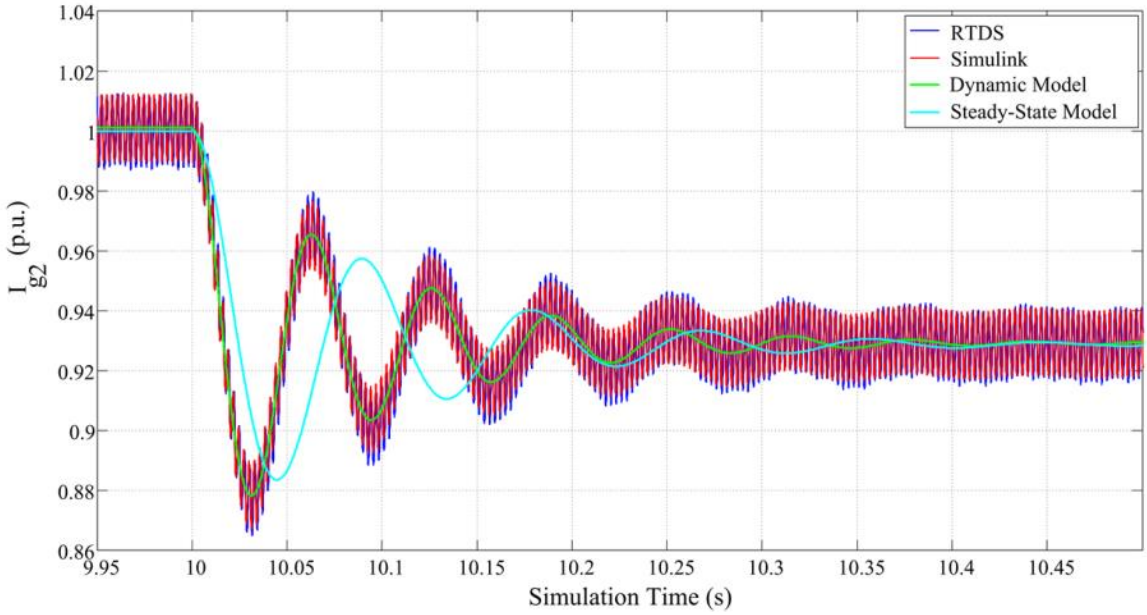

Figure 3.24 Auxiliary generator two current I_{g2}

3.3.3.3 Scenario III: Generator offline

For this scenario, it is assumed that: originally both of the generators are working normally while at simulation time T=10 sec, one of the generators (assume MTG) is damaged and gets tripped offline immediately. Due to the consideration of simplicity, it is assumed that the system remains within a stable region after the generator goes offline. The corresponding system bus voltage following the generator offline, as well as current outputs from each generator is shown in Figure 3.25, Figure 3.26, and Figure 3.27.

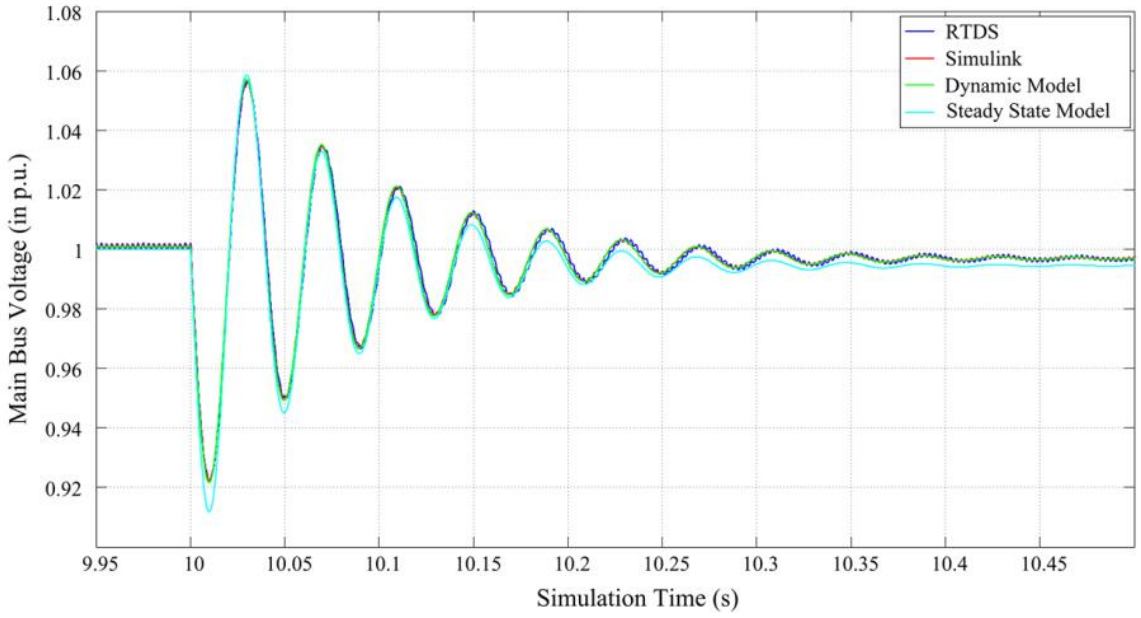

Figure 3.25 Main bus voltage V_{bus}

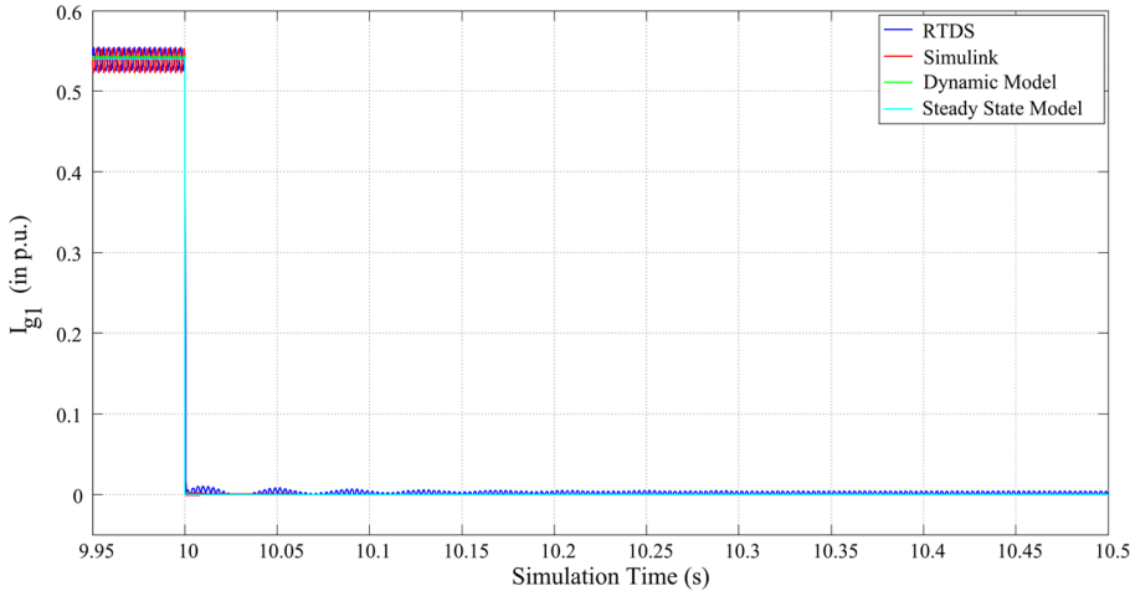

Figure 3.26 Main generator current I_{g1}

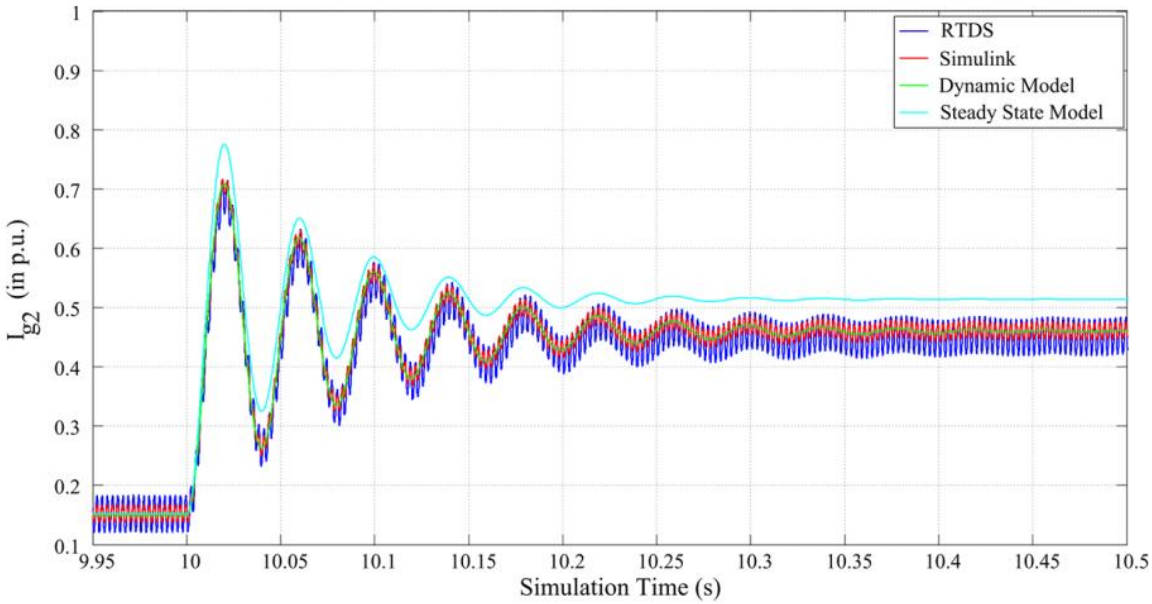

Figure 3.27 Auxiliary generator two current I_{g2}

3.3.4 Simulation Efficiency

In addition to the accuracy comparison, the simulation efficiency of each modeling method is also recorded and compared here as a performance criteria as it directly determines the computational resources required for the development of performance management controller. The elapsed time measurement here is based on a 10 seconds simulation time with a $1e^{-4}$ second step time.

From the elapsed time recorded in Table 3.5, we can conclude that the proposed *dynamic* modeling method takes relatively longer to finish compared with the *steady state* approach. However, it provides a more accurate approximation of the system responses and the simulation efficiency is still within the acceptable range compared with the notional high-fidelity baseline model which doesn't have any form of complexicity reduction or simplification and the equivalent Simulink model which is moderately simplified but still contains the switching details. It can be clearly shown that unlike the full-order model or the switching model, the average-value representation of the MVDC system is more practical for system-level studies from the perspective of simulation time.

Table 3.5 Simulation efficiency comparison between different modeling methods

Model Type	Execution Time
Dynamic model	0.087 (sec)
Steady-state	0.054 (sec)
Equivalent Simulink model	2.8 (sec)
High-fidelity baseline model	1894 (sec)

3.4 Conclusion

In this chapter, in order to facilitate the system-level analysis, the modeling strategy for the notional baseline MVDC system based on its functional decompositions

is illustrated in details. The conventional average-value modeling technique is modified to fit into the time frame of this dissertation. Combined with the standard SM model as well as the characteristics of onboard load modules, a novel simplified modeling approach for MVDC system in the form of DAE sets is set forth. The accuracy of this modeling approach is verified and validated against the corresponding Simulink model and RSCAD model implemented on RTDS simulator as the hardware benchmark. Its simulation efficiency is also justified to meet the requirement of system-level studies. The presented modeling approach can be used as a convenient simulation tool for research and application designs on shipboard DC power systems. The same modeling principle can be expanded for studies of short-term stability, governor and load control design, or even long term dynamics by including the appropriate level of details of the corresponding components.

CHAPTER IV

THE CONTROL-BASED PERFORMANCE MANAGEMENT STRUCTURE

4.1 Introduction

For the aforementioned shipboard power system, a variety of performance-related parameters need to be continuously tuned following a system disturbance to optimize the dynamic performance of the system especially during the transient period (i.e. suppress the amplitude of the transient swing and rapidly restore the system to steady state) in order to satisfy the stringent performance-related requirements for ship operation. Overall the dynamic performance management system must be able to utilize the existing shipboard resources, accommodate to the dynamic events, i.e. contingencies and ensure the response time to effectively and efficiently handle the situation.

The current performance management system still heavily relies on human effort and rule-based responsive machinery control framework. The operation relies on the classic feedback control concept to first observe the system states and then take corrective actions to achieve the specified goals. As the system becomes more and more complex, it also becomes more and more difficult to keep track of system changes and provide quick system solutions via manual tuning. In this case, an automated approach that has the capability to manage available resources to achieve the optimal dynamic system performance under time-varying operating environment needs to be derived. The control actions provided by this approach needs to be determined based on a series of

performance-related cost functions to adapt to the requirement of various safe-operation constraints and system specifications.

A predictive management framework is proposed in this dissertation where the optimal control actions that govern the system dynamics are obtained by optimizing the forecast system behaviors according to the specified criteria over a limited prediction horizon. The sequence of control inputs that results in the best system performance over the control horizon is obtained and the first control input of this sequence is applied to the current system while the others are discarded. This process is repeated every control cycle until the system is fully recovered.

In this chapter, the modeling strategy developed in the previous chapter is used to formulate the performance management problem and the design of a predictive controller that optimizes time-domain system behavior during the transient period is proposed. The performance of the controller is evaluated based on a series of criteria. It also discusses how this management technique can be applied to other performance management applications. To illustrate the design procedure and demonstrate the applicability of the proposed controller, two case studies are developed where the management framework is applied to the field controller design and load shedding operation system to optimize the system dynamic response following disturbances.

4.2 Management framework design

4.2.1 Overview

The main concept of Model Predictive Control (MPC) techniques has been briefly discussed in previous chapter and will be explained more in depth in this section. A generic model-based predictive control approach can be applied to the management of a

variety of dynamic systems in which the system performance can tuned with a set of control inputs. The key components include: 1) an abstracted system model that approximates the system behavior with the corresponding measurement units that are attached to the actual physical system, e.g. sensors or observers which provide the current actual system states; 2) performance specifications, utility functions and operation /system state constraints and 3) the controller (optimizer) which generates the optimal control solutions. A diagram showing those components and their interconnections can be found in Figure 4.1.

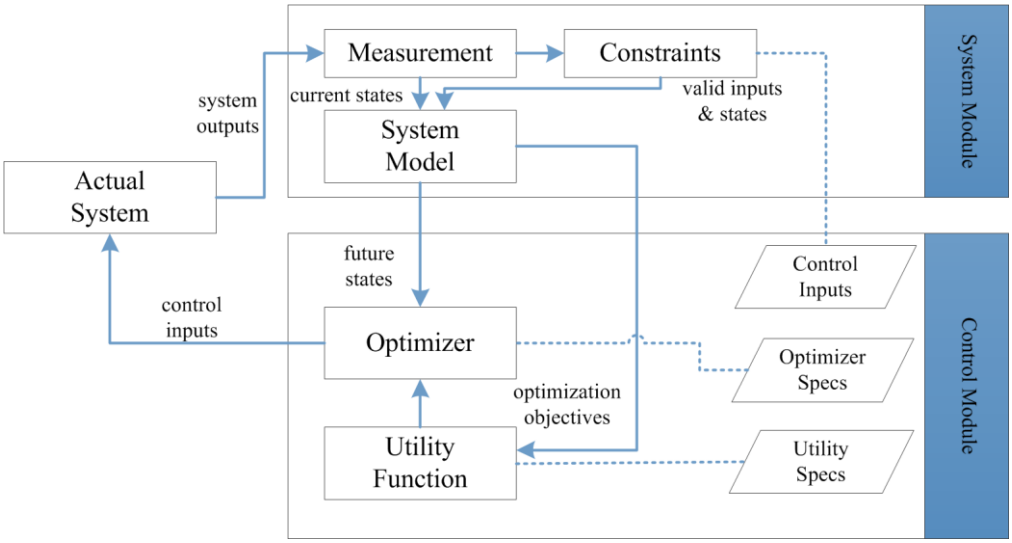

Figure 4.1 A generic MPC-based performance management framework

4.2.2 System model, performance specifications and controller design

4.2.2.1 System model formulation

A generic performance management framework targets at a variety of general classes of power system dynamics, and as noted in the previous chapters, such system dynamics can be represented with a set of continuous first-order DAEs as:

$$\begin{aligned} \dot{x} &= f(x, y, u) \\ 0 &= g(x, y, u) \end{aligned} \tag{4.1}$$

To solve the equations in the above form, a numerical integration method is required to be used here. The basic forward Euler method is introduced and used here [12].

The principle of applying Euler method is to approximate the curve representing the actual differential function by its tangent having a slope, in another word:

$$\Delta x(k) = \left.\frac{dx}{dt}\right|_{x=x(k)} \cdot \Delta t \tag{4.2}$$

The value of the state variable at the next time step can then be represented as:

$$x(k+1) = x(k) + \Delta x(k) = x(k) + \left.\frac{dx}{dt}\right|_{x=x_0} \cdot \Delta t \tag{4.3}$$

Given that $\left.\frac{dx}{dt}\right|_{x=x_0} = f(x_0, y, u)$

Such a system can be then discretized as:

$$\begin{aligned} x(k+1) &= x(k) + f(x(k), y(k), u(k)) \cdot \Delta t \\ 0 &= g(x(k), y(k), u(k)) \end{aligned} \tag{4.4}$$

In discrete-time form, $x(k) \in \Re^n$, $y(k) \in \Re^m$ and $u(k) \in U \subset \Re^j$ denote the system state variables, algebraic variables and control input variables at time instant k respectively while Δt indicates the sampling interval (normally the same as simulation time step). As the system is derived based on the discretization of a continuous system, to make the approximation hold, the state increment Δx needs to be obtained within a small time region to assure the accuracy of the discrete model. In another word, Δt needs to be relatively small to capture the complete dynamics without introducing numerical instability. In the following discussion due to convenience consideration, the system states including both differential state variables and algebraic state variables are combined and generally referred to as x. At the same time, as the operation region of the system is always compact due to the safety consideration and physical proximity, the system states x are always assumed to stay within the essential limits in the form of $x \in X$. Under this assumption, we can simplify the general system representation in the form of:

$$\begin{aligned} x(k+1) &= x(k) + f(x(k), u(k)) \cdot \Delta t \\ 0 &= g(x(k), u(k)) \end{aligned} \tag{4.5}$$

To further simply the representation, we will define a new function $f(x(k), u(k))$ which is equivalent to the previous function of $f(x(k), u(k)) \cdot \Delta t$. At the same time, we will assume that the function $0 = g(x(k), u(k))$ can be always met. Now the dynamics of the system can be rewritten in the general form of [93, 106, 107]:

$$x(k+1) = x(k) + f(x(k), u(k)) \tag{4.6}$$

where $x(k) \in X \subset \mathbb{R}^n$, $u(k) \in U = \{u_1, u_2, ...u_p\} \subset \mathbb{R}^m$, and $f : \mathbb{R}^n \times U \to \mathbb{R}^n$

4.2.2.2 Performance specifications

1) Performance specifications: In order to optimize the dynamic system performance, a series of operating specifications and system states need to be maintained within a specified range or follow a certain optimal trajectory during the transient period. The specific series of functions describing the specifications to be optimized are denoted as $H(x)$. Therefore the basic control principle of the controller is to, by tuning the control input variables, drive the system into a close neighborhood denoted as D ($D \in \mathbb{R}^n$) of the desired operating trajectory $H^*(x)$ in every time-step and maintain the system there [93]. A general form representing such specification can be found as:

$$J(x,u) = \left\| H(x) - H^*(x) \right\|_P + \left\| u \right\|_Q + \left\| \Delta u \right\|_R \tag{4.7}$$

subject to $\delta(x) \subset \Delta$

Here $\left\| * \right\|_A$ denotes the proper norm with weight A. The formulation of the performance specification considers the cost of control inputs themselves and the cost of their variations. The costs are decided based on their level of priorities or importance to the system and standardized to fit in the detailed problem.

2) Operating Constraints: All the system states and control inputs need to operate within their pre-specified operation constraints. Constraints can be generally expressed as: $u \in U$ and $\delta(x) \subset \Delta$ where U denotes the valid control input set and $\delta(x) \subset \Delta$ defines the permissible operation bounds that the system states to be maintained within. Any control solution that leads to system states violating the constraints shall be

discarded. Constraints can be generally classified into categories of inequality constraints denoted as $C_{ineq}(x,u) \le 0$ and equality constraints denoted as $C_{eq}(x,u) = 0$.

4.2.2.3 Control schemes

The basic design concept behind predictive control is to solve an optimization problem within a future time horizon based on the abstracted system model and current system states, roll this horizon forward over specified time intervals and then re-solve the control problem [93, 98]. In another word, the control policy should return solutions in the following format:

For each current system state set $x(k) \in \mathbb{R}^n$, return $u^* \in U$ so that

$$\left\| f(x,u^*) \right\| = \min_{u \in U} \left\| f(x,u) \right\| \tag{4.8}$$

The detailed control strategy described in (4.8) can be represented by the function **MPC()**. In the beginning of the operation, define x_0 as the initial system states and t_0 as the current simulation time. Then, the controller determines the optimal control input sequence "u_new " which results in the best cost function output based on the function "solve()". Both the system dynamics in the form of $f(x,u)$ and the cost function in the form of $J(x,u)$ need to be provided as well as the operation constraints $C_{ineq}(x,u)$ and $C_{eq}(x,u)$. The control input sequence that leads to the minimum cost at the end of the search is then selected and the first input of this sequence is applied to the system through the function "apply()". System states are updated accordingly based on "u_new" and the latest state variables are recorded as the new x_0 for the next control iteration.

Table 4.1 The MPC function

********** ***MPC***(N, Ts ,t0, x0, u0) **********
/*N: depth of the prediction horizon; Ts: Sampling time interval; t0: initial time
x0: initial system states; u0: initial estimation of control input*/
for each iteration
[t, x]=[t0, x0] /*step one: set the initial state*/
[u_new, x_new]= solve(x, N, Ts, u0, $C_{ineq}(x,u)$, $C_{eq}(x,u)$, $J(x,u)$, $f(x,u)$)
/*step two: solve the optimal control problem and obtain optimal control input*/
/* $C_{ineq}(x,u)$ and $C_{eq}(x,u)$ represent the overall operation constraints*/
/* $J(x,u)$ represents the cost functions*/
/* $f(x,u)$ represents the dynamics of the system (differential equations)*/
[t0, x0]= apply(t , x, Ts, u_new, $f(x,u)$)
/*step three: apply the obtained control input and generate the state updates*/
end for

4.2.3 Detailed framework design for SPS

The generic framework discussed in the previous section is modified to adapt to the detailed requirement for the dynamic performance management for shipboard power systems. Since this design practice serves as a preliminary investigation of the MPC concept implemented in power system, assumptions are made:

Assumption #1: An ideal latency-free communication system is assumed, so the signals and system states are transferred without delay.

Assumption #2: All the electrical losses during operation is neglected, therefore the power loss is not a valid criteria for this design practice.

The detailed procedure can be defined step by step as:

1. Select the contingency (contingencies) and apply it (them) to the system. Sensors within the system are assumed to detect the adverse operating conditions and initiate

the recording of system states to capture the system responses closely following the contingency.

2. After the contingency happens, fast component level controls and the operation of relays and other protections devices are assumed to start instantaneously, including relay tripping off, fast disconnection from distribution network, converter setting change and etc. It is considered that at this point, the system structure will stay unchanged with no other external control actions.
3. Identify the constraints $C_{ineq}(x,u) \le 0$ and $C_{eq}(x,u) = 0$ based on the system specifications and operating conditions.
4. Form the system level dynamic performance optimization function. Based on the aforementioned control design concept, the objective function that describes the performance optimization criteria can be defined as:

$$\min(J_1) \quad J_1 = \left\| F(x) - F_{desired}(x) \right\| \tag{4.9}$$

where formulation of $F(x)$ is based on the average-value model developed in Chapter III.

5. In order to demonstrate that the proposed management framework is flexible and can be integrated with other power management utilities onboard, we also consider the static system performance as an addition to the dynamic performance cost function. Objectives like optimal fuel optimization, minimizing power loss and optimal power dispatch can be performed using static optimization methods including economic dispatch and optimal power flow formulation. The objective function that describing the objective of the static optimization can be formulated similarly in the form of:

$$\min(J_2) \quad J_2 = \left\| S(x) - S_{desired}(x) \right\| \tag{4.10}$$

where function $S(x)$ is directly associated with the desired static optimization criteria and thus can be defined accordingly under different operating conditions.

6. Form the cost function for control inputs. In general case, maintaining the control inputs at their desired values takes certain amount of system effort. Meanwhile, control input variation also generates cost that needs to be taken into consideration from the system perspective. As the control input set may contain more than one element, elements involved within u_i need to be standardized i.e. converted to the same unit-less scale. The objective functions can be formulated separately as:

$$\min(J_3) \quad J_3 = \sqrt{\sum_{\forall i \in U} A_i \left(\frac{u_i - u_i^{desired}}{u_i^*}\right)^2} \tag{4.11}$$

$$\min(J_4) \quad J_4 = \sqrt{\sum_{\forall i \in U} B_i \left(\frac{\Delta u_i - \Delta u_i^{desired}}{\Delta u_i^*}\right)^2} \tag{4.12}$$

where A_i and B_i stand for the weighting factors for each elements that reflect the internal relationship/priority levels within the control input sets. u_i^* and Δu_i^* denote the minimum accessible values that can be derived solving $(\min \left\| u_i - u_i^{desired} \right\|, \forall i \in U)$ and $(\min \left\| \Delta u_i - \Delta u_i^{desired} \right\|, \forall i \in U)$ from off-line studies. For cases that u_i^* or Δu_i^* being zero, a very small number (typically $1e^{-3}$) is added to avoid the division by zero error.

7. For the overall optimization formulation, the optimization of system transient response trajectory J_1 is combined with steady-state optimization objective J_2 as

well as the control input cost J_3 and J_4 to finalize the overall objective function. After normalizing individual objectives into a uniform, dimensionless scale, the general system cost function can be represented as [96, 108, 109]:

$$\min \sqrt{W_{dyn} \cdot \left(\frac{J_1}{J_1^*}\right)^2 + W_{sta} \cdot \left(\frac{J_2}{J_2^*}\right)^2 + W_U \cdot \left(\frac{J_3}{J_3^*}\right)^2 + W_{Uc} \cdot \left(\frac{J_4}{J_4^*}\right)^2} \tag{4.13}$$

subject to constraints as: $C_{ineq}(x,u) \le 0$ and $C_{eq}(x,u) = 0$

as well as: $W_{dyn} + W_{sta} + W_U + W_{Uc} = 1$

The values of the *weighing factors* W_{dyn}, W_{sta}, W_U, W_{Uc} as well as A_i and B_i are decided for on a given operation scenario and therefore reflect the priority of optimization during the transient phase from a global perspective. By tuning the values, the management framework is going to be able to handle a variety of multi-objective optimization problems under different operating conditions.

In (4.7), J_1^* - J_4^* are called the *scaling factors* for each cost function as they have different units and orders of magnitude/dimension. In order to represent and compare their level of priorities on a unit-less, global scope, scaling factors are imperative when formulating multi-objective functions. For this practice, the minimum accessible values of each individual cost function J_1 - J_4 subject to the system constraints are used as the scaling factors. For every control iteration, each of the cost functions are solved first to derived J_1^* - J_4^*. Based on the latest values of J_1^* - J_4^* and the vector of pre-specified weighting factors, the objective function can be formulated and calculated. The generated solutions, i.e. optimal control inputs are feed back into the system to update the system

states. This process is repeated until the system reaches at a relatively stable operation point. The algorithm flow chart is illustrated in Figure 4.2.

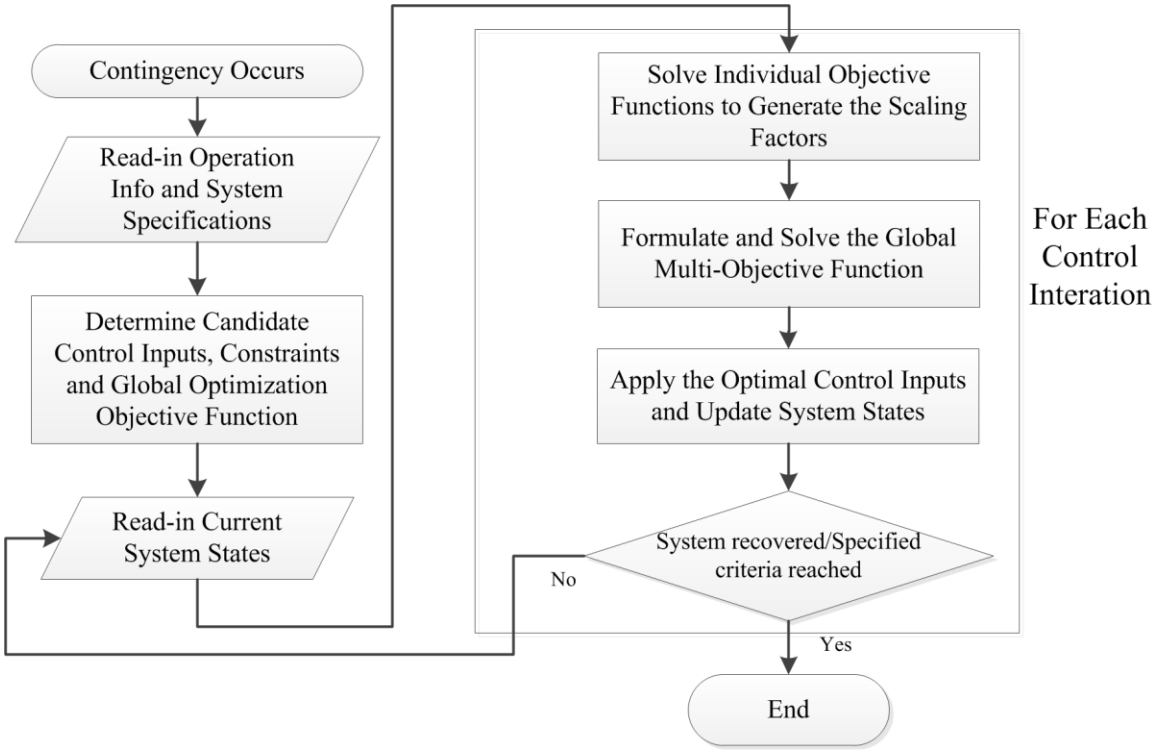

Figure 4.2 Algorithm flow chart of the proposed controller

4.2.4 Optimal search strategy

As mentioned in the previous chapter, the control scheme requires a core function "***solve()***" to search and determine the optimal control input over every step of the prediction horizon. The search algorithm is directly related to the efficiency of the whole controller and thus need to be selected carefully. While a variety of search methods can be applied to solve the optimization problem, we will start from the basic search strategy which is known as the "tree search" method [110-113].

Tree search strategy is suitable for discrete type of inputs. The detail of the tree search algorithm is demonstrated in Algorithm. 1. This function accepts the current system states, and uses them as a starting point to generate a tree of all the reachable system states up to the specified prediction horizon depth N based on the combination of the possible control inputs. Those predicted system states, as well as the control inputs are subject to constraints represented as "$C_{ineq}(x,u)$" and "$C_{eq}(x,u)$". The cost of each estimated system states is calculated based on the cost function $J(x,u)$. The state $x_{\min}$ corresponding to the minimum cost is selected and the first control input leading to the state $x_{\min}$ is returned as the output. This search is performed every control interval.

The tree search strategy introduced above is straightforward and can be implemented easily. However, the computational burden of this method increases exponentially with the increasing number of control inputs and length of prediction horizon. This is a major concern for systems that have a large set of control inputs as every possible combination of the control inputs needs to be considered in order to construct the tree data structure and in-order traversal of the tree requires the visit of every node that stores data for each control interval. In order to improve the calculation efficiency, complexity reduction strategies need to be applied to reduce the computational overhead for actual applications. In other word, instead of the exhaustive search, a more efficient algorithm is preferred to produce the control solution.

Table 4.2 Algorithm.1. The tree-search based solver algorithm

solve(x(t), N, $C_{ineq}(x,u), C_{eq}(x,u), J(x,u), f(x,u)$)

$s_0 := x(t)$

for *i=0 to N-1*

$s_{i+1} := \varnothing$

  for all $x \in s_i$ **and all** valid inputs u

    do

    $\hat{x} := f(x,u)$

    if $\hat{x}$ **satisfy** $C_{ineq}(\hat{x},u)$ **and** $C_{eq}(\hat{x},u)$

    $s_{i+1} := s_{i+1} \cup \{\hat{x}\}$

    $Cost(\hat{x}) = J(\hat{x},u)$

    end if

  end for

i=i+1

end for

$x_{\min} = \arg\min\{Cost(\hat{x}) | x \in s_N\}$

Return $u^*(t)$ *as initial input leading from x(t) to* $x_{\min}$

One approach that can help reduce the complexity of the search algorithm is to utilize the existing optimization algorithms in the AI community [93]. Such algorithms include: Genetic Algorithm (GA), Particle swarm optimization (PSO), A* search, Pruning Equivalent Nodes, and Greedy Search. Particularly, if the control input set is continuous, or discrete but with a large and uniformly distribution which can be approximated as a continuous domain, then a variety of traditional optimization techniques (linear or non-linear) can be implemented here as well [114].

To perform such type of multi-objective optimal search, an applicable tool that can be utilized here is the Matlab Global Optimization Toolbox™ [115] provided in Matlab version R2008 or newer. The Global Optimization Toolbox™ provides generic

methods that can be used to derive the global solutions for multi-objective optimization problems that contain multiple maxima and minima while the another tool Matlab Optimization Toolbox™ [116] is generally used to find local optimum. Compared with local optimum solvers that only find a point where the function value is smaller than or equal to the value of "nearby" points, the Global Optimization Toolbox™ is designed to search more than one basin of attraction in various ways.

The solvers that can be directly used for the purpose of this dissertation include: global search (**fmincon**), multi-start, pattern search, genetic algorithm (**ga**), and simulated annealing. The function of each solver can be found briefly in [117]:

- Global search solver and multi-start solver: They generate a number of points as the starting points and then call local solver to find the optima in the basins of attraction of the starting points. Function **fmincon()**, which is gradient-based and finds minimum of constrained nonlinear multivariable function, is the most commonly used local-optima solver.
- GA solver: it generates a series of random starting points, and iteratively produces better points from the starting points. GA is a population-based method and thus has no convergence proof.
- Simulated annealing solver: it performs a random search and accepts a point if it is better than the previous point. It will occasionally accept a worse point as well to make sure all the basin of attractions is covered.
- Pattern search solver: it examines a number of neighboring points before accepting the point of interest.

A comparison of those four different types of solvers have been conducted and the performance of each algorithm has been reported in [117] with regards to run time and accuracy. Particularly for the SPS, multi-objective genetic algorithm solver (**ga**) is used for discrete type of control inputs as it accepts integer value of control input (Mixed Integer Programming), supports linear and nonlinear constraints, and achieves relatively accurate optimization results within reasonable steps of iterations, while global search method utilizing **fmincon** solver is used for continuous type of control inputs for its best accuracy and efficiency in exploring different basins especially for non-linear optimization problems [118]. The optimization algorithms that are available to **fmincon** function include 'active-set', 'interior-point', 'trust-region-reflective' and etc. In contrast, **ga** function has a fixed algorithm which repeatedly modifies a "population" that consists of individual solutions. For each iteration, the algorithm selects individuals at random from the current "population" to be parents and uses them to produce the children for the next generation. As the best point within the population is selected for each iteration, over successive generations, the population "evolves" towards an optimal solution [119].

Notice here the detailed analysis of the optimization algorithms is not the main focus of this dissertation. The management framework selects and utilizes the existing algorithms provided by the Matlab toolbox directly without getting excessively involved with the concept explanation and detailed numerical derivation process. However, the performance of the aforementioned algorithms is still going to be evaluated respectively and compared to improve the control efficiency.

Table 4.3 Algorithm.2. The solver algorithm based on function **ga**

solve(x0, N, u_int, $C_{ineq}(x,u)$, $C_{eq}(x,u)$, $J(x,u)$, $f(x,u)$))

for *k=1:N*

determine [nvars, A, b, Aeq, beq, lb, ub, IntCon] based on x0, $f(x,u)$, u_int, and $C_{ineq}(x,u)/C_{eq}(x,u)$

% nvars is the number of design variables of the fitness function J

% IntCon indicates the listed variables only take integer values

end for

[u, ~, exitflag, output] = **ga** (@(u) $J(x,u)$, nvars, A, b, Aeq, beq, lb, ub, @(u) $C_{ineq}(x,u)/C_{eq}(x,u)$, IntCon, options)

Table 4.4 Algorithm.3. The solver algorithm based on function **fmincon**

solve(x0, N, u0, $C_{ineq}(x,u)$, $C_{eq}(x,u)$, $J(x,u)$, $f(x,u)$))

for *k=1:N*

determine [A, b, Aeq, beq, lb, ub] based on x0, u0, $f(x,u)$, and $C_{ineq}(x,u)/C_{eq}(x,u)$

end for

[u, ~, exitflag, output] = **fmincon** (@(u) $J(x,u)$, u0, A, b, Aeq, beq, lb, ub, @(u) $C_{ineq}(x,u)/C_{eq}(x,u)$, options)

4.3 Feasibility analysis of the management strategy

As the online search algorithms can only search limited space ahead, it is of importance to address the feasibility property of the control algorithms. By definition, the controller is "feasible" for a given set point if the control algorithm can guide the system from the initial states to a desired neighborhood of the set points and keep the system within that region. The feasibility can be seen and formulated as a joint problem of containability and reachability, which can be specified as: 1) The containability problem which is to determine a subset $S \subseteq D$ where $(\forall x \in S) f(x,u^*) \in S$; 2) The reachability

problem which is to decide if the region D is finitely reachable from the given initial state under the given control policy and the returned control solution u^*. The feasibility of the basic case with fixed system parameters [106] and more complicated case where the system parameters are uncertain and need to be predicted [93, 107] have been analyzed and discussed. In this section, the non-linear programming based computational procedure and the relative mathematical derivation process will be briefly reviewed and formulated in the form that can be solved as a nonlinear max-min problem.

First, for all $u_i \in U$, let

$$W_i := \{x \in \mathbb{R}^n \mid \|f(x,u_i)\| < \|x\|\} \tag{4.14}$$

Under this definition, W_i is the set of states that can be brought closer to the ideal trajectory by the control actions. Let Q be the summation of all W_i, in another word, Q includes all the system states that can be driven closer to the region D. Define $\mathbb{R}^+$ as the set of all non-negative real numbers, for an $r \in \mathbb{R}^+$ write $B(r)$ to represent the closed ball in $\mathbb{R}^n$ with the radius r, and write $\partial B(r)$ for the boundary of $B(r)$, so we can have:

$$\partial B(r) := \{x \in B(r) \mid \|x\| = r\} \tag{4.15}$$

Let $\bar{Q} = X - Q$ be the complement of Q with respect to the complete system state set X. As X is defined as compact, $\bar{Q}$ is also considered as compact. Let:

$$r^* = \max_{x \in \bar{Q}} \|f(x,u^*)\| = \max_{x \in \bar{Q}} \min_{u \in U} \|f(x,u)\| \tag{4.16}$$

With U being finite, r^* is also finite. Based on the definition of $\bar{Q}$, we have the basic representation of:

$$(\forall x \in \bar{Q})(\forall u \in U)\|x\| \le \|f(x,u)\| \tag{4.17}$$

Rewrite it based on the previous definition,

$$(\forall x \in \bar{Q})\|x\| \le \min_{u \in U}\|f(x,u)\| \le r^* \tag{4.18}$$

Therefore it can be proved that $\bar{Q} \subseteq B(r^*)$.

If $B(r^*) \subseteq X$, then $B(r^*)$ is a containable region. Furthermore, if there exists another region $B(r)$ that satisfies $\bar{Q} \subseteq B(r)$, then $r^* < r$. To calculate r^*, as $r^* = \max_{x \in \bar{Q}} \min_{u \in U}\|f(x,u)\|$ it is essentially a max-min problem which can be converted to a well-defined Non-Linear Programming (NLP) problem.

For systems with simple dynamics and constraints, the NLP problem can be solved in an analytical approach. But generally, the optimization tool as provided in Matlab or Mathemetica [120] can be used directly to solve the max-min problem.

4.4 Performance evaluation of the management framework

For a limited search strategy with a limited control input set and a finite prediction horizon, the proposed management strategy can only achieve the sub-optimal performance. The performance is directly related to several design factors and those factors can be listed as [93]:

- Length of the prediction horizon (N): increasing the length of the prediction horizon can typically improve the performance of the proposed

manager. However, as the future predictions are made only based on the current system states and the mathematical model, the positive effects of the increased prediction horizon will be countered by the accumulation of predication errors caused by the model mismatch as the control strategy explores deeper into the prediction horizon. At the same time, increasing the prediction would significantly increase the amount of computational effort for every control cycle. Therefore it is always desired to investigate the length of prediction horizon carefully for different systems/scenarios.

- Control set (U): for the purpose of this dissertation, the available control actions include a variety of different options. For some cases, the control inputs need to be selected from a finite set while for other cases, they need to be chosen from a continuous domain. Under certain conditions, a continuous control input region needs to be discretized based on the system requirements. Therefore it can be concluded that the definition of the control input set has direct impact on the performance of the controller from many aspects. As the result, the control input set is also considered as a design choice that needs to be optimized to improve the performance of the performance management controller.
- Sampling time interval (T_s): successful implementation of the performance management requires the system states to be sampled based on the operational frequency of the system and the objective functions that need to be optimized.

The effectiveness of the management strategy can be evaluated based on the criteria of fitness, robustness and computational overhead.

- Fitness: this index characterizes the ability of the control strategy to reach a suboptimal solution. The basic definition is to define fitness as the ratio of the average utility to the average utility. The average utility can be either computed offline for a given system model and a given disturbances or calculated online.
- Robustness: this criterion indicates the variations in the system utility in response to variability in the disturbances and system states. The controller performance can vary vastly depending on the magnitude/types of the disturbance.
- Computational overhead: this criterion defines the relevant computational time requirement for the management strategy. Especially for the transient performance management as the target of this research work, it has a very stringent requirement for the computational speed. The computational overhead is directly determined by the prediction horizon, control set, and the sampling time.

The above performance criteria are available to various application/systems. They are calculated for a specific design objective for a specific system model under given operating condition(s) to evaluate the capabilities and characteristics for the system management framework.

4.5 Case Study I: Field controller design for pulsed load starting up

Field oriented control of induction motor drives is considered as an effective and efficient approach as it allows the torque to be tightly controller instantaneously [58]. DC-link stabilizing field-oriented control has been proposed by Sodhuff in [58]. It is based on the assumption that torque control in a field oriented drive is very fast and can be seen as instantaneous. In the typical situation, the value of this torque is set equal to the desired torque as requested by the mechanical system governor. However, by modifying the conventional torque value, a very fast field oriented control can be applied.

The control implementation can be described as:

$$T_E^{new} = (V_{dc} / \tilde{V}_{dc})^n T_E^{req} \tag{4.19}$$

so that $P^{new} = (V_{dc} / \tilde{V}_{dc})^n P^{req}$

where the $\tilde{V}_{dc}$ is the filtered DC bus voltage that can be defined as:

$$d\tilde{V}_{dc} / dt = (V_{dc} - \tilde{V}_{dc}) / \tau \tag{4.20}$$

Within it, τ ($\tau \in [0,1]$) and n ($n \in [1,10]$) are considered to be time-varying and continuous within the desired range. By suitable selection of τ and n, a large variety of dynamic behavior can be obtained. The outline of this control process can be found as in Figure 4.3.

From the literature, the effect of varying n and τ has been analyzed in [58] and [121] based on the linearization of the non-linear dynamic equations using root-locus approach. It is demonstrated that of those two variables, n plays a more important role in the determination of system dynamic behavior during the stabilizing process compared to

τ . Therefore in this case study, we will use n as the control input for the model-based predictive control design and assume parameter τ staying as a constant during the transient phase with τ =4. The design solution to this problem is relatively simple and straightforward, therefore it is chosen here as a preliminary demonstration of the proposed management framework.

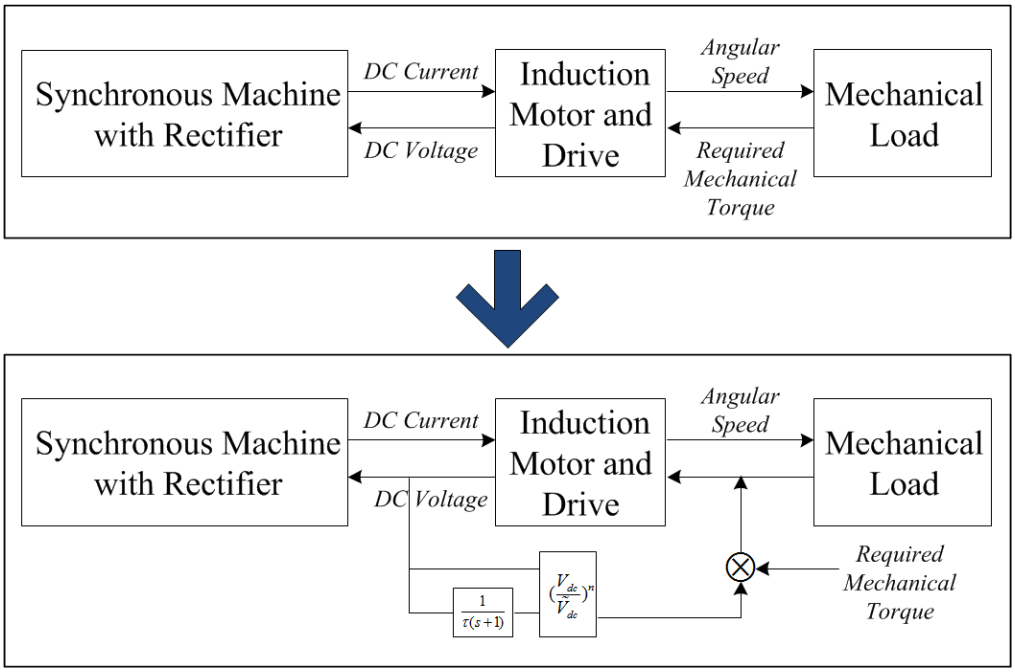

Figure 4.3 Field oriented stabilizing control concept

For demonstration purpose, the same testing system as used in Scenario I of Chapter III is used for this case study. We will focus on demonstrating the design practice of dynamic management on improving the DC bus voltage damping. Similarly, it is assumed that the load is running under half of the maximum generation capacity with P^* =0.5 p.u., and at time instant T=2.5 sec, another load (e.g. a pulse load) is picked up so

that the load is running under full capacity which indicates P^*=1.0 p.u.. The optimization objective can then be defined as:

$$\min(\left\|V_{bus}(x)-V_{bus}^{*}\right\|) \tag{4.21}$$

subject to: $n \in [1,10]$

Note that no other system constraints are necessary here, and for the demonstration purpose, the prediction horizon depth is set as N=1 time step.

The information exchange and the general system structure can be found as in Figure 4.4.

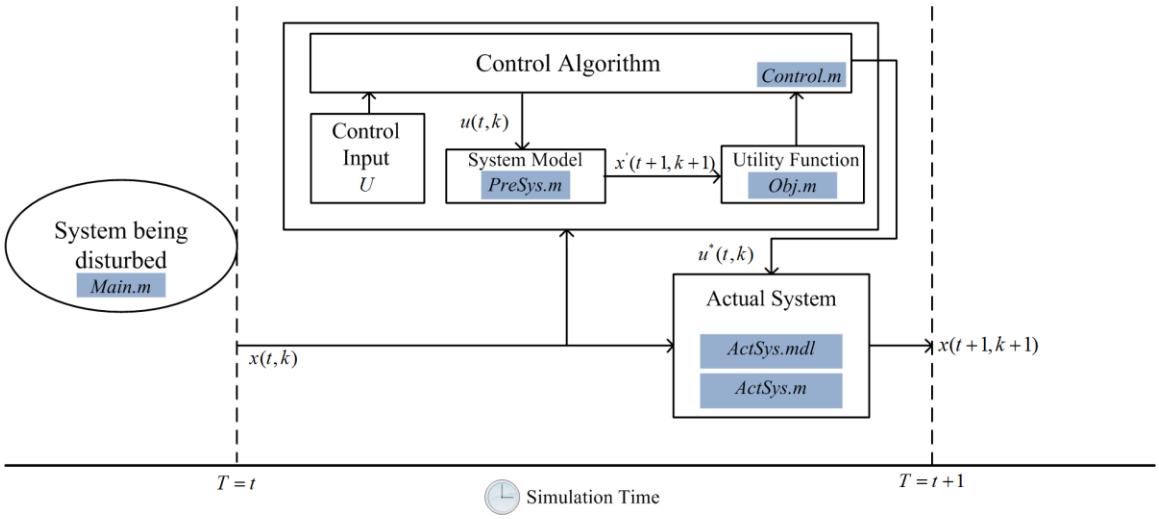

Figure 4.4 DC-Link stabilization control system structure

In the conventional approach presented in literature [58], the non-linear differential equations governing the DC-link dynamics with the presence of the control inputs are first linearized. Then the root loci of the characteristics equation with

$n = 1,3,5,7$ (n doesn't have to be an integer though) and τ varied from 0.1 to 1 is plotted. Based on the characteristics shown in the root loci plot and the complex pole pair damping diagram, a number of manually selected combinations of (τ, n) are compared. The final selection for the stabilizing controller is: $(\tau = 4, n = 1)$ for the testing system. In order to evaluate the performance of this control approach compared with the proposed control design, we implemented the optimal control inputs derived in [58].

The DC bus voltage damping of 1) system with no controller applied, 2) system with a fixed n ($n = 3$) and 3) system fully controlled , as well as the variation of control input n following the contingency can be found in Figure 4.5 and **Error! Reference source not found.**.

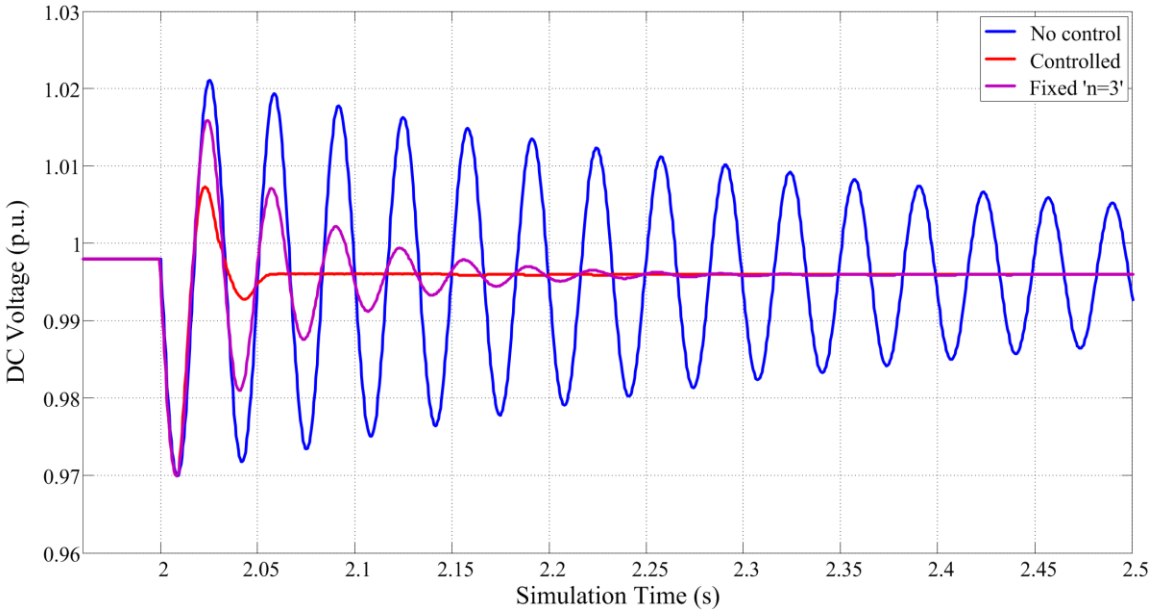

Figure 4.5 Detailed dynamic response comparison

The simulation results prove that the proposed performance management framework could effectively improve the voltage oscillation caused by the load step change.

To compare the controller's performance based on computational burden and the average fitness, we have tested the proposed management strategy subject to prediction horizon with different length N. The computer hardware used for the performance analysis includes an Intel I5-2500k processor with 16GB of memory.

Within the table, "fbest" denotes the averaged minimum value of the global cost function returned from **ga**, which reflects the fitness of the generated strategies. Naturally "fbest" is expected to be zero which indicates that the system is following its optimal operating trajectory. For this case study, "fbest" is assumed to characterize different management strategies and control solutions as it describes the ability of the control strategy to reach a suboptimal solution. The results can be found as follow:

Table 4.5 The effect of different prediction horizon on controller performance

Prediction horizon N	fbest	Execution time (sec)
1	0.6432	26.68
2	0.6531	31.04
3	0.7172	31.20
4	0.6346	34.11

From the simulation results, it can be observed that the increment of prediction horizon leads to longer simulation time, but it does not directly improve the performance of the proposed optimization strategy. Experiments performed in [93] has proven that for an ideal exhaustive tree-search strategy, with increased prediction horizon, the fitness increases upto a certain N and starts to fall afterwards as for longer prediction horizon,

the estimation error and mismatch between the mathematical model and the actual system behavior are expected which degrades the controller's performance. Particularly for the proposed framework design, another critical factor needs to be taken into consideration is the impact of the efficient search techniques. Instead of considering all the possible combination of system states and control input variables, efficient search algorithms like function **fmincon/ga** cuts the possible search region in order to reduce the computation time, thus provides a sub-optimal solution. Table 4.5 demonstrates and justifies this assumption. Depending on different system models, specifications, operating conditions and solvers, it is hard to come up with a general conclusion on the relationship among the prediction horizon, computational overhead, and performance. An overall evaluation is suggested to derive the optimal or sub-optimal controller specifications for a given case. Trade-off studies have to be performed based on the available computational resources and the desired fitness of the control strategy.

4.6 Case Study II: Generator offline and automatic Load shedding strategy

Based on the review in Chapter II, we could conclude that for a load shedding scheme, the following factors need to be taken into consideration:

- Total load demand and total generation capacity
- Working conditions of each generator unit including current power output, spinning reserve, and the corresponding control settings
- System configuration including available tier-line numbers and their status, working conditions of converters, loading conditions of all the loads, especially of the sheddable loads

- System transient response including system frequency response, voltage response, and the operation status of protective devices

A good load shedding system is able to incorporate all of the considerations into its decision-making process. In the following discussion, the proposed performance management system will be used to perform the optimal load shedding to minimize the voltage oscillation caused by the load shedding operation while satisfy the static QoS requirement.

As one of the recommended practice mentioned in Chapter II, the system response after sudden loss of a generator is studied here. It is assumed the ship is operated under cruise model where only one MTG and one ATG are online. The information of those two generators can be found in Table 4.6 while the load information can be found in 0. Then the ATG is tripped offline due to an internal failure and the MTG cannot provide sufficient power for the connected loads before the startup of back-up generator(s). Load shedding is performed by the dynamic performance management framework incorporating with a static dynamic load shedding controller to assure:

Obj1: the smallest combination of low priority loads to be shed that most quickly restores the system to stable conditions before the back-up power supply initiates

Obj2: the dynamic transients caused by the generator tripping and the load shedding operation are within a safe region to maintain the system stability.

Based on the discussion above, for this case study we use the simplified multi-machine model as developed in Chapter III as the system model and assume that each zonal load can be instantly switched on/off respectively via the management framework. Those loads also have different detailed functionalities which lead to the different priority

levels for a specific mission. Information of each load can be found as in 0. The information as listed was originally obtained for related load shedding operation in [84, 122], and is modified based on [18] and used here for demonstration purpose only which may not reflect the actual physical component properties. For simplification, all the loads here are considered to have a unity power factor.

Table 4.6 Generator information table

Generator Type	Load ID	Rated Power (kW)	Status
Main generator	G1	36000	On-line
Aux generator	G2	20000	On-line

Table 4.7 Load information table

Load Type	Load ID	Power Rating (kW)	Status	Priority Level	Equivalent Resistance
Propulsion load	P1	12000	Vital	100%	N/A
Propulsion load	P2	16000	Vital	95%	N/A
Motor load	M1	7000	Semi-vital	70%	N/A
Static load	S1	1000	Non-vital	20%	3.4611
Static load	S2	2000	Semi-vital	45%	8.6528
Static load	S3	4000	Vital	85%	2.1632
Total		42000			

Of the listed loads, it is assumed that static loads are presented in the form of equivalent resistance R_{equ} while motor and propulsion loads are represented in the form of equivalent constant power using current injection $\frac{P_{equ}}{V_{bus}}$ with filters. At this point, the system model has been successfully developed and in the next step, the optimization problem will be formulated.

To derive the optimal load shedding strategy, there are a variety of factors that need to be taken into consideration, including the cost of the connecting/disconnecting certain load (by switching on/off), the energy balance that needs to be maintained/capacity limits of the generators, the specific priority level of loads during the operation with regards to the QoS requirement and the bus voltage regulation. Based on the discussion of Section 4.2.3, we will formulate each individual optimization problem and combine them into a global optimization objective function with constraints. Solver **ga** will then be used to solve the problem and provide solutions in the form of optimal load shedding actions. With the detailed parameter settings, the optimization objective of this case study can then be formulated. Recall equation (4.7), the general global optimization cost function can be found as:

$$\min \sqrt{W_{dyn} \cdot \left(\frac{J_1}{J_1^*}\right)^2 + W_{sta} \cdot \left(\frac{J_2}{J_2^*}\right)^2 + W_U \cdot (\frac{J_3}{J_3^*})^2 + W_{Uc} \cdot (\frac{J_4}{J_4^*})^2} \qquad (4.22)$$

More specifically, for this case study, the control input can be defined as: $u_i = [u_1, u_2, u_3, u_4, u_5, u_6]$ where u_1, u_2 and u_3 determines the equivalent power ratings of propulsion load P1, P2 and motor load M1 in kW, and u_4, u_5, u_6 stands for the connection/disconnection status of the static resistive loads S1, S2 and S3. With this definition, it is obvious that $[u_4, u_5, u_6]$ are integers that are either 0 or 1 while $[u_1, u_2, u_3]$ are values within the range of their power ratings respectively, i.e. $\begin{cases} u_1 \in [0, 12000] \\ u_2 \in [0, 16000] \\ u_3 \in [0, 7000] \end{cases}$.

With regards to the individual cost functions, $J_1 = \min(\|F(x) - F_{desired}(x)\|)$ describes the performance criteria of the dynamic voltage performance. In this case study, as we want the voltage to return to the original status as soon as possible; thus, we choose $F_{desired}(x)$ to be the ideal system bus voltage magnitude under steady-state operation which is a constant 5000. Therefore J_1 can be represented as:

$$J_1 = \min(\|F(x) - 5000\|) \tag{4.23}$$

Moving to the next objective function, function $J_2 = \min(\|S(x) - S_{desired}(x)\|)$ describes the general static optimization objective. For this case study, as the QoS performance is directly connected with the control inputs rather than system states, J_2 can be rewritten based on the value of components within u_i. Ideally, we want all the loads to be on or working at its notional condition which puts the $S_{desired}$ at 4.15; thus, accordingly the cost function of J_2 can be specified as:

$$J_2 = \min \left\| \begin{matrix} 1 \cdot u_1 / 12000 + 0.95 \cdot u_2 / 16000 + 0.7 \cdot u_3 / 7000 \\ +0.2 \cdot u_4 + 0.45 \cdot u_5 + 0.85 \cdot u_6 - 4.15 \end{matrix} \right\| \tag{4.24}$$

With ATG tripped offline during the simulation, the power balance between the remaining generator G1 and the total amount of the system loads needs to be taken into consideration as well as the desired spinning reserve, which suggests that:

$$u_1 + u_2 + u_3 + 1000 \cdot u_4 + 2000 \cdot u_5 + 4000 \cdot u_6 \le 36000 \cdot 90\% = 32400 \tag{4.25}$$

subject to:

$$\begin{cases} u_1 \in [0,12000], u_2 \in [0,16000], u_3 \in [0,7000] \\ u_4 \in [0,1], u_5 \in [0,1], u_6 \in [0,1] \\ u_4 \in \square, u_5 \in \square, u_6 \in \square \end{cases} \tag{4.26}$$

With regards to the cost of control input implementation, it is apparent that maintain loads at their original conditions doesn't cost extra system resources; thus, it is considered that $W_U = 0$, which suggests cost function J_3 is ignored. However, tripping off certain static loads or reducing the power rating of CPL loads would still require a certain amount of system/human effort. To start defining and quantifying the operation cost for each control input, the general cost function of J_4 can be recalled as:

$$J_4 = \min(\sqrt{\sum_{\forall i \in U} B_i (\frac{\Delta u_i - \Delta u_i^{desired}}{\Delta u_i^*})^2}) \tag{4.27}$$

From the system perspective, it is apparently desired that all the loads are staying at their original working condition, i.e. $\Delta u_i^{desired} = [0,0,0,0,0,0]$. Similarly, Δu_i^* can be derived as: $\Delta u_i^* = [\mu, \mu, \mu, \mu, \mu, \mu]$ where μ stands for a tiny value, e.g. $1e^{-3}$. The value of $B_1 \cdots B_6$ can be defined based on different operating conditions; however, to simply the case study, a fixed set of $B_1 \cdots B_6$ is used here as $B = [1/12000, 1/16000, 0.8/7000, 1, 0.6, 0.8]$. Thus, J_4 becomes an optimization problem that can be described as:

$$\min(\sqrt{\sum_{\forall i \in U} B_i (\frac{\Delta u_i}{\Delta u_i^*})^2}) \tag{4.28}$$

subject to:

$$\begin{cases} \Delta u_1 \in [0,12000], \Delta u_2 \in [0,16000], \Delta u_3 \in [0,7000] \\ \Delta u_4 \in [0,1], \Delta u_5 \in [0,1], \Delta u_6 \in [0,1] \\ u_4 \in \square, u_5 \in \square, u_6 \in \square \end{cases} \tag{4.29}$$

Considering that fact that the remaining generator capacity has to be larger than or equal to the total remaining load power:

$$\begin{aligned} &\Delta Load = \Delta u_1 + \Delta u_2 + \Delta u_3 + 1000 \cdot \Delta u_4 + 2000 \cdot \Delta u_5 + 4000 \cdot \Delta u_6 \\ &\geq 42000 - 36000 \cdot 90\% = 9600 \end{aligned} \tag{4.30}$$

At this point, combining each of the derived individual cost function, the global optimization problem can be formulated as well as the system constraint. Once all the weighting factors are determined, we could start calculate the scaling factors J_1^*, J_2^*, J_4^* and solve the global objective function using the proposed performance management system using Algorithm 2 with **ga** solver. In the following section, we will demonstrate the implementation and solving procedure of this optimization problem.

4.6.1 Implementation and result analysis

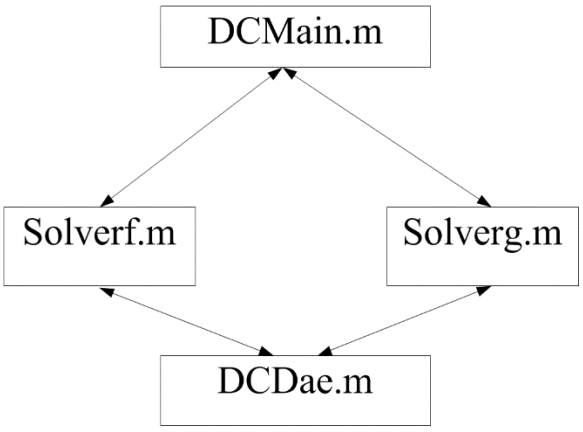

Figure 4.6 Matlab script structure

The structure of the Matlab scripts performing the optimization strategy can be found in Figure 4.6. The main script is called "DCMain". It defines all the relevant simulation parameters/global variables and the dynamic event. The dynamic event is generally represented in the way of the change of critical parameters. For every simulation step time t_s, "DCMain" calls "Solverg" to pass f. "Solverg" then calls forth "DADae" which contains the essential DAEs as derived in Chapter III to generate the updated system states using ODE23s solver for the next simulation step time, and the generated state information is sent back to "DCMain". After the system disturbance, relative specifications are changed in “DCMain”. Constraints are formulated, and for every control time interval t_c, “DCMain” calls **ga** to generate the optimal control inputs utilizing function “solverf”. Like “solverg”, “solverf” calls “DCDae” to generate the system states over the prediction horizon N. It also contains the general form of all the individual cost functions as well as the global multi-objective function. Based on system's request, the predicted system states information is used to formulate every detailed individual objective function $J_1,...J_4$. **ga** will be called multiple times in "DCMain" to assure that all the corresponding scaling factors $J_1^*,...J_4^*$ are derived. Then, since all the reference values, weighting factors, as well as the scaling factors are available, the detailed global cost function can be formulated in “solverf”. After **ga** solves the global multi-objective optimization problem, it returns the optimal control solutions to “DCMain”, those optimal control inputs are implemented via “Solverg” to update the system states. This control loop is repeated until the system recovers or the total simulation time is up.

For this case, the prediction horizon is set as 1 initially. The option setting of the ga solver is defined as:

```
opts = gaoptimset(...
        'PopulationSize', 50, ...
        'Generations', 50, ...
        'EliteCount', 5, ...
        'TolFun', 0.1);
```

To verify this approach, we will implement the proposed design algorithm and evaluate the generated control solutions with regards to the system dynamic response and QoS rating. The performance of the acquired control strategies are compared respectively based on different operation priorities. Notice that the priority parameters used in this case study are solely defined for the demonstration purpose and do not reflect the actual priorities during mission operations.

4.6.1.1 Scenario I

For Scenario I, the top priority is to optimize the dynamic voltage damping of the system during the transient phase. QoS performance and the control actions are considered less important. A set of weighting factors can then be determined as in Table 4.8.

Table 4.8 Weighting factors for Scenario I

W_{dyn}=85%	W_{sta}=10%	W_{Uc}=5%

The generated control input, system voltage response and the QoS rating following the ATG offline can be found as:

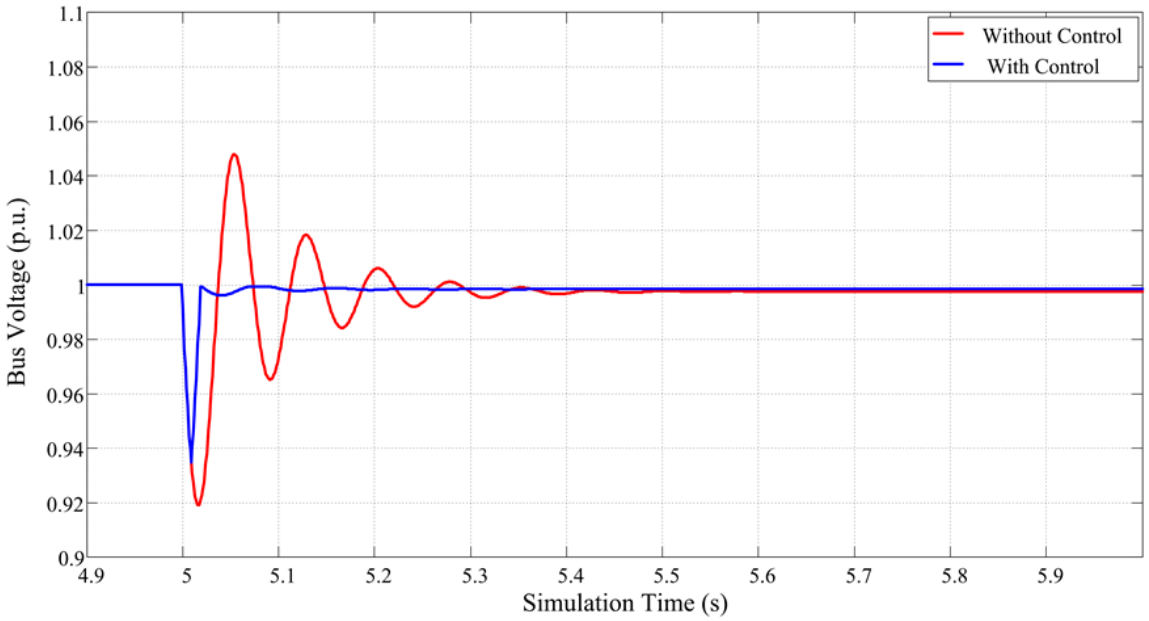

Figure 4.7 Bus voltage comparison

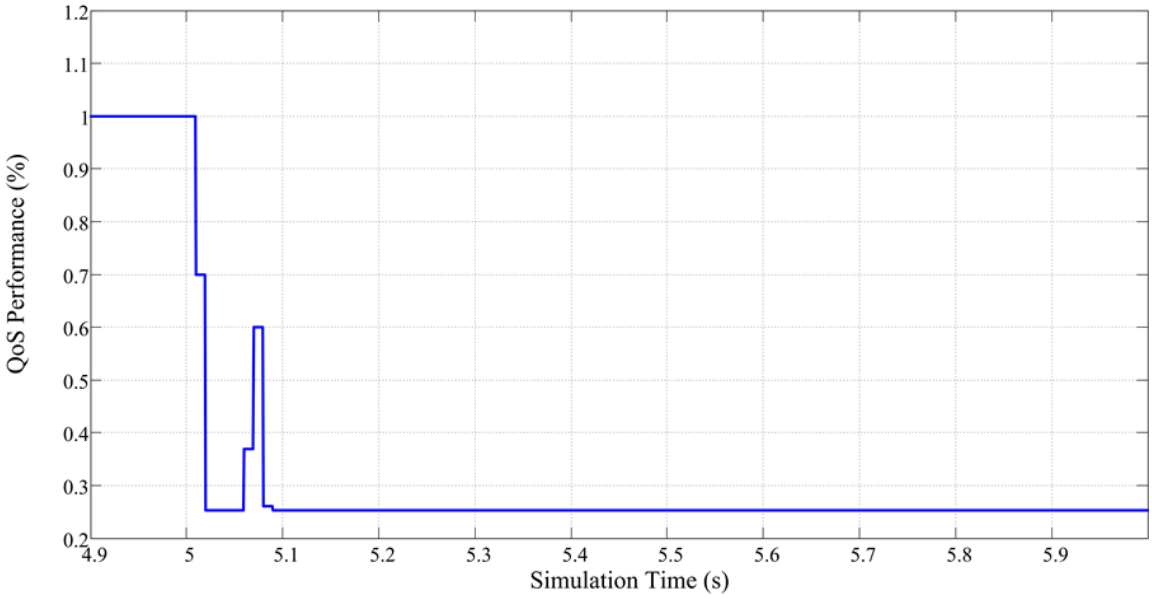

Figure 4.8 QoS performance

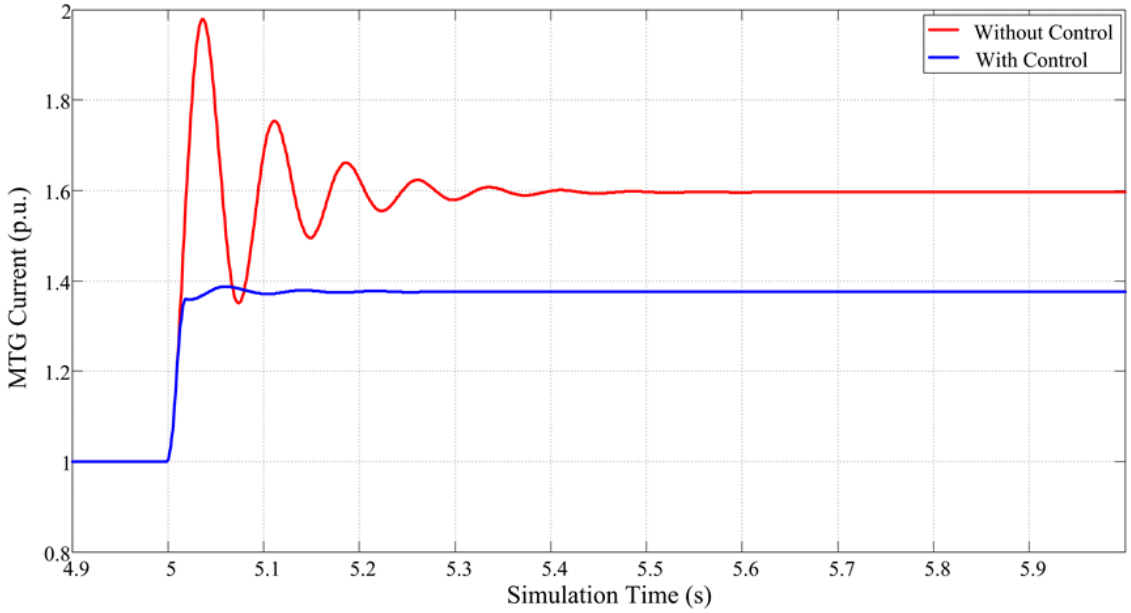

Figure 4.9 MTG current output comparison

From the result comparison, it can be observed that the bus voltage has been greatly optimized compared with cases where no control actions are applied. The current output of MTG is also optimized to avoid over-current. In contrast, the QoS performance is relatively bad as it decreases to less than 30% of the normal operation level.

4.6.1.2 Scenario II

For Scenario II, what is different than the first scenario is that the top priority is to optimize the QoS. The dynamic response and the cost of control action implementation are set as less important objectives for the operation. A set of weighting factors can then be determined as:

Table 4.9 Weighting factors for Scenario II

W_{dyn}=10%	W_{sta}=85%	W_{Uc}=5%

The generated control input, system voltage response and the QoS rating can be found as:

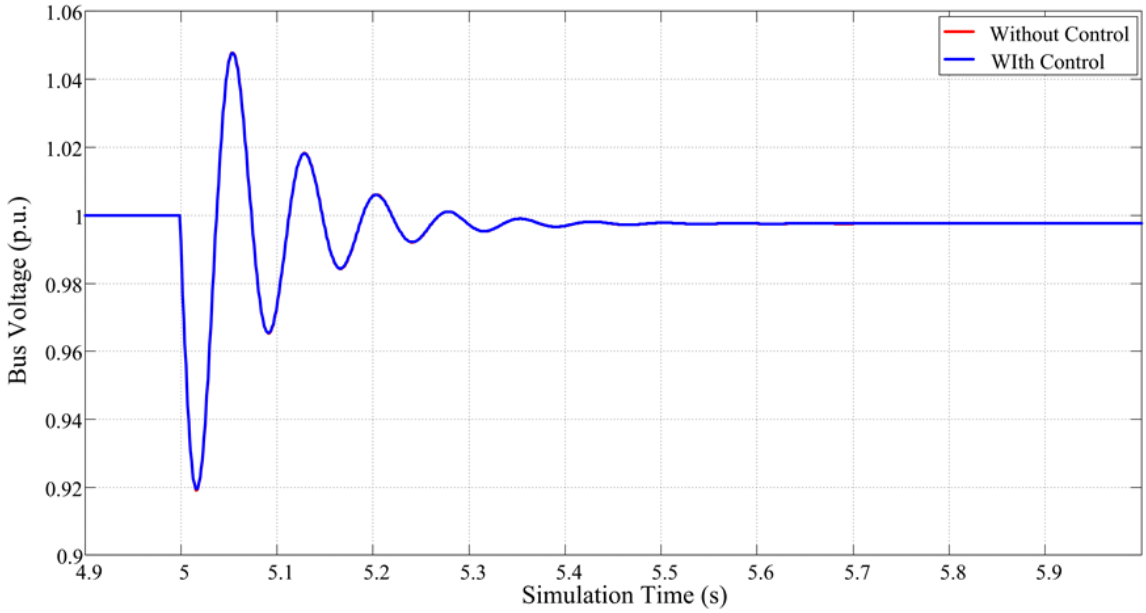

Figure 4.10 Bus voltage comparison

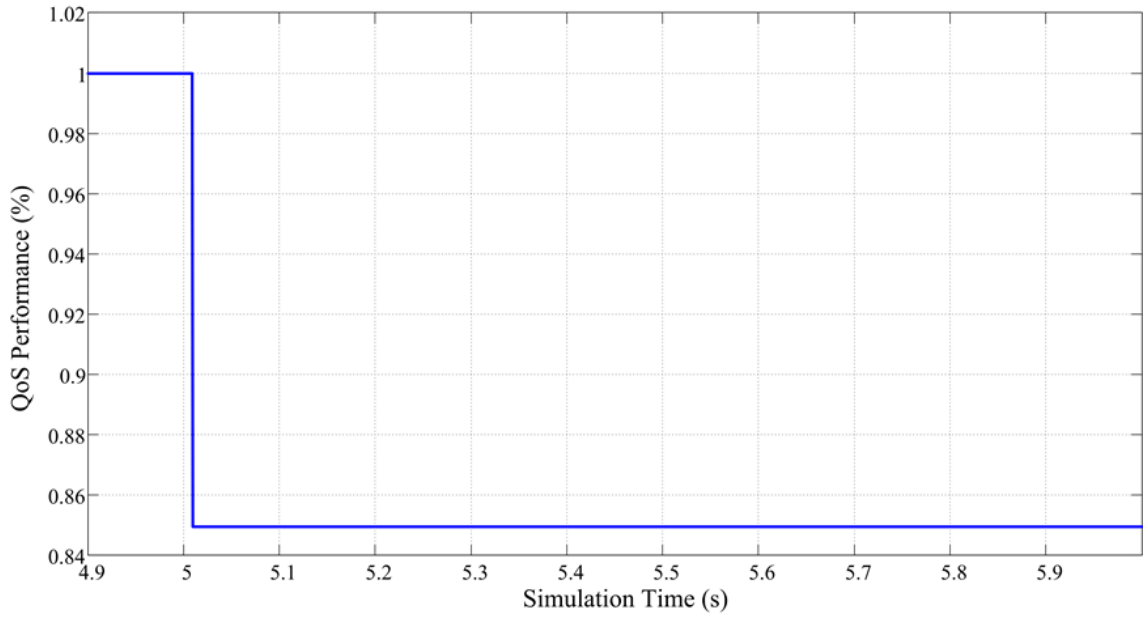

Figure 4.11 QoS performance

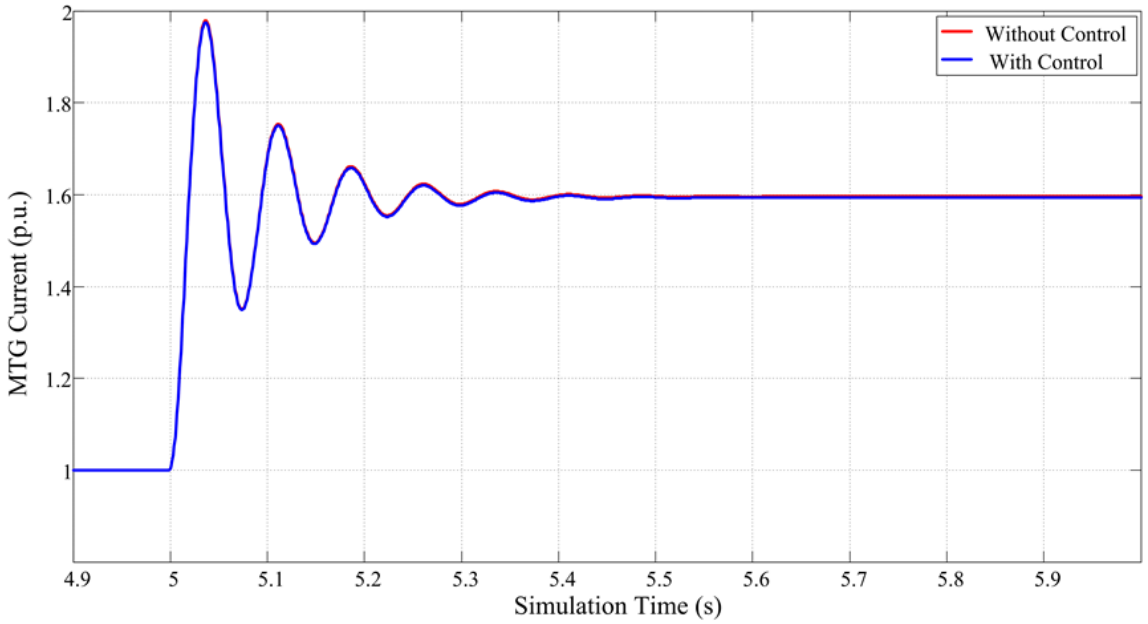

Figure 4.12 MTG current output comparison

The simulation results have demonstrated that the system QoS performance has been maintained at its maximum level via control inputs as it has the highest priority level. However, the bus voltage and MTG current output is not optimized as they are not considered to be important.

4.6.1.3 Scenario III

For Scenario III, the priority for the dynamic voltage response optimization and QoS optimization is set as equal; thus, we want the system to achieve optimal voltage performance while maintaining an optimal QoS rating. The weighting factor can be found as:

Table 4.10 Weighting factors for Scenario III

W_{dyn}=45%	W_{sta}=45%	W_{Uc}=10%

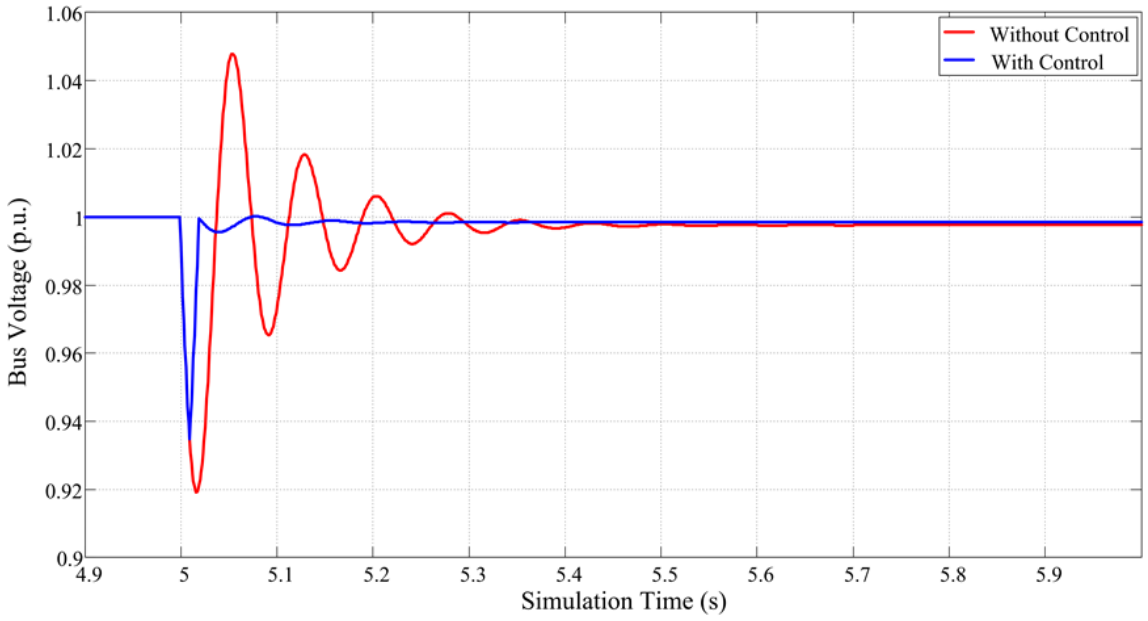

Figure 4.13 Bus voltage comparison

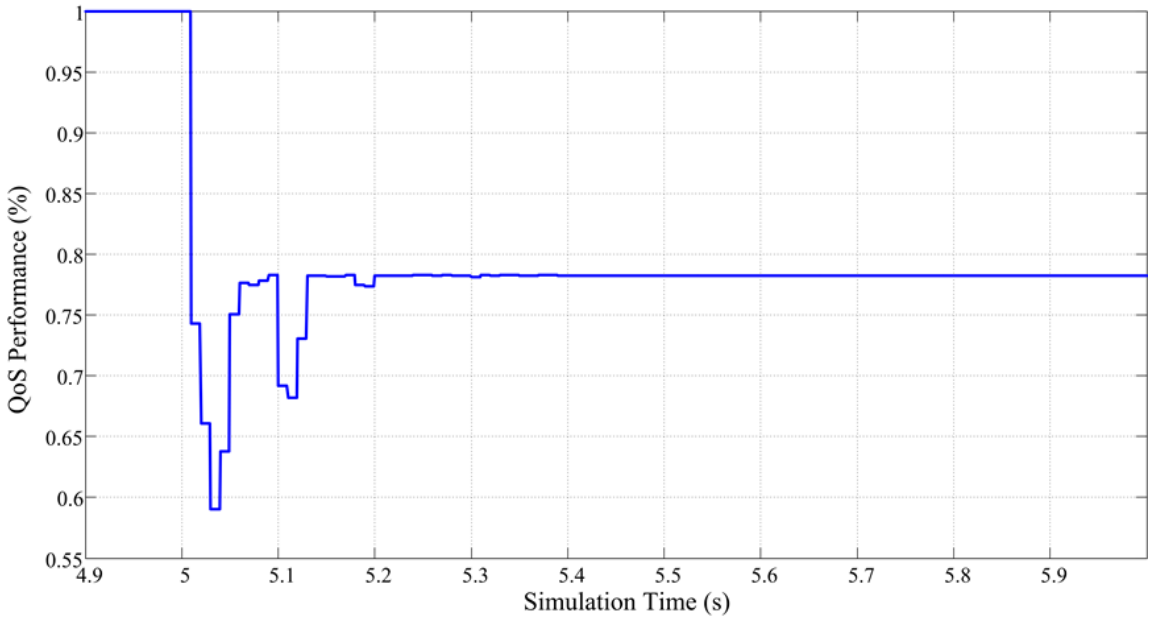

Figure 4.14 QoS performance

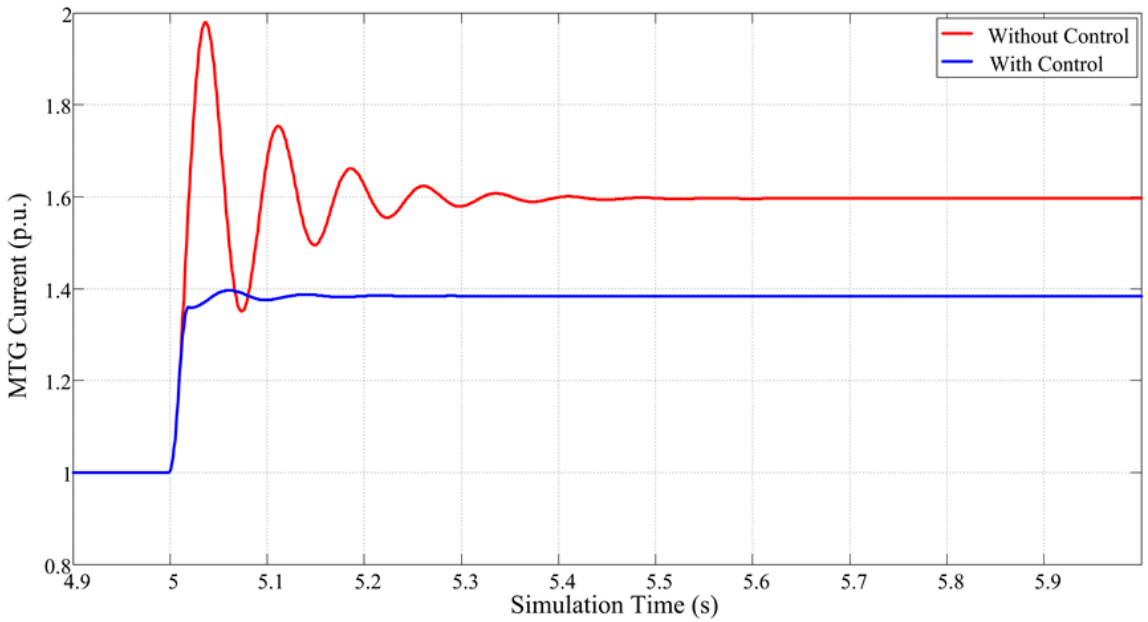

Figure 4.15 MTG current output comparison

This scenario has demonstrated that the QoS performance can optimized in parallel with bus voltage damping optimization. The performance management framework manages to drive the bus voltage to the optimal level within 0.15 sec while maintaining the QoS rating at a relatively high level (>60%). Compared with the previous two scenarios, the performance of Scenario III is more balanced between different objective functions.

4.6.2 Performance analysis

Compared with typical load shedding strategy development approaches as reviewed in Chapter 2.6.3, the proposed framework has a variety of advantages include:

- Capability of including the transient performance optimization criteria
- Highly flexible and customizable
- Proven effectiveness

Table 4.11 summarizes the performance of the management framework based on different prediction horizon setting N. The results are collect from repetitive runs of Scenario III which finds the balanced control inputs to optimize the overall system performance.

Table 4.11 The effect of different prediction horizon on controller performance

Prediction horizon N	fbest	Execution time (sec)
1	1.3238	280
2	1.3125	294
3	1.3106	302
4	1.3078	311

Based on the comparison of the performance analysis results, we can conclude that for this case study, prediction horizon increment leads to longer execution time; however, increasing the prediction horizon doesn't greatly increase the performance of the proposed management framework.

The profile for running the function "DCmain.m" is attached as in Figure 4.16. From the simulation profile we could observe that solving **ga** and its related functions takes most of the execution time compared with other parts of the function. Based on this observation, it can be concluded that in order to improve the simulation efficiently of the proposed management framework for actual onboard applications, the computational speed of **ga** needs to be greatly increased. A few approaches to achieve this goal have been illustrated in [119] including lowering the setting of **ga** and introducing parallel processing in Global Optimization Toolbox.

Function Name	Calls	**Total Time**	Self Time*	Total Time Plot (dark band = self time)
DCMain	1	280.711 s	0.366 s	
ga	40	272.124 s	0.024 s	
globaloptim\private\gaminlp	40	271.811 s	0.009 s	
globaloptim\private\gaminlpengine	40	271.797 s	0.010 s	
globaloptim\private\galincon	40	271.122 s	0.119 s	
...gaminlppenaltyfcn(x,problem,conScale)	1040	266.732 s	0.026 s	
globaloptim\private\gaminlppenaltyfcn	1040	266.706 s	0.151 s	
globaloptim\private\fcnvectorizer	1040	266.423 s	0.393 s	
...ateAnonymousFcn>@(x)fcn(x,FcnArgs{:})	52040	266.231 s	0.834 s	
@(p)solveg(ti,fo,p)	52040	265.397 s	0.494 s	
solveg	52040	264.903 s	1.771 s	
globaloptim\private\stepGA	1000	258.712 s	0.114 s	
ode23s	58041	258.428 s	89.396 s	
funfun\private\odenumjac	651855	108.370 s	76.422 s	
dceqmul	4080372	66.600 s	66.600 s	
odeget	928656	14.524 s	6.648 s	
odeset	58041	12.580 s	10.372 s	
globaloptim\private\makeState	40	12.193 s	0.012 s	

Figure 4.16 Simulation profile of "DCMain.m"

CHAPTER V

MODEL-BASED DESIGN ENVIORNMENT DEVELOPMENT

5.1 Overview

Based on the previous discussion, the dynamic system responses caused by disturbance under different operation scenarios, especially under the adverse conditions, are critical to the mission of SPS design. Careful modeling and simulation to analyze such contingent scenarios is critical for the design of SPS..

Based on the review in Chapter II, currently several conventional simulation platforms exist such as Matlab, Matlab Simulink, PSSE, PSCAD, and VTB. These tools provide the ability to model and analyze the performance of shipboard power applications. However, those simulation environments are also heavily constrained:

- The application designer needs to have very explicit knowledge of the simulation tools that the system model is developed based on in order to assure the application design suitable for the desired specifications without making syntactic mistakes or violating hierarchical component dependencies and other constraints
- Although similar design concepts and application development principles can be used across different tools, it is still relatively time-consuming and expensive to move the application model from one simulation

environment to another simulation environment due to the incompatibilities among different simulation environments and tools

- The model development is greatly limited to the current available tool-specific syntactic rules and constraints. Therefore it is hard to expand an existing design for future technologies and system updates

To solve those issues and further facilitate the design practice for application engineers, the Model-Integrated Computing (MIC) concept has been proposed as an ultimate solution for diverse domains [123-126]. In this chapter, a model-based software environment based on the principle of MIC is developed to support and simplify the modeling and simulation process for SPS that has been illustrated in Chapter III and the corresponding control and management framework design presented in Chapter IV. The design principle of this environment is similar to the definition of "Automatic Control Modeling Environment" (ACME) that has been developed and demonstrated in [93] for computer system. Therefore the proposed environment can be named as "Automatic Power system Modeling Environment" (APME). The general objective of this environment is to provide a flexible and extensible model-integrated graphical software tool to facilitate the rapid evaluation/analysis of SPS and possibly other micro-grid power system, as well as the implementation of the performance management strategy applications according to various testing scenarios. The contribution of this effort can be summarized as:

- The system design is categorized and represented in a modular and component based form which facilitates the development process

- With the introduction of meta-models, designers are now able to work on the application development with no particular knowledge of the simulation tools which significantly optimizes the life-cycle cost and improves the design efficiency
- The synthesized applications and system models can automatically be translated to scripts based on user's specification which can then be directly computed by the numerical solver to perform simulation and other types of analysis
- It can be seen as a seamless vertical integration environment which is capable to employ various power system tools, existing simulators and even user-specified tools for SPS application design and overall for other micro-grid system designs

This chapter is organized as follows: Section 5.2 provides a brief review of the MIC modeling principle and the software infrastructure of the proposed design. In Section 5.3, the system model formulation as discussed in Chapter III and the management strategy design as discussed in Chapter IV are integrated with the proposed modeling environment to create a convenient tool for applications designers. A brief conclusion is made in Section 5.4.

5.2 Model Integrated Computing

The concept of MIC is to facilitate the environment designers or application designers, by enabling the definition of the syntax and semantic specifications in a way that yields a better overall experience during building and simulating practice of complex applications [127]. For the implementation of MIC, the complete design process is

divided into two different levels. Of them, software or system engineers operate on the meta-level for specifying and configuring a specific domain; while domain engineers work on the application level to create application models and run simulations. Figure 5.1 demonstrates the structure of a typical MIC design process.

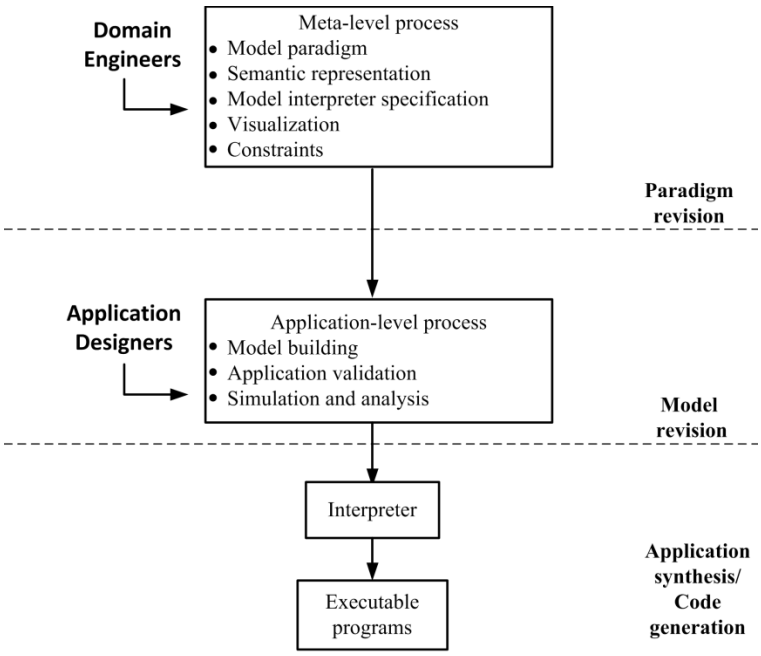

Figure 5.1 MIC concept

In the diagram, meta-level is a domain-independent abstraction that defines a domain specific environment in terms of modeling concepts, component relations, model-composition principles and constraints. In other words, meta-level is the specification of modeling paradigms of system configurations. It contains the base knowledge of rules and constraints of a specific domain and the corresponding representations.

On the other hand, application level provides an environment for application model customizations. The objective is to let the environment designers build the model,

synthesize executable applications, and analyze the simulation results. Principles of application operations are based on the semantic representations and paradigms defined on the meta-level. With changes and updates applied to the system, designers can easily modify the model and re-synthesize application files without building a new system from scratch.

A model interpreter is used to convert the knowledge captured from the application models into other types of useful artifacts [128]. For example, it can be used to generate executable scripts and configurations files. Upon user's request, attributes and relationships of system components will be acknowledged and synchronized to an numerical solver, which is normally provided by the specific domain. The interpreter will then invoke the solver and generate output in the form of data files, graphs, etc [126].

5.2.1 An essential tool: Generic Modeling Environment (GME)

Developed by the Institute of Software Integrated System at Vanderbilt University, Generic Modeling Environment (GME) is an open source, highly configurable toolkit that provides a generic solution for model design and application development for different domain-specific modeling environments [129].

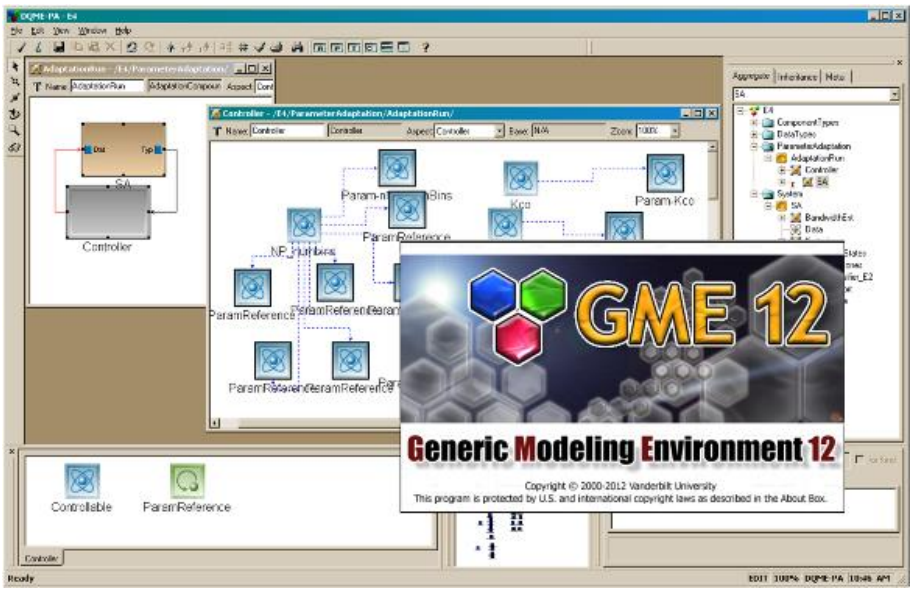

Figure 5.2 GME interface

A set of generic concepts are embedded in GME to facilitate the creation of sophisticated systems. Typical modeling concepts provided by GME include: aspects, attributes, hierarchy, set, reference, and constraints [126, 130]. Within a GME project, model, atom, reference, connection and set are classified as first-class objects (FCOs) which will be the main elements to be utilized to develop the meta-model paradigm [129]:

- Atom: the basic, elementary object, which cannot contain any objects inside
- Model: the comprehensive object that can contain other objects and inner structures
- Hierarchy: the containment relationships between objects. Every object must have one parent and the parent must be a model

- Aspect: the control unit of visibility that determines which part of the model is visible or hidden
- Connection: expresses the relationship between objects within the same model. In order to make a connection, the connected objects must be visible to each other, i.e. in the same aspect
- Reference: expresses relationships between objects in different system levels or different systems
- Set: relationships among a group of objects under the same folder with the same aspect
- Attribute: in order to capture information that has no graphical representations, FCOs are affiliated with attributes. The common available attributes are test, integer, double, boolean and enumerated
- Constraint: rules made specifically for model-composition and attribute specification.

Apart from the support of MIC based development, GME also offers a user-friendly graphical design interface. Developing a system model, especially a system with sophisticated components and hierarchical composition is an error-prone process. However, instead of the typical, textual representation, GME offers designers a better option of a more expressive and readable system representation in the GUI. In this way, the tedious code-based design becomes an easier, more straightforward and more visualized process [131].

As a summary, GME is a comprehensive software toolkit that integrates the meta-model editor, meta-model interpreter, application model editor, domain specific codes generator and simulation execution environment.

5.2.2 Design procedure

In author's previous work [132, 133], a similar environment has been developed primarily for the power flow and optimal power flow analysis for AC SPS applications. The developed environment is demonstrated to be capable of integrating with MatPower [134]/PSAT toolkit [135, 136] which are Matlab based power system analysis tools, and VTB environment [137] to perform the model design and simulation analysis. In this dissertation, the proposed APSME will be developed based on the same design principle, but modified to adapt to the requirement of modeling, analysis and performance management strategy design for MVDC SPS.

The general design procedure can be defined as: **i)** Preparing of the input data matrices that defines all the relevant system parameters in an appropriate form; **ii)** Invoking the main function to compile the system, perform the desired simulation or analysis/calculation and generate the results, and **iii)** Displaying the results and saving simulation data in predefined structures and directories. In the following section, the specific environment design that utilizes the MatPower toolbox to perform basic power flow analysis is provided as a simple and intuitive example to illustrate the generic design procedure of the development procedure of such environment.

To start with, the modeling principle of Matpower is briefly reviewed. Modeling of Matpower is based on the standard static power flow analysis models [134]. Equations describing system components and connections are represented in the form of matrices in

the Matlab structure. The common fields of the Matlab structure consist of **bus**, **branch**, **generator** and **load** for optimal power flow analysis. Among them, **branch** includes all forms of transmission lines, transformers and phase shifters, and is modeled as a standard pi transmission line with series impedance and charging capacitance. **Generator** is modeled in the form of power injections at a specific bus with an active part which stands for active power injection and a reactive part that denotes the reactive power injection. **Load** is modeled as constant consumption of active and reactive power from its interconnected **bus**. After the specifying the Matpower ***struct,*** a ***case*** file that combines and summarizes the system information and component specifications can be formulated. Commands like ***runpf*** and ***runopf*** are then invoked to solve the system and provide simulation results. The solver of Matpower is relying on the Matlab extension (MEX) files.

5.2.2.1 Step.1: Create the meta-model

Based on the Matpower format requirement, the main components in the system can be summarized into "Generators", "Buses" and "Loads". "Generator" blocks contain most of the attributes for the ***gen*** matrices in the MatPower data file, "Bus" blocks contain most of the attributes for the ***bus*** matrices, and the "Load" blocks contain the active and reactive power flow data for the ***bus*** matrices. There are also three types of connections in the system: "branch connection", "generator connection", and "load connection". Of them, the "branch connection" contains data for the ***branch*** matrices indicating the destination and source bus for a given connection. The "generator connection" includes data specifying the bus that each generator is connected to, along with the generator status for the ***gen*** matrices. The "load connection" includes the

information of the bus number each load is connected to and status attributes indicating the connection status of loads. Once all the components and their attributes are set in the Meta model, it can be complied and the Meta-model paradigms can be registered for the design of application model. The complete meta-model is shown as in Figure 5.3 and Figure 5.4. After compilation, the generated component library as well as the component property inspector can be found as in Figure 5.5 and Figure 5.6. They are resources that directly available to designers to drag and drop to formulate the system schematics for application system models.

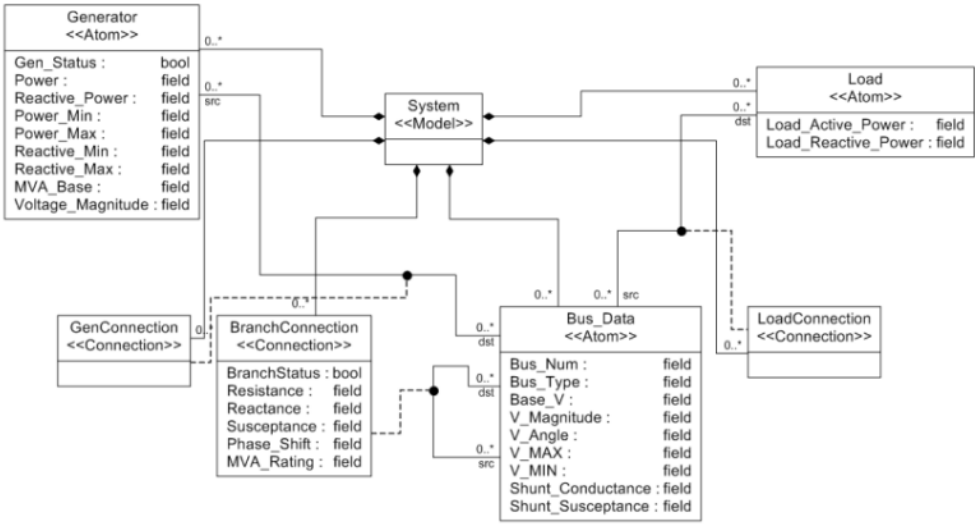

Figure 5.3 General architecture of the Meta model

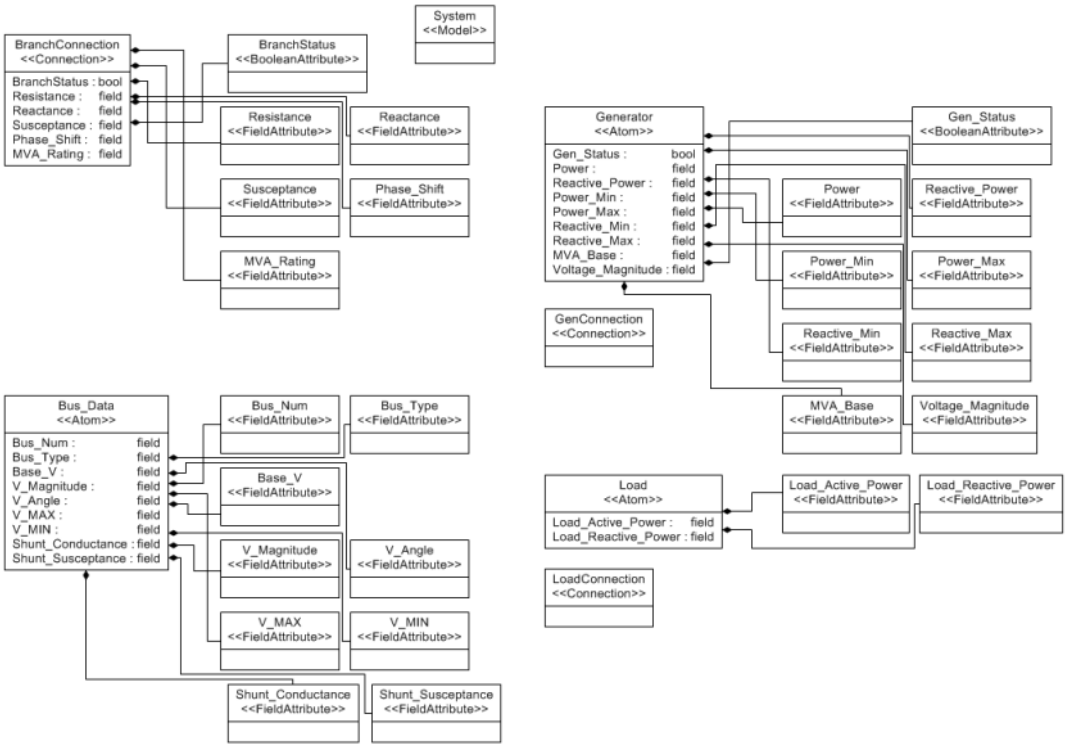

Figure 5.4 Attributes definition for the Meta-model components

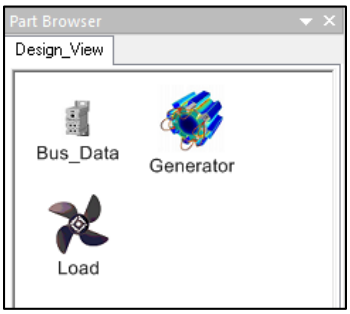

Figure 5.5 Component library generated from Meta-model compilation

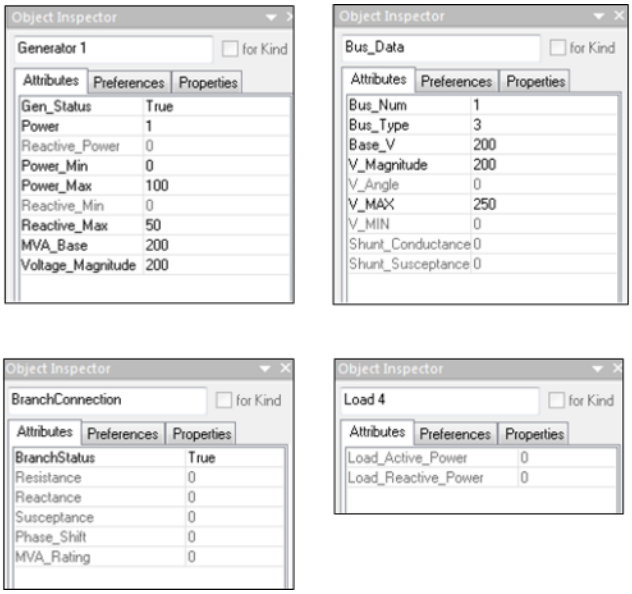

Figure 5.6 Parameter/Specification settings for each type of components

5.2.2.2 Step.2: Create the application model

The application model is created to mimic the model of the notional AC shipboard power system. Similarly to the MVDC system investigated in this dissertation, the fundamental topology of an AC SPS includes four turbo-generators connected to a ring-bus which supplies two propulsion motors and four zonal loads. Other components like energy storage system or high-level pulsed load are not included for simplicity. The main focus on the application model design is to evaluate the static state optimal power flow within the system, therefore the control units and other dynamic components within the system are also removed. The application model is demonstrated as in Figure 5.7.

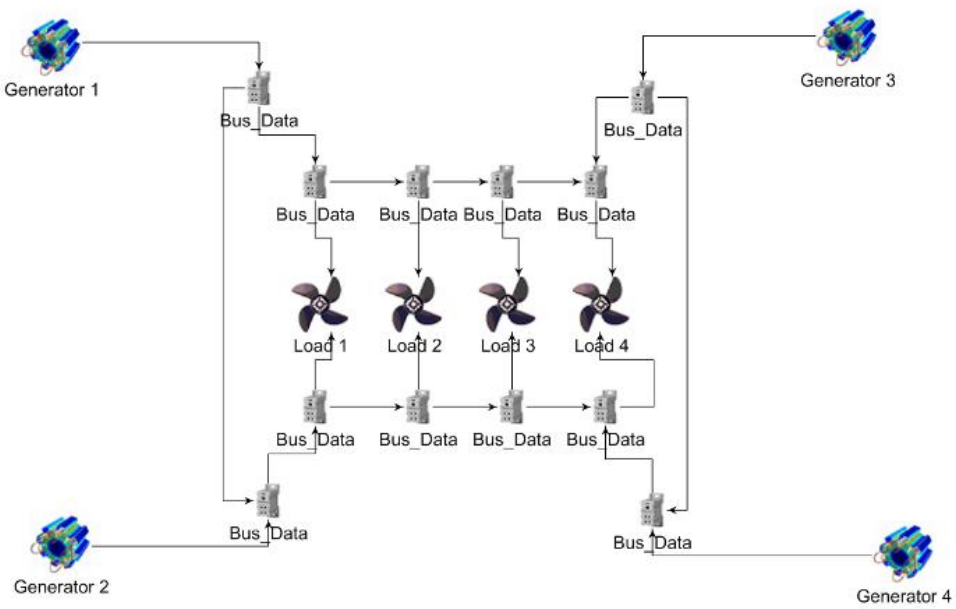

Figure 5.7 Application model design for a notional AC SPS

5.2.2.3 Step.3: Interpreter design-collect system data

The interpreter has three major functions. First of all, it examines the application model, extracts and collects data from the graphical design interface and save them in the correct formats. Secondly, it checks the values of each parameter and system settings to ensure that all the system constraints are satisfied. Last but not least, the interpreter automatically organizes the system information, creates the Matlab script file and sends the script to Matlab engine to solve and produce the simulation results. The interpreter is programmed in Visual C++ environment and can be directly opened by user from the graphic interface.

In order to collect the system information, the interpreter uses a dynamically allocated two-dimensional array to save the data. Sample below shows a section of the interpreter script which collects ***Bus*** data entities from the application model.

"***getAttribute()***" is one of the main functions used to collect attributes of particular elements from the system model.

```
%% Bus_Data_Collection
...
if((*it)->getObjectMeta().name() == "Bus"){
bus_array[0][buses]= (*it)->getAttribute("Bus_Num")->getIntegerValue();
bus_array[1][buses]=(*it)->getAttribute("Bus_Type")->getIntegerValue();
bus_array[4][buses]=(*it)->getAttribute("Shunt_Conductance")->getRealValue();
...
```

5.2.2.4 Step.4: Interpreter design-define constraints

As shown in the sample script below, a list of system constraints can be defined and added to the interpreter. Some of the simple numerical constraints can be checked based on the values of "flags" or "counters" once the data collection is complete. Other logic constraints, such as the statement that "every bus needs to have a unique bus number", are checked using multiple ***"for"*** loops during the data processing. If any of the constraints is found to be true, it indicates a violation and an "error flag" is set to prevent the furthering processing. In addition, an error message will be displayed on the console of GME describing the error information for the user. If no error has occurred, the interpreter will continue with the file generation.

```
%% Generator_Connection_Check
...
if(gen_conn_check < total_gens){
error = true; Console::Out::WriteLine("Error: Generator(s) not Connected."); }
else if(gen_conn_check > total_gens){
error = true;
Console::Out::WriteLine("Error: Multiple connections from a single
Generator.");}
```

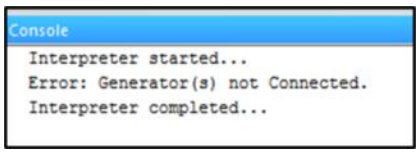

Figure 5.8 Error message displayed if constraints are violated

5.2.2.5 Step.5: Interpreter design-synthesis of configuration information

Sample script below shows the approach to generate the executable Matlab script. A variety of **"for"** loops are used to traverse through the arrays to retrieve the data and print them out in the correct format. At the end of the script, the interpreter also creates the command lines to execute the case file based on the type of analysis that indicated by the user. Once the data file is ready, the interpreter will invoke the Matlab engine.

```
%% Configuration_File_Synthesis
...
fprintf(matlab_file, "function mpc = case_1");
fprintf(matlab_file, "mpc.version = '2'");
fprintf(matlab_file, "mpc.baseMVA = 10");
fprintf(matlab_file, "mpc.bus = [  \n");

%% Print_Bus_Array
For (counter1 = 0;counter1 < total_buses;counter1++){
  For (counter2 = 0;counter2 < 11;counter2++){
    If (counter2 == 6)
     fprintf(matlab_file,"\t1");
    if (counter2 == 9)
    fprintf(matlab_file,"\t1");
  fprintf(matlab_file,"\t%.2f",bus_array[counter2][counter1]); }
fprintf(matlab_file,";\n");}
...
```

5.2.2.6 Step.6: Interpreter design-invoke Matpower solver

Matlab engine contains a series of API functions which supports C/C++, Fortran among many [138]. These functions can be used to invoke Matlab engine and execute Matlab scripts directly in the programming environments. Data (variables, arrays, matrices, etc.) can be transferred between the C++ workspace and Matlab workspace bi-directionally. The sample below shows the basic command lines used to call Matlab engine from C++.

```
%% Invode_Matlab_Engine_and_Solve
...
Engine *ep;  %% define Matlab engine pointer
char MatlabPath[100];  %%current Matlab Path
char p[6000];  %%Matlab return buffer
int n=6000;  %%Matlab return buffer size
ep=engOpen(NULL);
engOutputBuffer(ep, p, n);   %%push the Matlab output into the buffer
TCHAR NPath[MAX_PATH];   %%current C++ project path
GetCurrentDirectory(MAX_PATH, NPath);
strcpy(MatlabPath,"cd ");
strcat(MatlabPath, NPath);
engEvalString(ep,MatlabPath);  %%change the Matlab project path to the C++
path
engEvalString(ep,"Matpower");  %%execute the m-file
Console::Out::WriteLine(p);
...
```

5.2.2.7 Step.7: Display the simulation results

The simulation results are automatically generated and presented to user as shown in Figure 5.9.

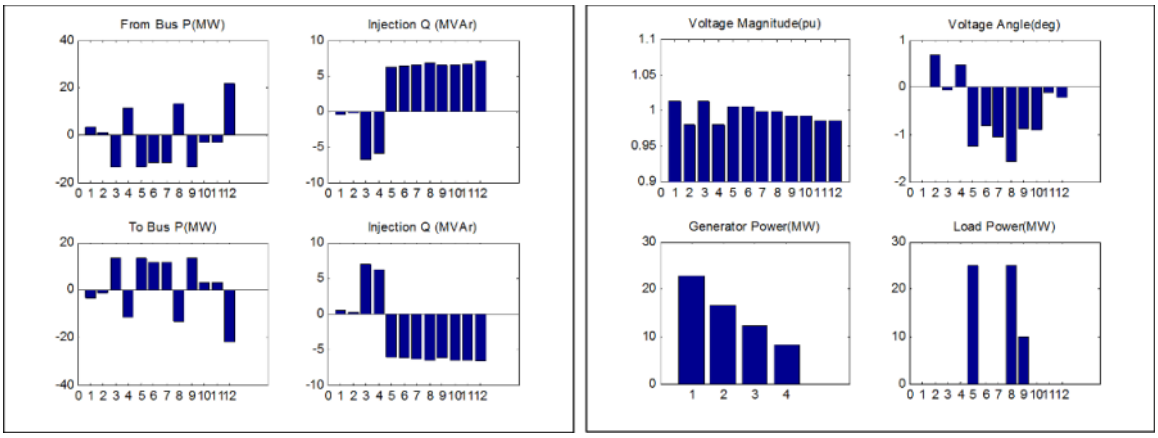

Figure 5.9 Simulation outputs

5.3 APME design

To include the contents proposed in this dissertation covering the model definition, application development and management strategy implementation, the existing environment has been expanded and modified for the APME platform.

APME essentially contains three main components: the dynamic power system model, the interface model, and the management system model. Among them, the system model generally refers to the complete power system represented in the form of DAE sets. For the purpose of this dissertation, we will use the model developed and validated in Chapter III as the dynamic system. Management system model, however, refers to the management framework developed in Chapter IV. Last but not least, the interface model provides the necessary means of information exchanging in between.

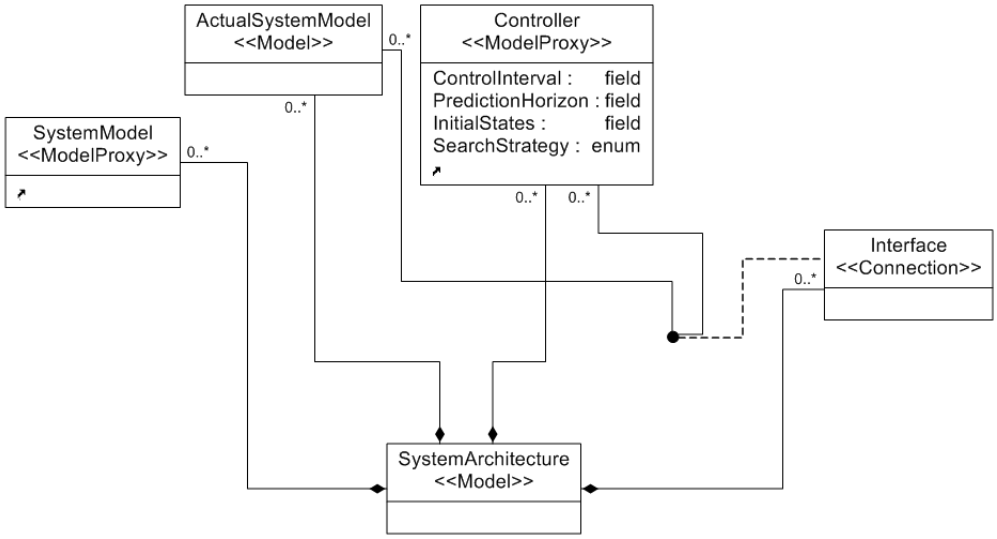

Figure 5.10 Architecture of the system meta-model

The architecture diagram of the Meta model for the APME design can be found in Figure 5.10 . Among them, the elements **ActualSystem**, **SystemModel**, **Controller** and **Interface** are the essential components under the main **SystemArchitecture** class. Those classes can be seen as the corresponding representations for the system component "Actual System", "System Module", "Controller Module", and "Measurement" as shown in Figure 4.1 respectively. The detailed architecture and decomposition are specified within each model.

The **ActualSystem** model refers to the actual system that the control management system will be applied to. It could be the physical or hardware testbed for MVDC SPS simulation or the equivalent form of the detailed baseline Simulink model.

The **SystemModel** model is developed based on the DAE sets as set forth in Chapter III. Unlike **ActualSystem**, it can be seen as an abstracted form to approximate the actual system behaviors.

The **Interface** model contains the necessary components to capture the system state variables for the controller. It acts like an interface to connect the physical system which is represented as "**ActualSystem**" and the abstracted system which is represented as "**SystemModel**". For this dissertation, it is assumed that all the related system states such as machine dynamics and the voltage/current measurements can be directly accessed and accurately transmitted by the **Interface** component.

Last but not least, the **Controller** model refers to the performance management system that has been developed in Chapter IV. The generic control principle function *MPC()* along with the basic search strategies like *Algorithm 1* and *Algorithm 2* proposed in Chapter IV can be set with appropriate specifications including the depth of the prediction horizon, the initial system states, the control input sets, and the constraints to be utilized.

The detailed meta-model of **SystemModel** can be found as in Figure 5.11. Based on the development in Chapter III, the essential components that need to be used to form a complete system include: switches, generators, different types of loads, propellers represented in the form of induction motors with filters, and the main DC distribution bus. The attributes of each type of the component are also defined and the specific values of those parameters need to be filled by application engineers later based on the operation scenarios.

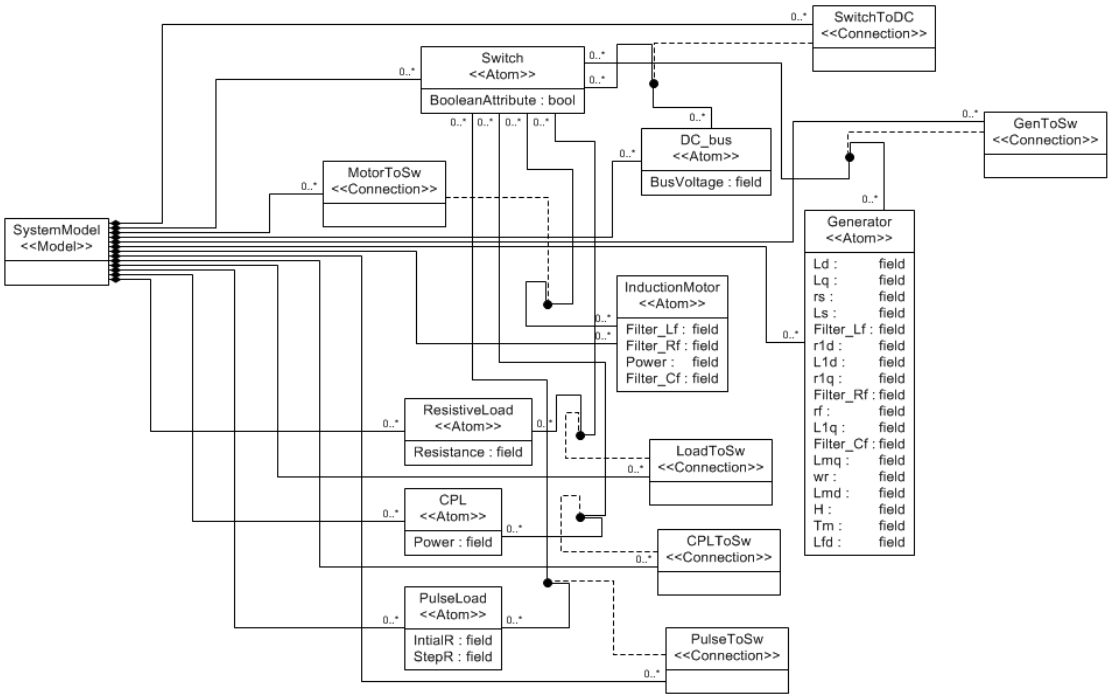

Figure 5.11 Detailed attributes settings for the "SystemModel"

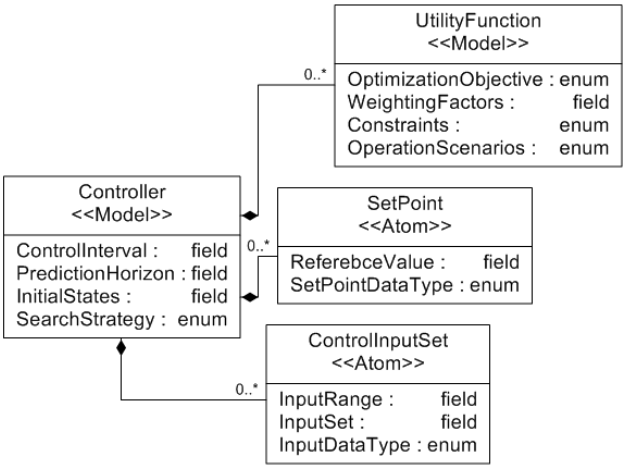

Figure 5.12 Meta-model for the "Controller"

In a similar way, the meta-model of the **Controller** model can also be developed as shown in Figure 5.12. The prediction horizon, control sampling interval, basic search

strategy (*Algorithm I/II* for discrete control input sets or *Algorithm III* for continuous control input sets) and the initial system values can be set to define the basic operation principles and properties of the controller. "ControlInputSet" determines the candidate control inputs that can be available for use which includes the data type, the possible range of the input data set, or a detailed set of inputs under certain circumstances. The reference system state trajectory or reference point for the **Controller** is specified in "SetPoint". Currently off-line calculation result is used to determine the optimal system trajectory or optimal reference point. The "UtilityFunction" model determines the utility functions, the system constraints and the detailed working scenarios. For the preliminary model development, we limit the utility functions that can be achieved with the proposed environment. Designers have to choose from a series of preset optimization functions under the specific conditions that are covered in Chapter IV. Customized utility functions/constraints/operation scenarios are not yet supported in this version. However, the detailed values of the utility function specifications, working constraints, weighting factors for different system elements and operation scenarios can still be changed.

Once the meta-model is created and successfully complied, the application model can be developed accordingly. The interface for the system architecture design is shown in Figure 5.13. An example of application model created based on the **SystemModel** is shown in Figure 5.14 while the **Controller** setting interface is shown in Figure 5.15.

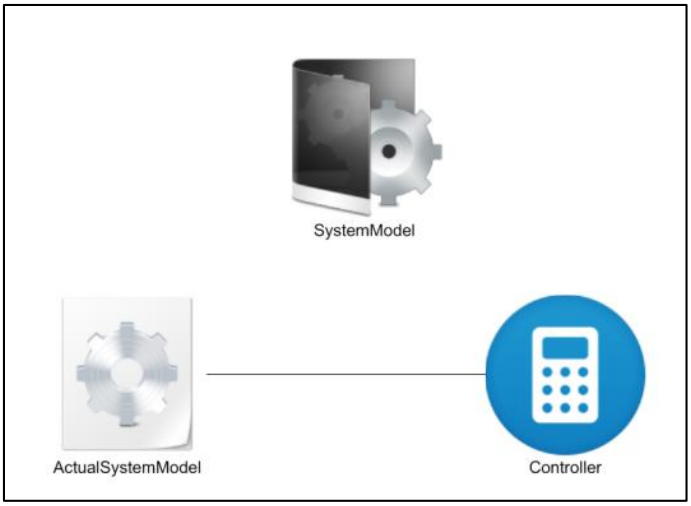

Figure 5.13 The design interface for the system architecture

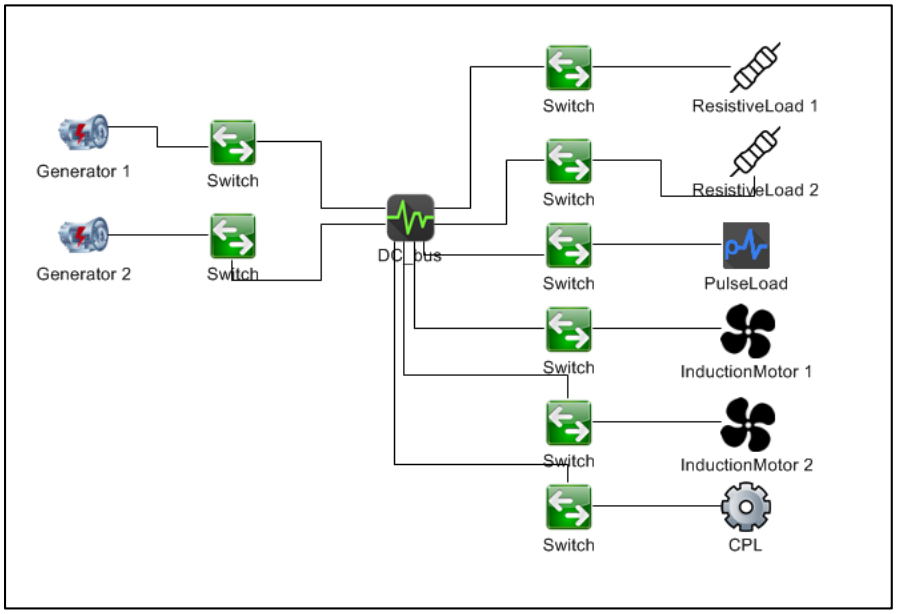

Figure 5.14 The design interface for application system model development

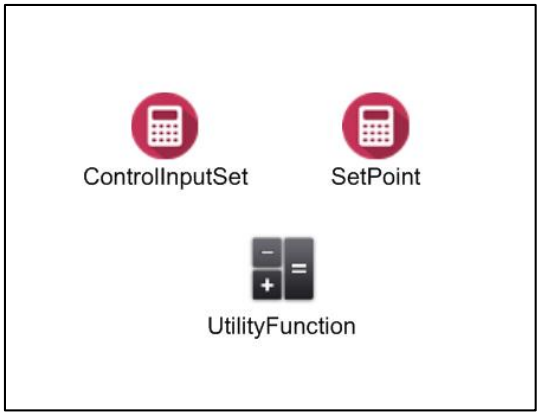

Figure 5.15 The interface to set the Controller parameters

Once the designer finishes the system structure development as well as the detailed specifications for each components, the created system model can then be processed by the interpreter to extract the necessary information, automatically generate the script file, and invoke Matlab engine to simulate the system and provide the results to users in the form of figures as demonstrated in Section 5.2.2. The detailed procedure is similar to the previous case study and will not be listed here for simplicity.

5.4 Conclusion

In this chapter, the development a MIC-based modeling, simulation and analysis environment is illustrated. The proposed software environment is capable of incooperating with the previously proposed system modeling strategy and the performance management framework developed to provide a generic solution for application designs and control strategy synthesis.

CHAPTER VI

CONCLUSION AND FUTURE WORK

6.1 Conclusion

This dissertation presents three categories of research work towards the design of an automated performance management system for MVDC SPS during transient period: 1) Power system modeling and simulation: a highly simplified representation of the notional baseline MVDC SPS model is developed which facilitates the subsequent design. The proposed modeling strategy is tailored specifically for the time frame of this dissertation and is proven accurate and efficient based on a series of testing scenarios. 2) Control framework design: The detailed designing procedure of the proposed management framework is illustrated. A series of case studies utilizing the proposed management system for different system-level applications are included to validate the MPC-based designing concept. An in-depth evaluation of the performance of the proposed management system is also presented based on the case studies. Specific performance indices, controller settings and essential factors have been identified to characterize the effectiveness and efficiency for a given control strategy. The simulation results demonstrate and support the statement that the proposed performance management system could effectively optimize the system dynamic behaviors during the transient phase. 3) Software implementation and tool development: a model-based software environment is developed in GME to allow easy creation of system models and

automatic application synthesis. This tool provides direct support for application designers to create system models using the proposed modeling strategy, develop control strategies based on the proposed management framework concept and automatically implement the design.

6.2 Future work directions

The research contributions presented in this dissertation can be further extended as follow:

- Further improve the simulation speed of the proposed management framework for practical application designs. Currently for complicated systems or complicated optimization problems, as indicated by the testing results from the case studies I/II, the generation of control strategy still takes significantly long even with the use of efficient optimization functions or solvers. This issue can be solved via two approaches, one is to distribute the centralized control hierarchy into different nodes so the calculation can be partitioned and executed in parallel as seen in [139]. The other approach is to 1) either parallelize the process of the optimization solver such as **ga** and **fmincon**, so the time required for each iteration of the complete system optimization can be reduced; 2) or to parallelize the power system model, thus different parts of the system can be evaluated and optimized simultaneously on different cores/threads as seen in [140].
- More case-studies can be added to further evaluate the performance of the proposed management framework under different operation scenarios. A

variety of suggested case studies is made available from ESRDC document and therefore provides good sources of information with regards to the system-level dynamic studies especially under large system disturbances.

- Other system components can be added in order to expand the applicable scale of the model library such as detailed model of isolated DC-DC converters, AC transformers and other types of service loads. By doing so, the modeling principle proposed in this dissertation can be expanded for studies of short-term stability, governor and load control design, or even long term dynamics by including the appropriate level of details of the corresponding components.

REFERENCES

1. Doerry, N., *Designing Electrical Power Systems for Survivability and Quality of Service.* Naval Engineering Journal, 2007. **119**(2): p. 25 - 34.

2. Chalfant, J.S. and C. Chryssostomidis. *Analysis of various all-electric-ship electrical distribution system topologies*. in *Electric Ship Technologies Symposium (ESTS), 2011 IEEE*. 2011.

3. Amy, J.V., Jr. *Considerations in the design of naval electric power systems*. in *Power Engineering Society Summer Meeting, 2002 IEEE*. 2002.

4. Ali, H., et al. *Cross-platform validation of notional baseline architecture models of naval electric ship power systems*. in *Electric Ship Technologies Symposium (ESTS), 2011 IEEE*. 2011.

5. Qunying, S., et al. *Power and Energy Management in Integrated Power System*. in *Electric Ship Technologies Symposium (ESTS), 2011 IEEE*. 2011.

6. Taylor, C.W. *The future in on-line security assessment and wide-area stability control*. in *Power Engineering Society Winter Meeting, 2000. IEEE*. 2000.

7. Larsson, M., D.J. Hill, and G. Olsson, *Emergency voltage control using search and predictive control.* International Journal of Electrical Power & Energy Systems, 2002. **24**(2): p. 121-130.

8. Licheng, J., R. Kumar, and N. Elia, *Model Predictive Control-Based Real-Time Power System Protection Schemes.* Power Systems, IEEE Transactions on, 2010. **25**(2): p. 988-998.

9. Ford, J.J., G. Ledwich, and Z.Y. Dong, *Efficient and robust model predictive control for first swing transient stability of power systems using flexible AC transmission systems devices.* Generation, Transmission & Distribution, IET, 2008. **2**(5): p. 731-742.

10. Zweigle, G. and V.M. Venkatasubramanian. *Model prediction based transient stability control*. in *Transmission and Distribution Conference and Exposition (T&D), 2012 IEEE PES*. 2012.

11. Larsson, M. and D. Karlsson, *Coordinated system protection scheme against voltage collapse using heuristic search and predictive control.* Power Systems, IEEE Transactions on, 2003. **18**(3): p. 1001-1006.

12. Kundur, P., *Power System Stability and Control*. 1994: New York: McGraw-Hill.

13. W.Sauer, P. and M.A.Pai, *Power System Dynamics and Stability*. 2006, Champaign, Illinois 61820: Stipes Publishing L.L.C.

14. Yasar, M., et al. *Integrated Electric Power System supervision for reconfiguration and damage mitigation*. in *Electric Ship Technologies Symposium, 2009. ESTS 2009. IEEE*. 2009.

15. Ramanujam, R., *Power system dynamic: analysis and simulation*. 2009, Delhi: PHI learning private limited.

16. Ericsen, T., N. Hingorani, and Y. Khersonsky, *Power electronics and future marine electrical systems.* Industry Applications, IEEE Transactions on, 2006. **42**(1): p. 155-163.

17. Sudhoff, S.D., *Stability technical report*. Aug, 2012, Purdue University.

18. ESRDC, *Documentation for Notional Baseline System Models (Version 0.2)*. 2010.

19. Bash, M., et al. *A Medium Voltage DC Testbed for ship power system research*. in *Electric Ship Technologies Symposium, 2009. ESTS 2009. IEEE*. 2009.

20. Arcidiacono, V., R. Menis, and G. Sulligoi. *Improving Power Quality in All Electric Ships Using a Voltage and VAR Integrated Regulator*. in *Electric Ship Technologies Symposium, 2007. ESTS '07. IEEE*. 2007.

21. Arcidiacono, V., A. Monti, and G. Sulligoi, *Generation control system for improving design and stability of medium-voltage DC power systems on ships.* Electrical Systems in Transportation, IET, 2012. **2**(3): p. 158-167.

22. Vicenzutti, A., D. Bosich, and G. Sulligoi. *MVDC power system voltage control through feedback linearization technique: Application to different shipboard power conversion architectures*. in *Electric Ship Technologies Symposium (ESTS), 2013 IEEE*. 2013.

23. Sulligoi, G., et al. *Linearizing control of shipboard multi-machine MVDC power systems feeding Constant Power Loads*. in *Energy Conversion Congress and Exposition (ECCE), 2012 IEEE*. 2012.

24. Andersson, G. *Modeling and Analysis of Electric Power Systems ETH Zurich*. 2008; Available from: http://www.eeh.ee.ethz.ch.

25. *IEEE Recommended Practice for 1 kV to 35 kV Medium-Voltage DC Power Systems on Ships*. IEEE Std 1709-2010, 2010: p. 1-54.

26. Kundur, P., et al., *Definition and classification of power system stability IEEE/CIGRE joint task force on stability terms and definitions*. Power Systems, IEEE Transactions on, 2004. **19**(3): p. 1387-1401.

27. Li, Q., *AC SYSTEM STABILITY ANALYSIS AND ASSESSMENT FOR SHIPBOARD POWER SYSTEMS*, in *Electrical Engineer*. 2004, Texas A&M University. p. 189.

28. Huaxi, Z., R.A. Dougal, and M.H. Ali. *Transient stability of high frequency AC power systems*. in *Electric Ship Technologies Symposium (ESTS), 2013 IEEE*. 2013.

29. Farasat, M., A.S. Arabali, and A.M. Trzynadlowski. *A novel control principle for all-electric ship power systems*. in *Electric Ship Technologies Symposium (ESTS), 2013 IEEE*. 2013.

30. Barati, F., L. Dan, and R.A. Dougal. *Voltage regulation in medium voltage DC systems*. in *Electric Ship Technologies Symposium (ESTS), 2013 IEEE*. 2013.

31. Steurer, M., et al., *Development of a model-based specification of a medium voltage DC amplifier for DC shipboard system studies*, in *Proceedings of the 2011 Grand Challenges on Modeling and Simulation Conference*. 2011, Society for Modeling & Simulation International: Hague, Netherlands. p. 116-123.

32. Kwasinski, A., *Stability and Control of DC Micro-grids*. May, 2011, University of Texas.

33. Amy, J., Jr., *Composite System Stability Methods Applied to Advanced Shipboard Electric Power Systems*. 1992, Massachusetts Institute of Technology: Cambridge, MA.

34. Peniston, B., *No Higher Honor: Saving the USS Samuel B. Roberts in the Persian Gulf*. 2006: Annapolis: Naval Institute Press.

35. *USS Princeton (CG-59)*. [cited 2014; Available from: http://www.navysite.de/cg/cg59.html.

36. U.S.Navy, *USS Zumwalt*. U.S. Navy photo illustration/Released.

37. Andrus, M., *NGIPS MVDC baseline architecture definition-RTDS implementation*. Auguest 2010, Florida State Univ.

38. *IEEE Recommended Practice for Excitation System Models for Power System Stability Studies.* IEEE Std 421.5-2005 (Revision of IEEE Std 421.5-1992), 2006: p. 0_1-85.

39. Sulligoi, G., et al. *Considerations on the design of voltage control for multi-machine MVDC power systems on large ships*. in *Electric Ship Technologies Symposium (ESTS), 2013 IEEE*. 2013.

40. Khalil, H.K., *Nonlinear Systems*. 3 ed. 2001: Prentice Hall.

41. Marx, D., et al., *Large Signal Stability Analysis Tools in DC Power Systems With Constant Power Loads and Variable Power Loads—A Review.* Power Electronics, IEEE Transactions on, 2012. **27**(4): p. 1773-1787.

42. Emadi, A., et al., *Constant power loads and negative impedance instability in automotive systems: definition, modeling, stability, and control of power electronic converters and motor drives.* Vehicular Technology, IEEE Transactions on, 2006. **55**(4): p. 1112-1125.

43. Rivetta, C., G.A. Williamson, and A. Emadi. *Constant power loads and negative impedance instability in sea and undersea vehicles: statement of the problem and comprehensive large-signal solution*. in *Electric Ship Technologies Symposium, 2005 IEEE*. 2005.

44. Emadi, A., M. Ehsani, and J.M. Miller, *Vehicular Electric Power Systems: Land, Sea, Air, and Space Vehicles*. 2003: New York: Marcel Dekker.

45. Emadi, A., B. Fahimi, and M. Ehsani, *On the concept of negative impedance instability in advanced aircraft power systems with constant power loads.* Soc. Automotive Eng. (SAE), 1999. **vol. 1**.

46. Emadi, A., B. Fahimi, and M. Ehsani, *On the concept of negative impedance instability in advanced aircraft power systems with constant power loads.* SAE Technical paper, 1999.

47. Abdelwahed, S., et al. *Reduced order modeling of a shipboard power system*. in *Electric Ship Technologies Symposium (ESTS), 2013 IEEE*. 2013. IEEE.

48. Chiniforoosh, S., et al., *Definitions and Applications of Dynamic Average Models for Analysis of Power Systems.* Power Delivery, IEEE Transactions on, 2010. **25**(4): p. 2655-2669.

49. Chiniforoosh, S., et al., *Dynamic Average Modeling of Front-End Diode Rectifier Loads Considering Discontinuous Conduction Mode and Unbalanced Operation.* Power Delivery, IEEE Transactions on, 2012. **27**(1): p. 421-429.

50. Sun, J., et al., *Averaged modeling of PWM converters operating in discontinuous conduction mode.* Power Electronics, IEEE Transactions on, 2001. **16**(4): p. 482-492.

51. Sun, J. and H. Grotstollen, *Symbolic analysis methods for averaged modeling of switching power converters.* Power Electronics, IEEE Transactions on, 1997. **12**(3): p. 537-546.

52. Krein, P.T., et al., *On the use of averaging for the analysis of power electronic systems.* Power Electronics, IEEE Transactions on, 1990. **5**(2): p. 182-190.

53. Lian, K.L., B.K. Perkins, and P.W. Lehn, *Harmonic Analysis of a Three-Phase Diode Bridge Rectifier Based on Sampled-Data Model.* Power Delivery, IEEE Transactions on, 2008. **23**(2): p. 1088-1096.

54. Grotzbach, M. and R. Redmann, *Line current harmonics of VSI-fed adjustable-speed drives.* Industry Applications, IEEE Transactions on, 2000. **36**(2): p. 683-690.

55. Carpinelli, G., et al., *Analytical modeling for harmonic analysis of line current of VSI-fed drives.* Power Delivery, IEEE Transactions on, 2004. **19**(3): p. 1212-1224.

56. Krause, P.C., O. Wasynczuk, and S.D. Sudhoff, *Analysis of Electric Machinery and Drive Systems (2nd Edition)*. 2002: NJ: IEEE Press.

57. Sudhoff, S.D., et al., *Transient and dynamic average-value modeling of synchronous machine fed load-commutated converters.* Energy Conversion, IEEE Transactions on, 1996. **11**(3): p. 508-514.

58. Sudhoff, S.D., et al., *DC link stabilized field oriented control of electric propulsion systems.* Energy Conversion, IEEE Transactions on, 1998. **13**(1): p. 27-33.

59. Sudhoff, S.D. and O. Wasynczuk, *Analysis and average-value modeling of line-commutated converter-synchronous machine systems.* Energy Conversion, IEEE Transactions on, 1993. **8**(1): p. 92-99.

60. Qiang, H., K. Hee-Sang, and J. Jatskevich. *Effect of stator resistance on average-value modeling of BLDC motor 120- degree inverter systems*. in *Electrical Machines and Systems, 2007. ICEMS. International Conference on*. 2007.

61. Han, Q., N. Samoylenko, and J. Jatskevich, *Average-value modeling of brushless DC motors with 120 voltage source inverter.* Energy Conversion, IEEE Transactions on, 2008. **23**(2): p. 423-432.

62. Zhu, H., *New Multi-Phase Diode Rectifier Average Models for AC and DC Power System Studies*, in *Electrical and Computer Engineering*. 2005, Virginia Polytechnic Institute and State University.

63. Zhu, H., et al. *Average modeling of three-phase and nine-phase diode rectifiers with improved AC current and DC voltage dynamics*. in *Industrial Electronics Society, 2005. IECON 2005. 31st Annual Conference of IEEE*. 2005.

64. Zhu, H., et al. *Evaluation of average models for nine-phase diode rectifiers with improved AC and DC dynamics*. in *Applied Power Electronics Conference and Exposition, 2006. APEC '06. Twenty-First Annual IEEE*. 2006.

65. Defense, D.o., *Interface standard Section 300B: Electric Power, Alternating Current*. 2008.

66. Doerry, N.H. and J.V. Amy. *Implementing Quality of Service in shipboard power system design*. in *Electric Ship Technologies Symposium (ESTS), 2011 IEEE*. 2011.

67. Butler-Purry, K.L. and N.D.R. Sarma. *Intelligent network reconfiguration of shipboard power systems*. in *Power Engineering Society General Meeting, 2003, IEEE*. 2003.

68. Ding, Z., *Realtime Dynamic Load Shedding for Shipboard Power Systems*, in *Electrical Engineering*. 2006, Florida State University.

69. Shen, Q., *A distributed control approach for power and energy management in a notional shipboard power system.* 2012.

70. Kwasinski, A. and C.N. Onwuchekwa, *Dynamic Behavior and Stabilization of DC Microgrids With Instantaneous Constant-Power Loads.* Power Electronics, IEEE Transactions on, 2011. **26**(3): p. 822-834.

71. Nagaraj, K.C., et al. *Perspectives on Power System Reconfiguration for Shipboard Applications*. in *Electric Ship Technologies Symposium, 2007. ESTS '07. IEEE*. 2007.

72. Butler, K.L., N.D.R. Sarma, and V.R. Prasad. *A new method of network reconfiguration for service restoration in shipboard power systems*. in *Transmission and Distribution Conference, 1999 IEEE*. 1999.

73. Butler-Purry, K.L. *Multi-agent technology for self-healing shipboard power systems*. in *Intelligent Systems Application to Power Systems, 2005. Proceedings of the 13th International Conference on*. 2005.

74. Abdeljalil, L., M.A. Ahmed, and M.F. Benkhoris. *Dynamic modelling of shipboard electric network compared to power flow problem's solution*. in *Electric Ship Technologies Symposium, 2005 IEEE*. 2005.

75. Bose, S., et al. *Analysis of robustness for shipboard power system with non-radial power flow*. in *Electric Ship Technologies Symposium (ESTS), 2011 IEEE*. 2011.

76. Haifeng, L., et al., *Planning Reconfigurable Reactive Control for Voltage Stability Limited Power Systems.* Power Systems, IEEE Transactions on, 2009. **24**(2): p. 1029-1038.

77. Yorino, N., et al., *A new formulation for FACTS allocation for security enhancement against voltage collapse.* Power Systems, IEEE Transactions on, 2003. **18**(1): p. 3-10.

78. Vaahedi, E., et al., *Dynamic security constrained optimal power flow/VAr planning.* Power Systems, IEEE Transactions on, 2001. **16**(1): p. 38-43.

79. Feng, Z., V. Ajjarapu, and D.J. Maratukulam. *A comprehensive approach for preventive and corrective control to mitigate voltage collapse*. in *Power Engineering Society Winter Meeting, 2000. IEEE*. 2000.

80. Baran, M.E. and N. Mahajan. *System reconfiguration on shipboard DC zonal electrical system*. in *Electric Ship Technologies Symposium, 2005 IEEE*. 2005.

81. Cuzner, R. and A. Jeutter. *DC zonal electrical system fault isolation and reconfiguration*. in *Electric Ship Technologies Symposium, 2009. ESTS 2009. IEEE*. 2009.

82. Carroll, J., et al. *Dynamic reconfiguration preserving stability*. in *Electric Ship Technologies Symposium, 2005 IEEE*. 2005.

83. Shokooh, S., et al., *Intelligent Load Shedding Need for a Fast and Optimal Solution*, in *IEEE PCIC*. 2005: Europe.

84. Shrestha, A., E.L. Foulks, and R.W. Cox. *Dynamic load shedding for shipboard power systems using the non-intrusive load monitor*. in *Electric Ship Technologies Symposium, 2009. ESTS 2009. IEEE*. 2009.

85. Mair, A.J., et al., *Progress in the development of adaptive control for shipboard power systems through modeling and simulations*, in *Proceedings of the 2010 Conference on Grand Challenges in Modeling & Simulation*. 2010, Society for Modeling & Simulation International: Ottawa, Ontario, Canada. p. 195-202.

86. Soman, R.R., E.M. Davidson, and S.D.J. McArthur. *Using functional failure mode and effects analysis to design the monitoring and diagnostics architecture for the zonal MVDC shipboard power system*. in *Electric Ship Technologies Symposium, 2009. ESTS 2009. IEEE*. 2009.

87. Otomega, B., M. Glavic, and T. Van Cutsem, *Distributed Undervoltage Load Shedding.* Power Systems, IEEE Transactions on, 2007. **22**(4): p. 2283-2284.

88. Wen, J.Y., et al., *Optimal coordinated voltage control for power system voltage stability.* Power Systems, IEEE Transactions on, 2004. **19**(2): p. 1115-1122.

89. Qiang, W., et al., *Voltage security enhancement via coordinated control.* Power Systems, IEEE Transactions on, 2001. **16**(1): p. 127-135.

90. Akhrif, O., et al., *Application of a multivariable feedback linearization scheme for rotor angle stability and voltage regulation of power systems.* Power Systems, IEEE Transactions on, 1999. **14**(2): p. 620-628.

91. Okou, F.A., O. Akhrif, and L.-A. Dessaint, *A novel modelling approach for decentralized voltage and speed control of multi-machine power systems.* International Journal of Control, 2003. **76**(8): p. 845-857.

92. Rubaai, A. and F.E. Villaseca, *Transient stability hierarchical control in multimachine power systems.* Power Systems, IEEE Transactions on, 1989. **4**(4): p. 1438-1444.

93. Abdelwahed, S., et al., *On the application of predictive control techniques for adaptive performance management of computing systems.* Network and Service Management, IEEE Transactions on, 2009. **6**(4): p. 212-225.

94. Marler, R.T. and J.S. Arora, *Survey of multi-objective optimization methods for engineering.* Structural and multidisciplinary optimization, 2004. **26**(6): p. 369-395.

95. Stadler, W., *A survey of multicriteria optimization or the vector maximum problem, part I: 1776–1960.* Journal of Optimization Theory and Applications, 1979. **29**(1): p. 1-52.

96. Marler, T. and J.S. Arora, *Multi-Objective Optimization: Concepts and Methods for Engineering*. 2009: VDM Verlag.

97. Rawlings, J.B., *Tutorial overview of model predictive control.* Control Systems, IEEE, 2000. **20**(3): p. 38-52.

98. Grüne, L. and J. Pannek, *Nonlinear Model Predictive Control: Theory and Algorithms*. 2011: Springer.

99. Findeisen, R. and F. Allgower, *An Introduction to Nonlinear Model Predictive*, in *Control, 21st Benelux Meeting on Systems and Control*. 2002: Veidhoven. p. 1 - 23.

100. Martinson, W.S. and P.I. Barton, *A differentiation index for partial differential-algebraic equations.* SIAM Journal on Scientific Computing, 2000. **21**(6): p. 2295-2315.

101. Zahedi, B. and L.E. Norum, *Modeling and Simulation of All-Electric Ships With Low-Voltage DC Hybrid Power Systems.* Power Electronics, IEEE Transactions on, 2013. **28**(10): p. 4525-4537.

102. Ong, C.-M., *Dynamic Simulation of Electric Machinery*. 1998, Upper Saddle River, New Jersey 07458: Prentice Hall PTR.

103. Kulkarni, S. and S. Santoso. *Estimating transient response of simple AC and DC shipboard power systems to pulse load operations*. in *Electric Ship Technologies Symposium, 2009. ESTS 2009. IEEE*. 2009.

104. RTDS. *Real Time Digital Simulator - RTDS.* [cited 2014; Available from: http://www.rtds.com/index/index.html.

105. RTDS. *Technical Publications*. [cited 2014; Available from: http://www.rtds.com/about-us/technical-publications/technical-publications.html.

106. Su, R., S. Abdelwahed, and S. Neema, *Computing finitely reachable containable region for switching systems.* Control Theory and Applications, IEE Proceedings - , 2005. **152**(4): p. 477-486.

107. Rong, S. and S. Abdelwahed. *A practical stability analysis for a class of switching systems with uncertain parameters*. in *American Control Conference, 2006*. 2006.

108. Kargarian, A., et al. *Multiobjective optimal power flow algorithm to enhance multi-microgrids performance incorporating IPFC*. in *Power and Energy Society General Meeting, 2012 IEEE*. 2012.

109. Chattopadhyay, D. and J. Momoh, *A multiobjective operations planning model with unit commitment and transmission constraints.* Power Systems, IEEE Transactions on, 1999. **14**(3): p. 1078-1084.

110. Nagarajan, K., S. Abdelwahed, and J.P. Hayes. *Self-optimization in computer systems via on-line control: application to power management*. in *Autonomic Computing, 2004. Proceedings. International Conference on*. 2004.

111. Abdelwahed, S., et al., *Online fault adaptive control for efficient resource management in Advanced Life Support Systems.* Habitation (Elmsford), 2005. **10**(2): p. 105-15.

112. Nagarajan, K., S. Abdelwahed, and M. Khandekar. *A Hierarchical Optimization Framework for Autonomic Performance Management of Distributed Computing Systems*. in *Distributed Computing Systems, 2006. ICDCS 2006. 26th IEEE International Conference on*. 2006.

113. Abdelwahed, S., N. Kandasamy, and S. Neema, *A control-based framework for self-managing distributed computing systems*, in *Proceedings of the 1st ACM SIGSOFT workshop on Self-managed systems*. 2004, ACM: Newport Beach, California. p. 3-7.

114. Lewis, F., L. and V. Syrmos, L., *Optimal Control*. 1995: Wiley-Interscience.

115. MathWorks, *Matlab 2014a Documentation*, in *Global Optimization Toolbox*. 1999-2014.

116. MathWorks. *Constrained Nonlinear Optimization Algorithms*. 1999-2014; Available from: http://www.mathworks.com/help/optim/ug/constrained-nonlinear-optimization-algorithms.html.

117. Mathworks, *Global optimization toolbox- Comparison of Four Solvers*. 1999-2014.

118. Works, M. *Choosing a solver*. 1999-2014; Available from: http://www.mathworks.com/help/optim/ug/choosing-a-solver.html.

119. Mathworks, *What Is the Genetic Algorithm?* 1999-2014.

120. Mathematica. *Virtual Book: Constrained optimization*. Mathematics and algorithms; Available from: http://reference.wolfram.com/mathematica/tutorial/ConstrainedOptimizationOverview.html.

121. Lee, W.J. and S.K. Sul, *DC-Link Voltage Stabilization for Reduced DC-Link Capacitor Inverter.* Industry Applications, IEEE Transactions on, 2014. **50**(1): p. 404-414.

122. Shaw, S.R., et al., *Nonintrusive Load Monitoring and Diagnostics in Power Systems.* Instrumentation and Measurement, IEEE Transactions on, 2008. **57**(7): p. 1445-1454.

123. Sztipanovits, J., et al., *Model-based Integration Technology for Next Generation Electric Grid Simulations.* Computational Needs for Next Generation Electric Grid, 2011: p. 4.11-4.44.

124. Karsai, G., et al., *Model-integrated development of embedded software.* Proceedings of the IEEE, 2003. **91**(1): p. 145-164.

125. Sztipanovits, J. and G. Karsai, *Model-integrated computing.* IEEE Computer, 1997: p. 110-111.

126. Ledeczi, A., M. Maroti, and P. Volgyesi, *The generic modeling environment*, in *\ldots on Intelligent Signal \ldots*. 2004, Vanderbilt University. p. 1-14.

127. Karsai, G., J. Sztipanovits, and H. Franke, *Towards specification of program synthesis in model-integrated computing.* Proceedings IEEE ECBS, 1998: p. 226-233.

128. Bakshi, A., V. Prasanna, and A. Ledeczi, *MILAN: A model based integrated simulation framework for design of embedded systems.* ACM Sigplan Notices, 2001.

129. GME Toolkit. *http://www.isis.vanderbilt.edu/Projects/gme*.

130. Ledeczi, A., M. Maroti, and A. Bakay, *The generic modeling environment.* Proceedings of the IEEE International Workshop on Intelligent Signal Processing, 2001.

131. Volgyesi, P. and A. Ledeczi, *Component-based development of networked embedded applications.* Proceedings. 28th Euromicro Conference, 2002: p. 68-73.

132. Shi, J., et al. *Generic modeling and analysis framework for shipboard system design*. in *Electric Ship Technologies Symposium (ESTS), 2013 IEEE*. 2013.

133. Shi, J., R. Amgai, and S. Abdelwahed. *Generic Modeling and Analysis Environment Design for Shipboard Power System*. in *3rd and 4th MARINELIVE Workshops*. 2012.

134. Matpower. *http://www.pserc.cornell.edu/matpower/*.

135. Milano, F., *An Open Source Power System Analysis Toolbox.* IEEE Transactions on Power Systems, 2005. **20**(3): p. 1199-1206.

136. PSAT. *Http://www.uclm.edu/area/gsee/Web/Federico/psat.htm*.

137. VTB Example Systems. *http://vtb.engr.sc.edu/vtbwebsite*.

138. *Matlab Documentation: Call Matlab Engine*.

139. Rajat, M., *Model-based autonomic performance management of distributed enterprise systems and applications*, in *Electrical and computer engineering*. 2012, Mississippi State University.

140. Amgai, R.S., J; Abdelwahed, S; Fu, Y., *Research Trends In High Performance Computing Application On Large Scale Power System Operation*, in *Grand Challenges in Modeling & Simulation*. 2012: Italy. p. 112-117.